Kinetic Alfvén Waves in Tokamaks

Ph. Lauber, T. Hayward-Schneider, V.-A. Popa, F. Vannini, A. Biancalani[1],
A.Bottino, G. Meng, Z.-X. Lu, X. Wang, and ASDEX Upgrade Team

IPP Garching, Germany
[1]Léonard de Vinci Pôle universitaire, Research center, Paris la Défense, France & IPP Garching

acknowledgements:

F. Zonca, M. Falessi, N. Carlevaro, ENEA Frascati
A. Bierwage QST,
S. D. Pinches, M. Schneider, O. Hoenen, ITER
M. Fitzgerald, CCFE

support within Eurofusion TSVV & Enabling Research Projects: MET (F. Zonca), ATEP(Ph. Lauber&M. Falessi), TSVV#10 (A. Mishchenko)

This work has been carried out within the framework of the EUROfusion Consortium and has received funding from the Euratom research and training programme 2014-2018 and 2019-2020 under grant agreement No 633053 and IO Contract No. IO/18/CT/ 4300001657. Part of this work has been supported by the following Enabling Research projects: Part of this work has been supported by the following Enabling Research projects: CfP-AWP17- ENR-MPG-01 (Ph. Lauber), CfP-AWP19-ENR-ENEA-01 (F. Zonca), EnR-MOD.01.MPG (Ph. Lauber), ITER is the Nuclear Facility INB no. 174. The views and opinions expressed herein do not necessarily reflect those of the European Commission nor the ITER Organization.

Outline

- motivation, introduction & history
- the role of kinetic Alfvén waves (KAWs) in Tokamaks:
  - JET (Culham, UK)
  - ITER (Cadarache, France)
  - ASDEX Upgrade (Garching Germany)
- conclusions & outlook

motivation

- KAWs are rarely directly investigated or measured in Tokamak plasmas: short wave-length (mm-cm) due to small gyro-radii/strong guide-field
- KAWs are absent in electrostatic limit: instabilities dominating thermal particle and heat transport in present-day experiments (e.s. drift modes, ion temperature gradient or trapped electron modes) are/were often discussed without coupling to Alfvénic branches
- for fusion relevant betas (~5%) this is certainly not true any more: electromagnetic codes advanced considerably within last decade
- fusion plasmas with energetic α-particles (~100 times more energetic than thermal ions) introduce additional spatial and temporal scales
- meso-scale and global Alfvénic modes interact most efficiently with energetic particles (EPs) - mode conversion to KAWs crucial for their stability
- KAW physics often dominates linear damping of EP-driven modes, and has significant consequences for non-linear saturation and related transport → KAWs influence crucially the self-organisation of a burning fusion plasma.

Tokamaks

- **strong guide-field:** several T (ITER: 5.3T)
  - gyro-radii for thermal ions ~ several mm
  - gyro-radii for energetic ions ~ several cm
  - gyro-radius ρ /minor radius a ~1/(100-1000)
- **low beta:** constraints of helicity (safety factor q)
  - $q_0 \gtrsim 1$, $q_a > 3\text{-}5$ due to MHD stability limitations
  - $\beta = 2\,\mu_0\, p\,/B^2 \approx 1/100\, \beta_p \rightarrow\ \beta \sim 1\%\text{-}10\%$
- **Alfvén velocity**: $v_A \approx B/\sqrt{(\mu_0\, m_i\, n_i)} \approx 10^6$ m/s; $\omega_{ci}/(v_A\, R) \sim 10^3 \rightarrow$ MHD phenomena and cyclotron physics can be decoupled with respect to time scales
- in plasma core: **collisionless plasma**
- **kinetic Alfvén waves (KAW)**: wavelength of main species gyro-radius ≈ several mm coupling of MHD scales [m], orbit width [cm] and KAWs [mm] lead to **multi-scale-length problem**

[IPP, C. Brandt]

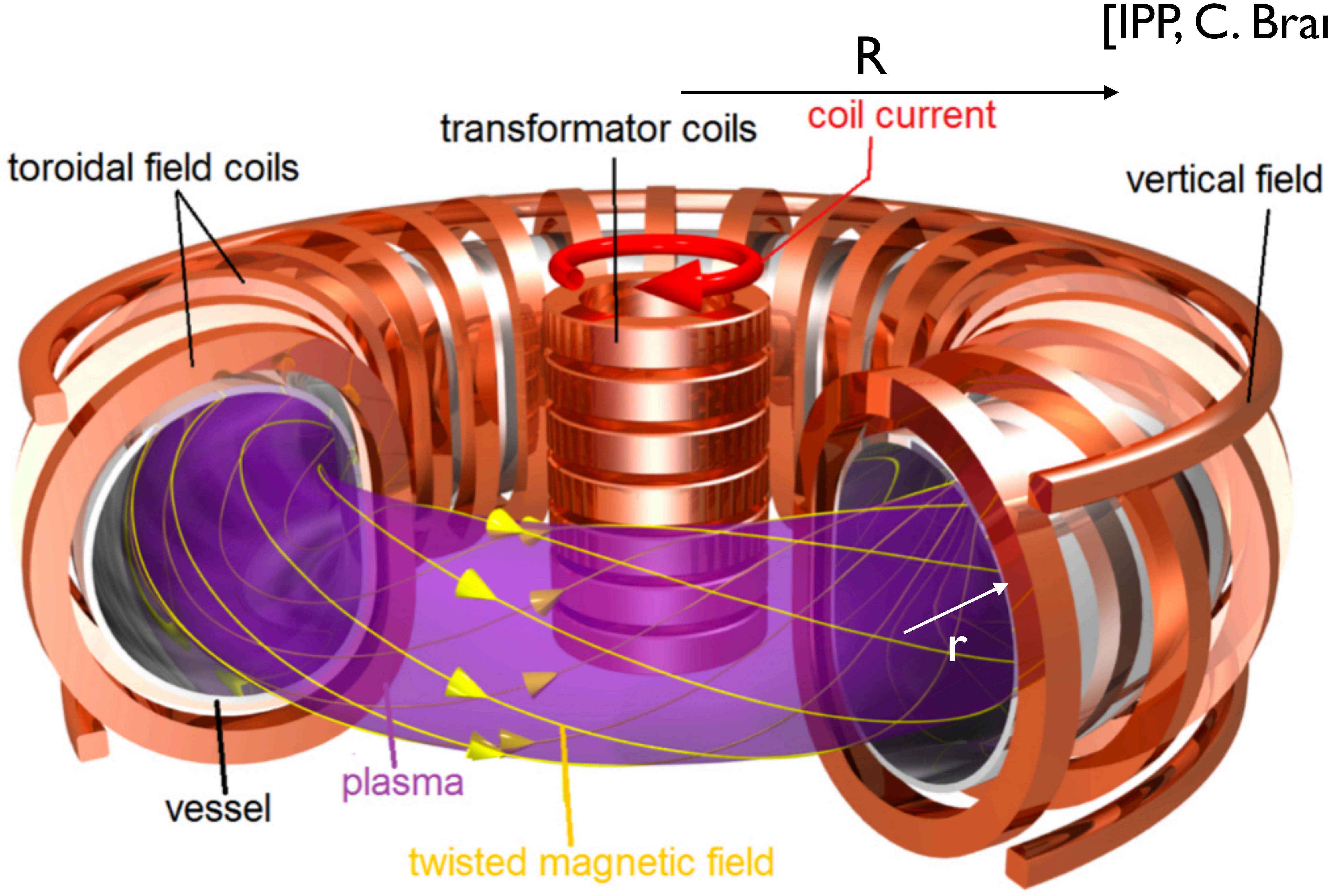

A=R/r ~3

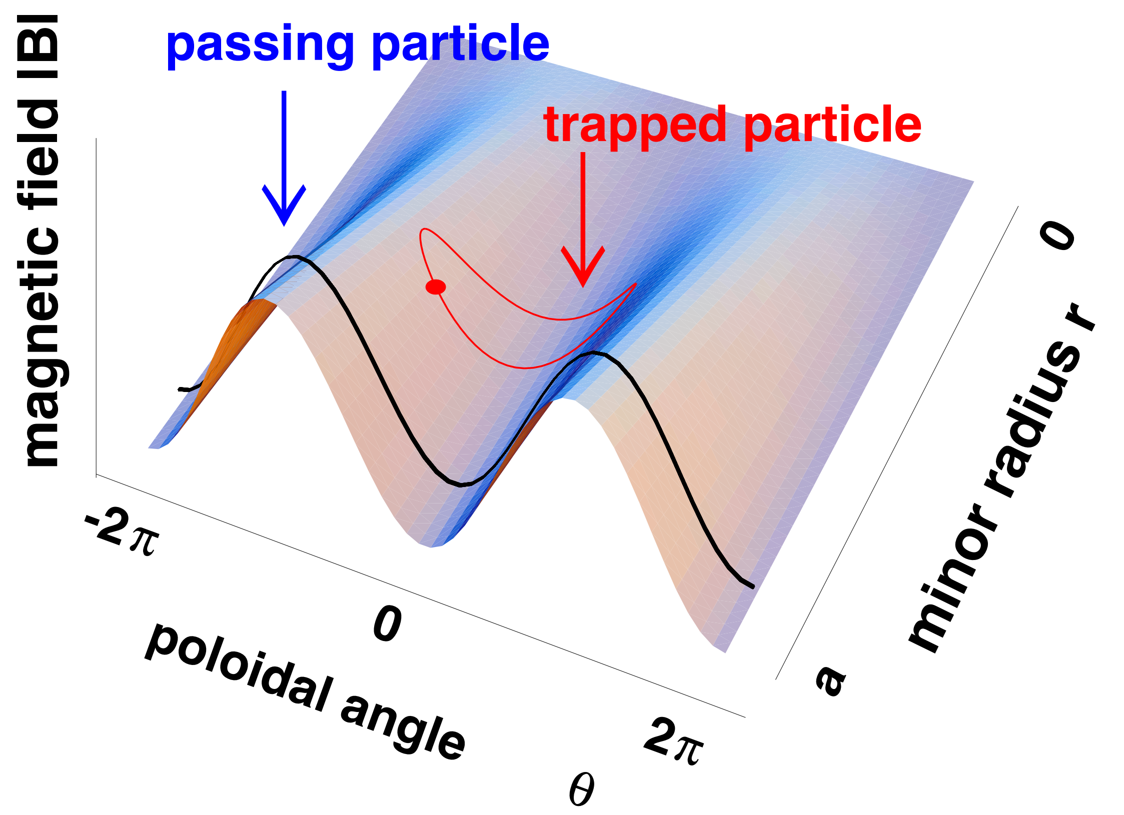

shear Alfvén waves in a cylindrical plasma with radial non-uniformity

dispersion relation: $\omega = k_{\|} v_A;$

periodic cylinder: phase mixing, i.e. strong damping

$$k_{\|} = \frac{1}{R_0}\left(n - \frac{m}{q(r)}\right); \quad v_A(r) = B(r)/\sqrt{\mu_0 m_i n(r)}; \; q(r) = rB_z/RB_\theta$$

n: toroidal/axial mode number m: poloidal mode number

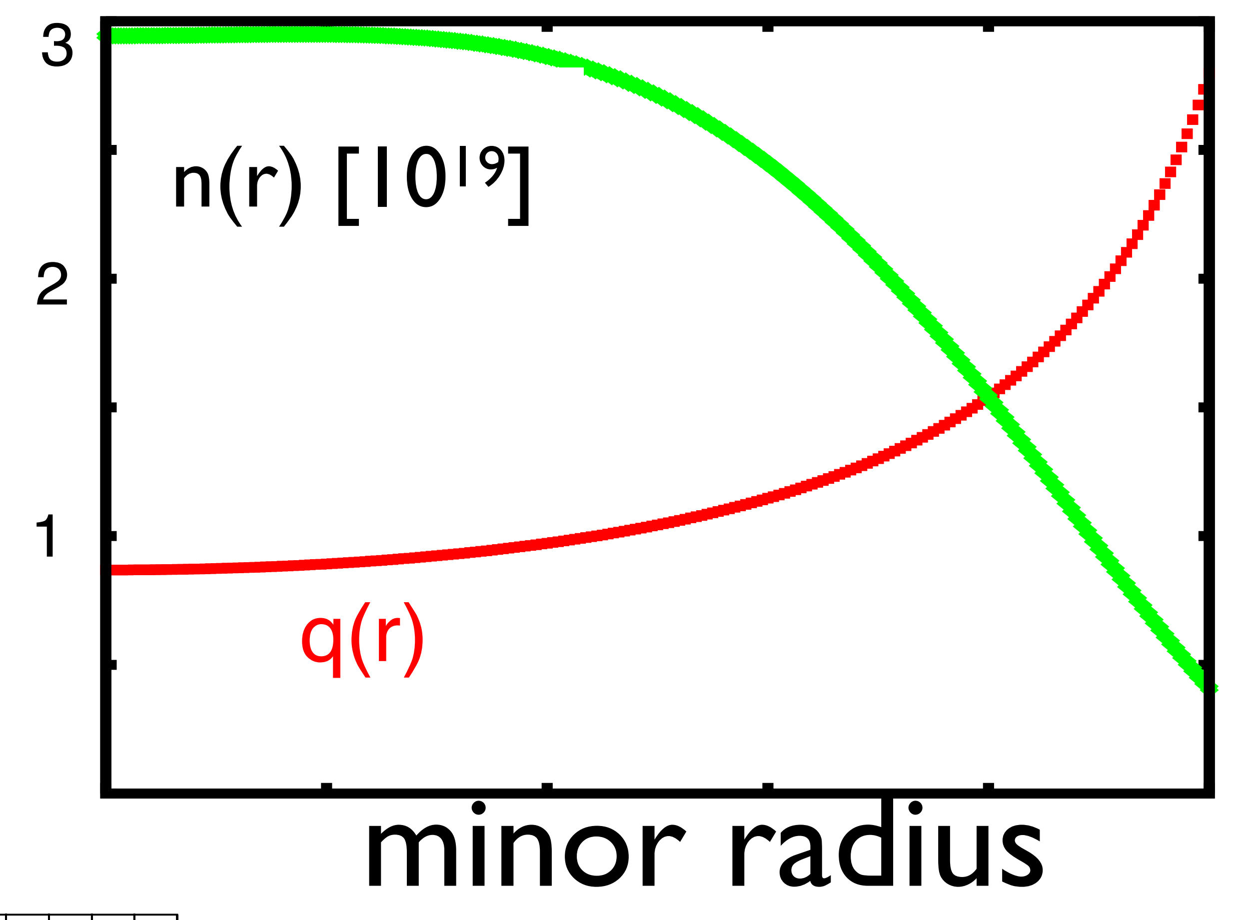

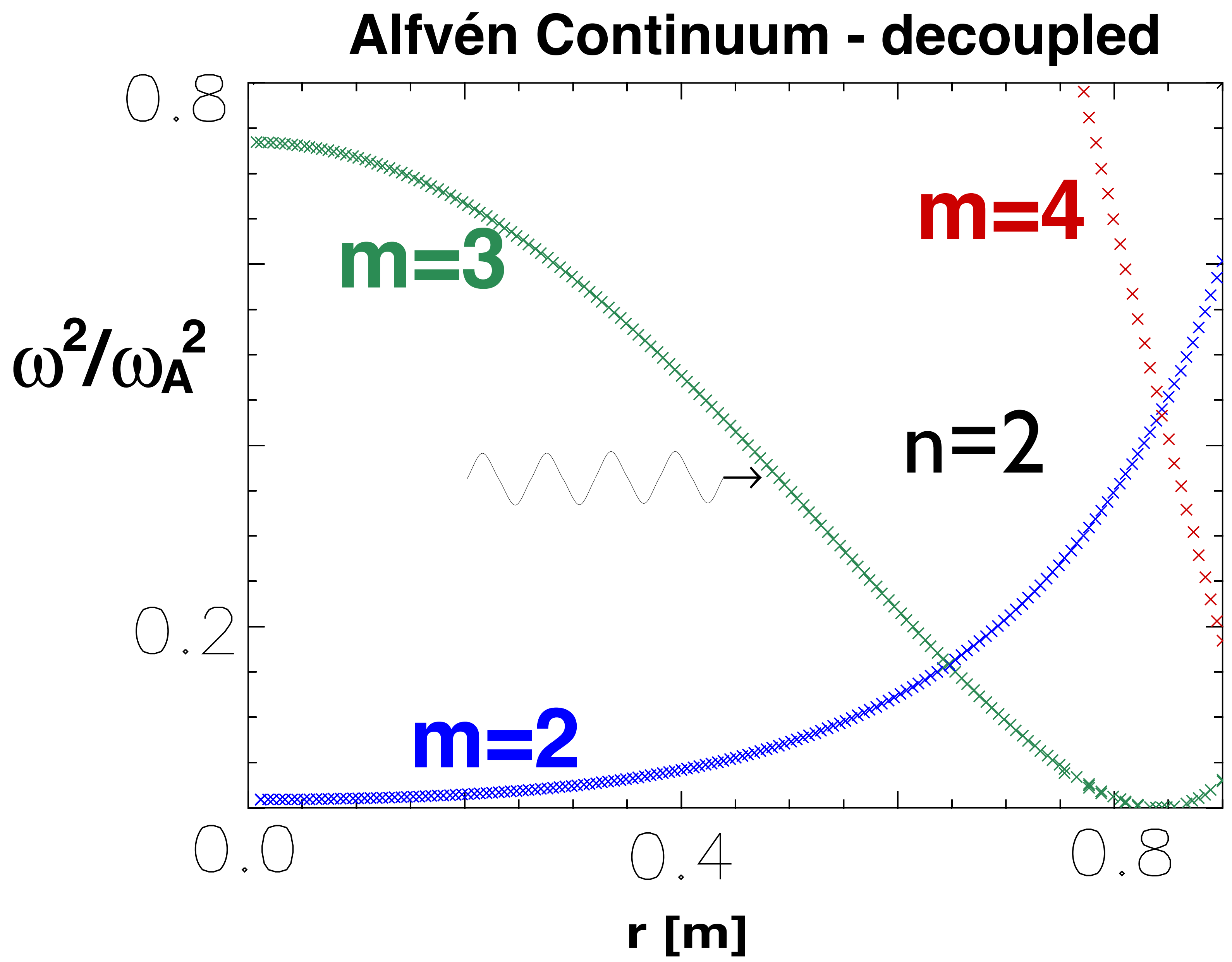

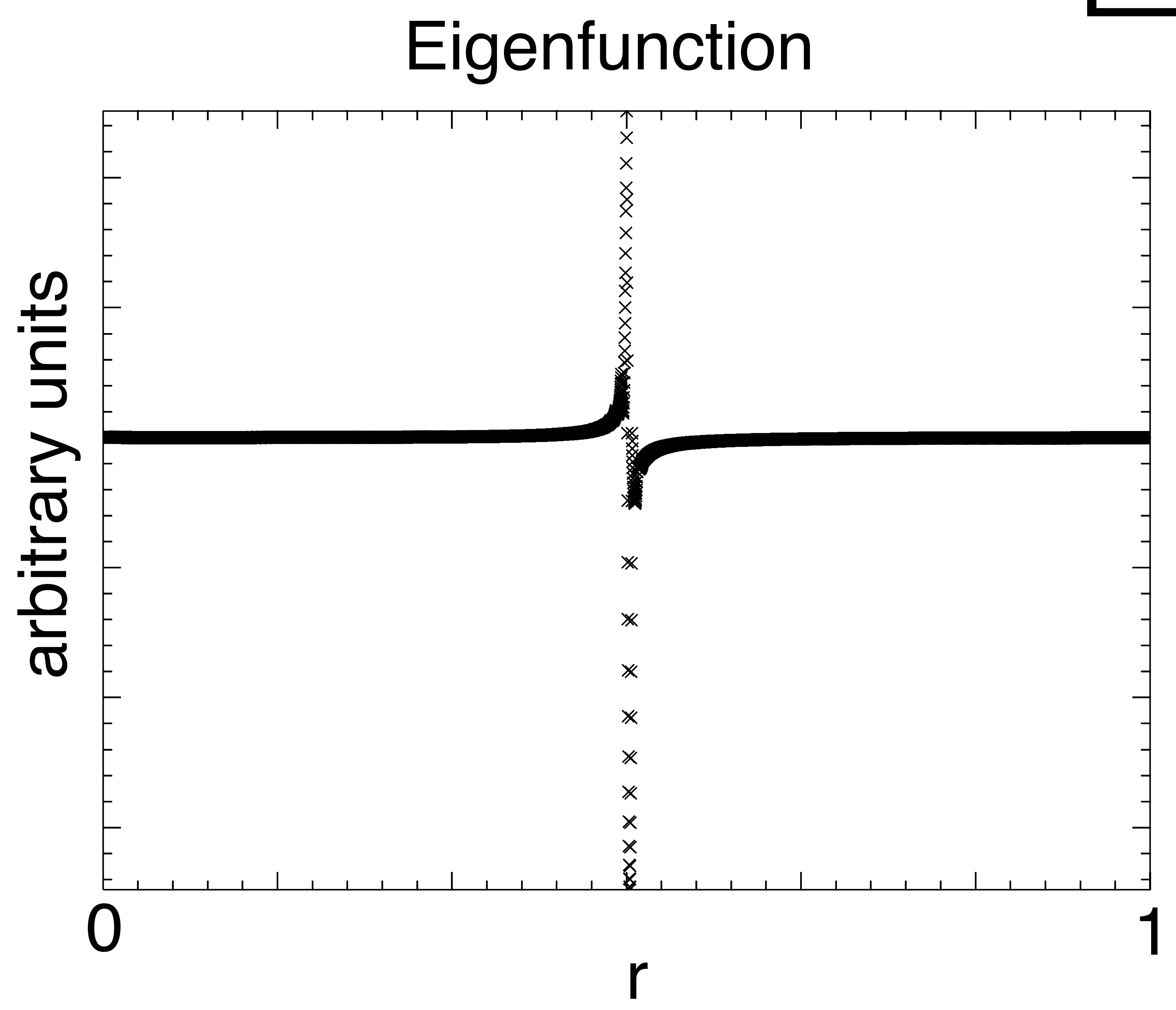

idea of Alfvén wave heating: efficient absorption of external wave at resonant location

[W. Grossmann, J. Tataronis, Z. Phys. 261, 217 (1973); A. Hasegawa, L. Chen, Phys. Rev. Lett. 35, 370 (1975)]

from reduced MHD to (gyro-)kinetics

- it was early recognised that kinetic effects need to be included to understand the absorption mechanism [A. Hasegawa, L. Chen, Phys. Rev. Lett. 35, 370 (1975), A. Hasegawa, L. Chen, Phys. Fluids 19 (1976) 1924]

- use quasi-neutrality and shear-Alfvén law including lowest order finite Larmor radius effects and Landau damping-like terms (LD):

$$\mathbf{E} = -\nabla\phi - \frac{\partial \mathbf{A}}{\partial t}; \qquad A_\parallel = \frac{1}{i\omega}(\nabla\psi)_\parallel$$

$$[1 + \xi_e Z(\xi_e) + 1 + \xi_i Z(\xi_i)](\phi - \psi) \quad = \quad T_e/T_i \varrho_i^2 \nabla_\perp^2 \phi$$

$$\nabla_\perp \cdot \frac{\omega^2}{v_A^2}\nabla_\perp\phi + \frac{\partial}{\partial s}\nabla_\perp^2 \frac{\partial\psi}{\partial s} \quad = \quad \frac{3}{4}\varrho_i^2 \frac{\omega^2}{v_A^2}\nabla_\perp^4\phi$$

- if mode is purely Alfvénic, $\Phi = \psi$ and $E_{//} = k_{//}(\Phi - \psi) = 0$

- polarisation gives important information on nature of perturbation: in Tokamaks, predominantly Alfvénic, predominantly electrostatic and mixed polarisation are very common

KAW: dispersion relation and global solutions

$$\left.\begin{array}{c} S(\phi - \psi) = T_e/T_i \varrho_i^2 \nabla_\perp^2 \phi \\ \nabla_\perp^2 \frac{\omega^2}{v_A^2}\phi + \nabla_\perp^2 k_\parallel^2 \psi = \frac{3}{4}\varrho_i^2 \frac{\omega^2}{v_A^2} \nabla_\perp^4 \phi \end{array}\right\} \Rightarrow \omega^2 = k_\parallel^2 v_A^2 \left[1 + k_\perp^2 \varrho_i^2 (3/4 + T_e/T_i)\right]_{\text{long-wavelength-limit}}$$

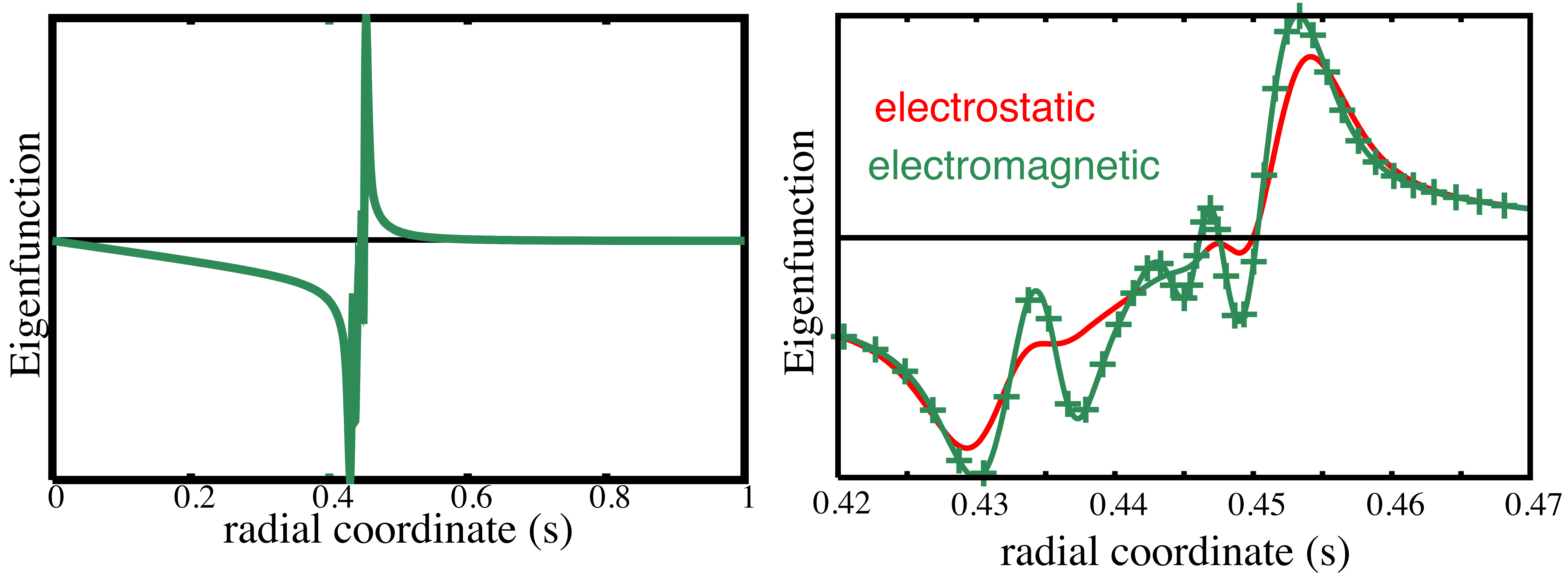

Singularity of the MHD operator is resolved by fourth order terms

deviations due to KAW coupling 'break Alfvénic state' [Walén 1944, Chen&Zonca RMP 2016]

experimental measurements of KAWs in Tokamaks (I)

experimentally confirmed: TCA [Weisen, PRL 1989]

antenna excitation - imaging interferometer array probing ñ

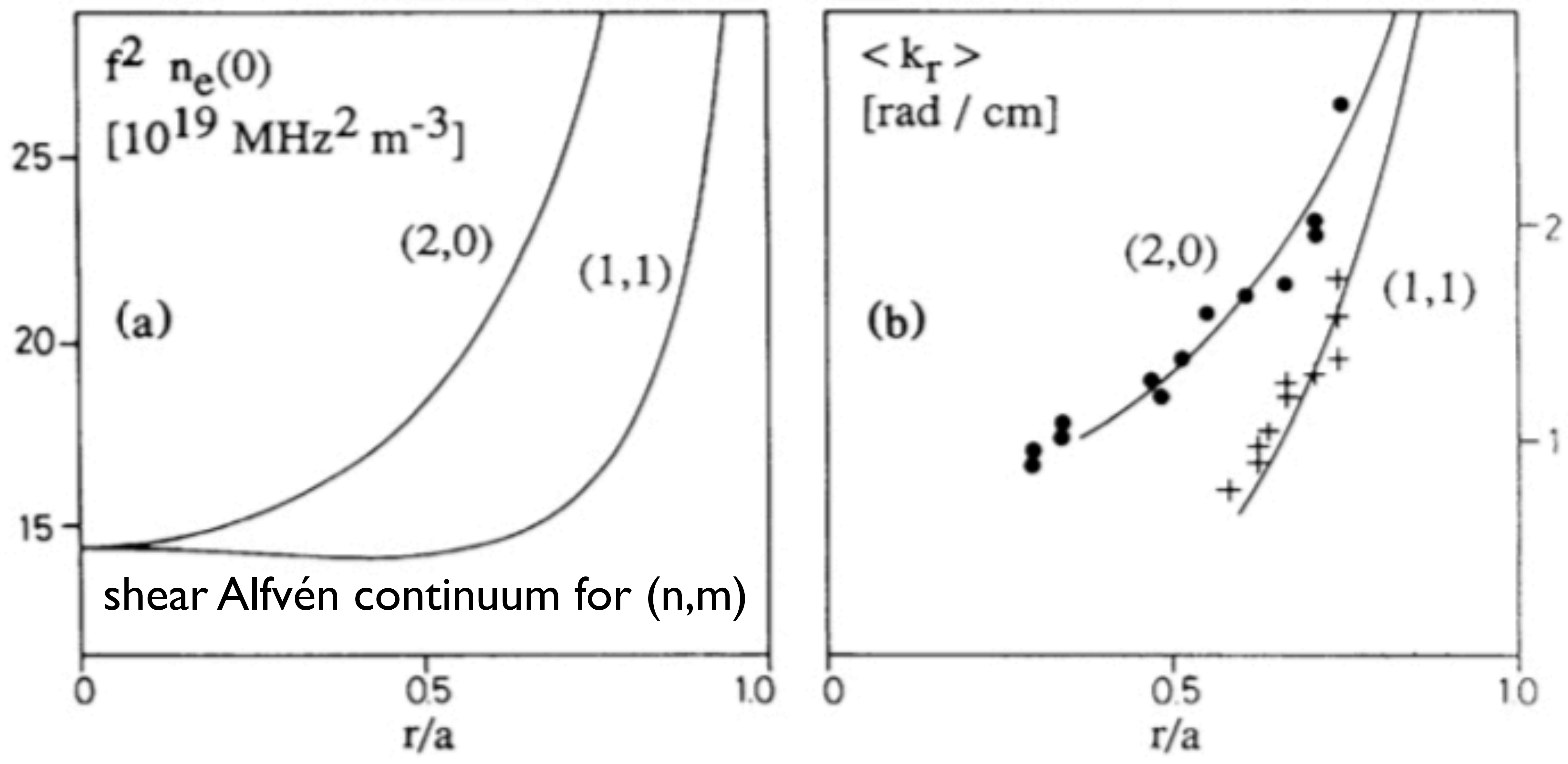

FIG. 1. (a) Resonance position as a function of frequency and central density for modeled mass density and current profiles. (b) Mean radial wave number as a function of position (averaged over one cycle of propagation). The solid lines are obtained from the KAW dispersion relation.

toroidal Alfvén eigenmodes (TAE)

[Cheng, Chen & Chance Ann. Phys.1985, Cheng & Chance 1986 Phys. Fluids 29]

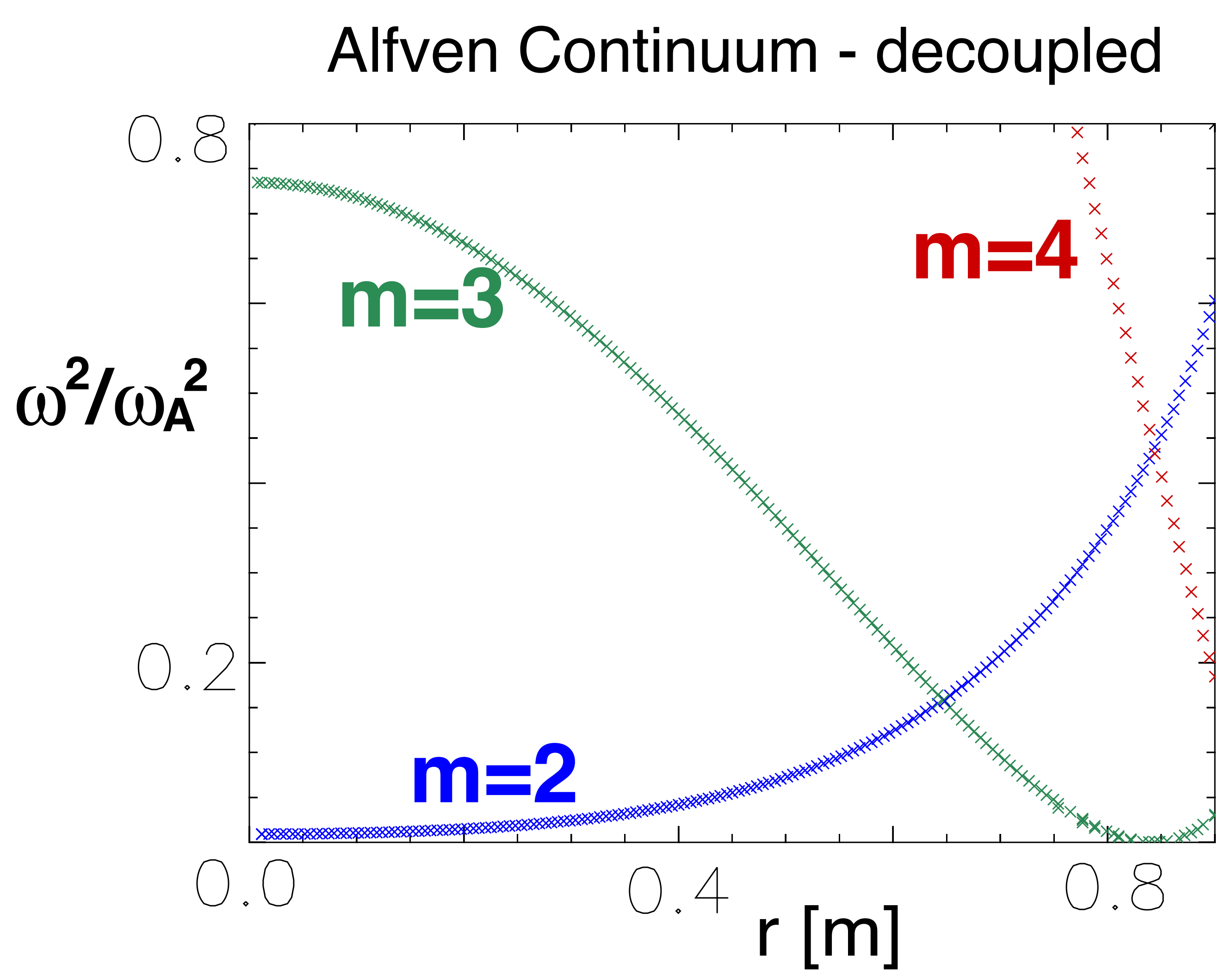

(n=2)

$\Rightarrow$

$$R \approx R_0(1+\epsilon\cos\theta)$$

$$B \approx B_0(1-\epsilon\cos\theta)$$

$$\epsilon = r/R_0$$

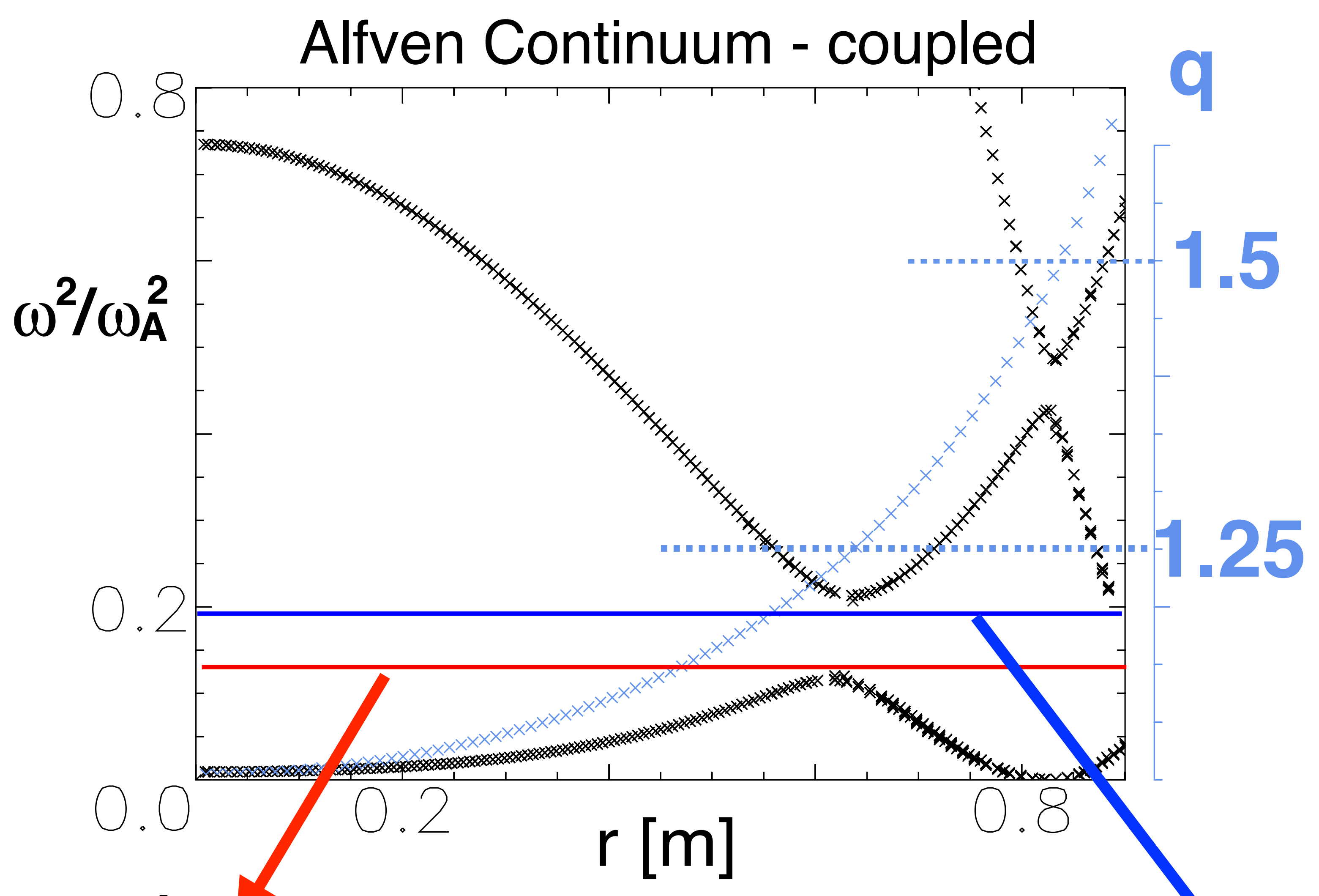

TAE: even mode

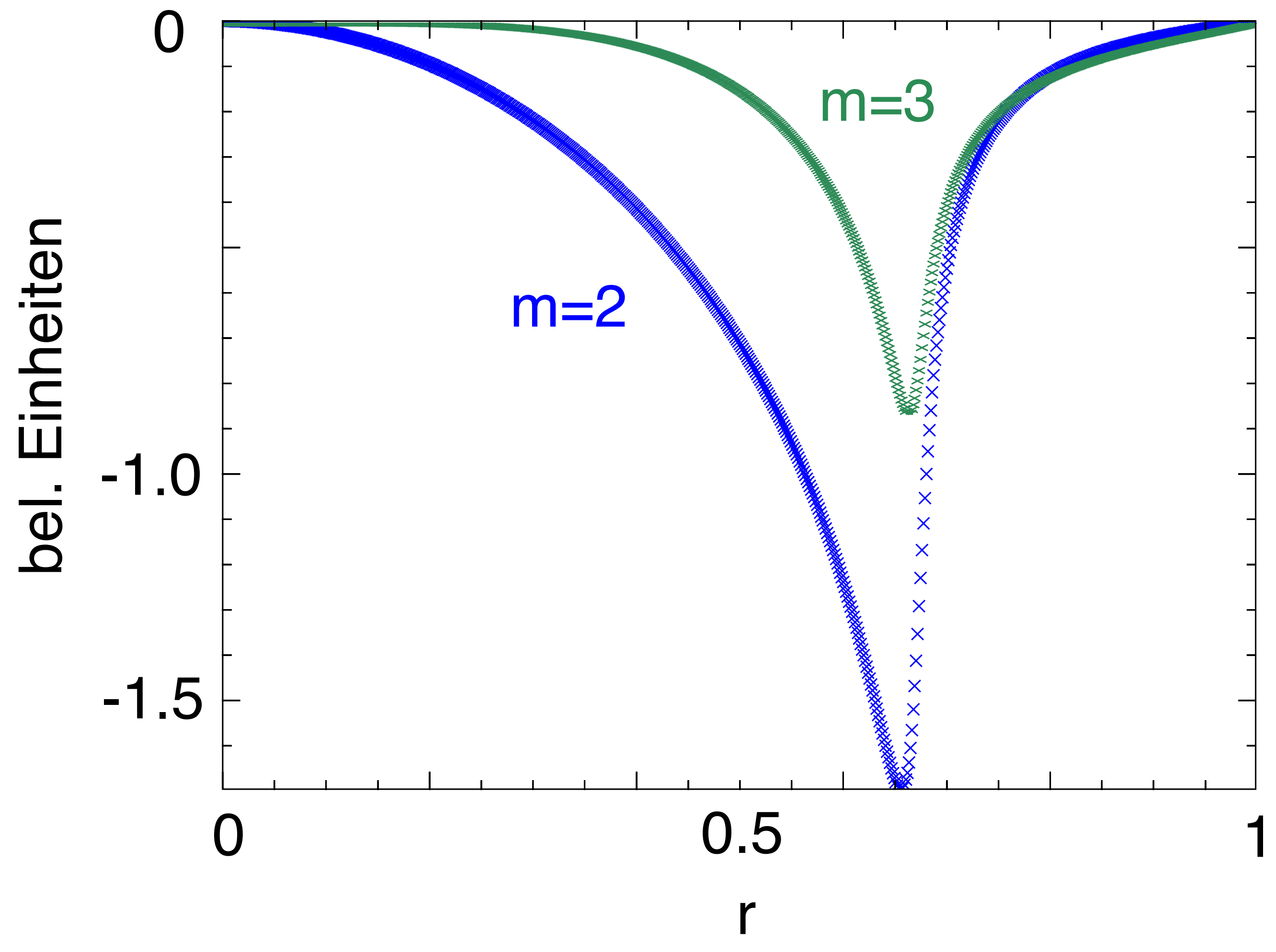

niedrigere Frequenz

TAE: odd mode

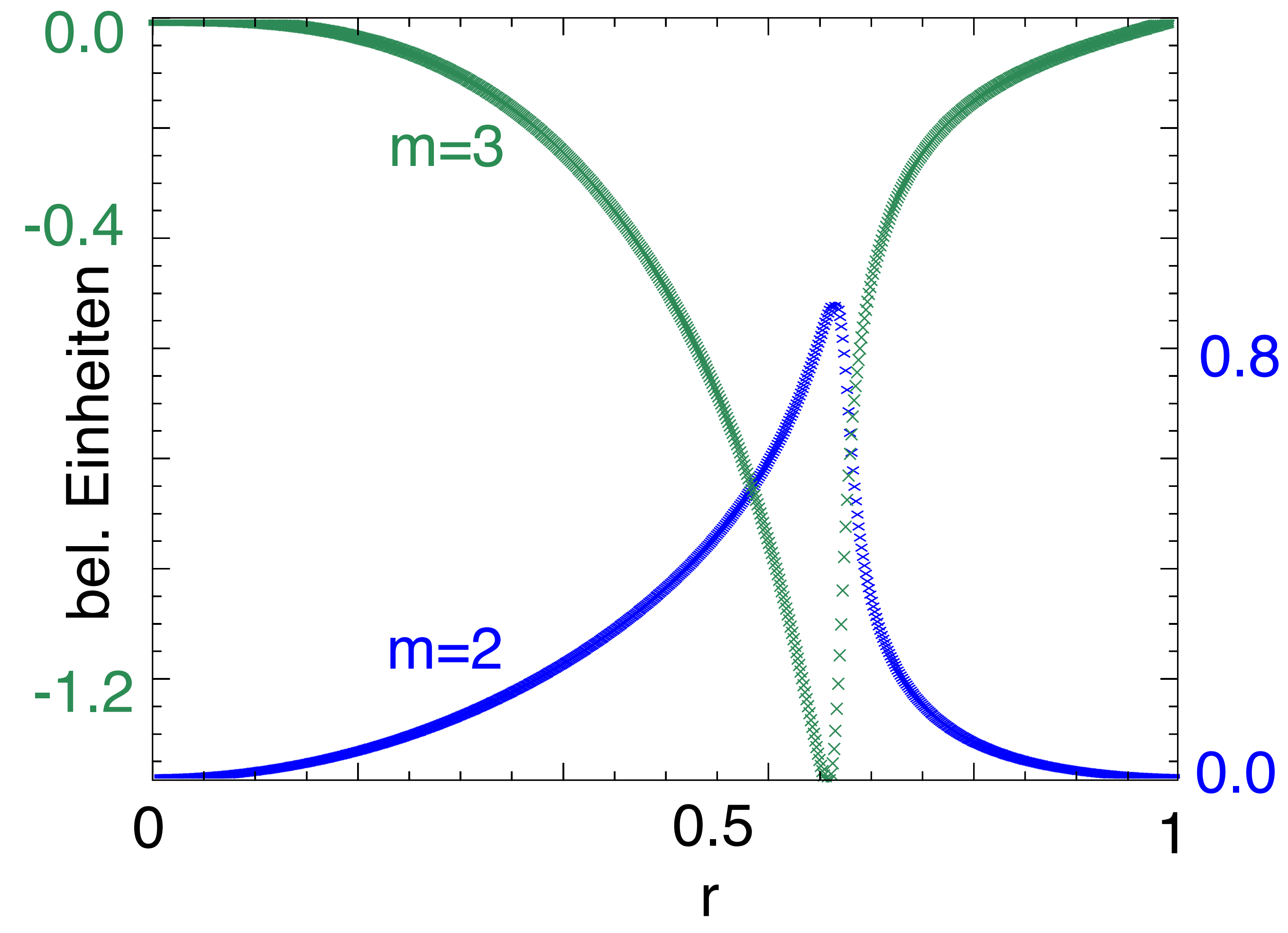

höhere Frequenz

analogous to electron bands in solid state physics

$q_{TAE}=(m+1/2)/n$

symmetry-breaking induces more gaps

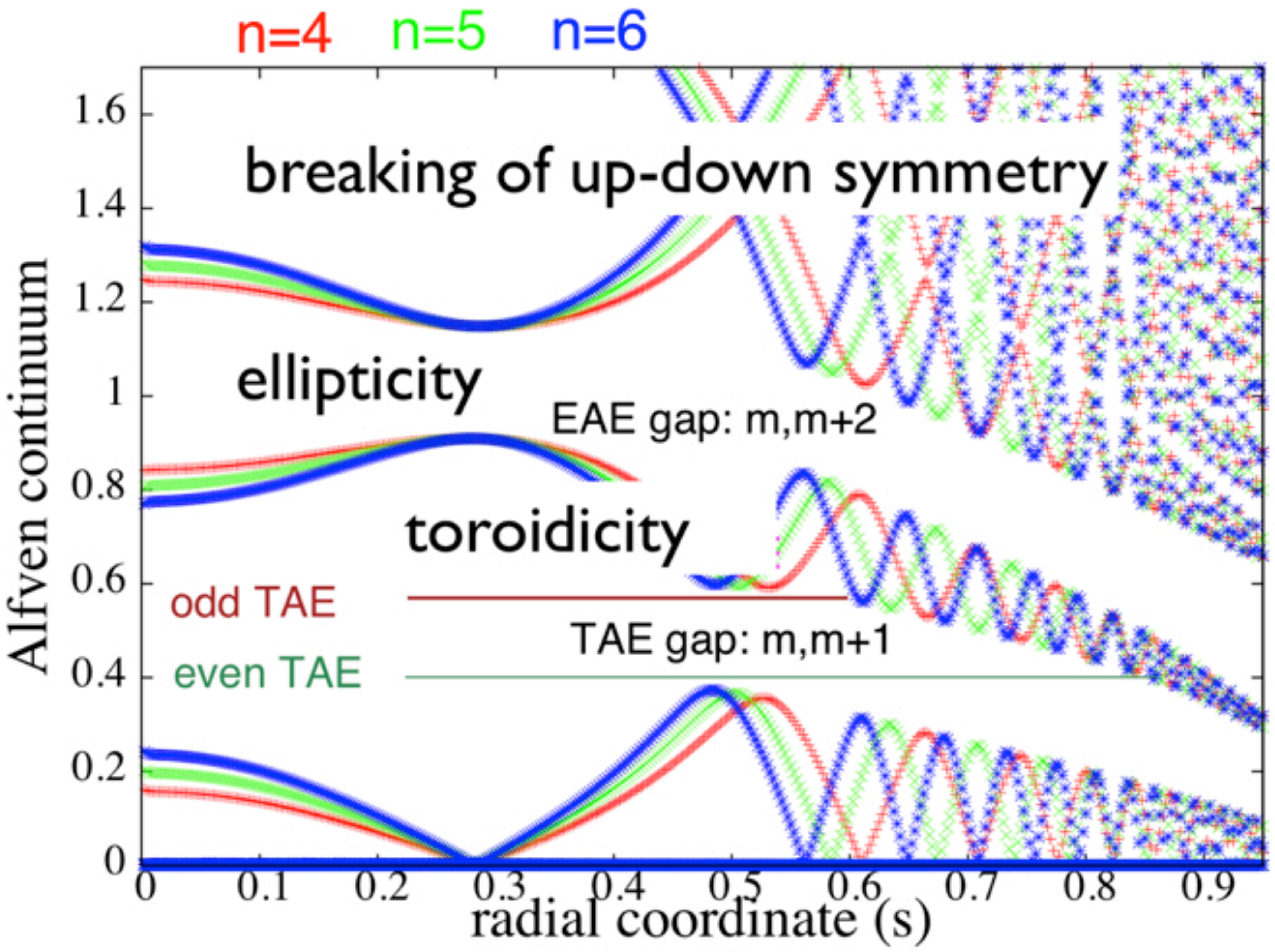

ASDEX Upgrade Alfvén continuum

AUG: magnetic perturbations

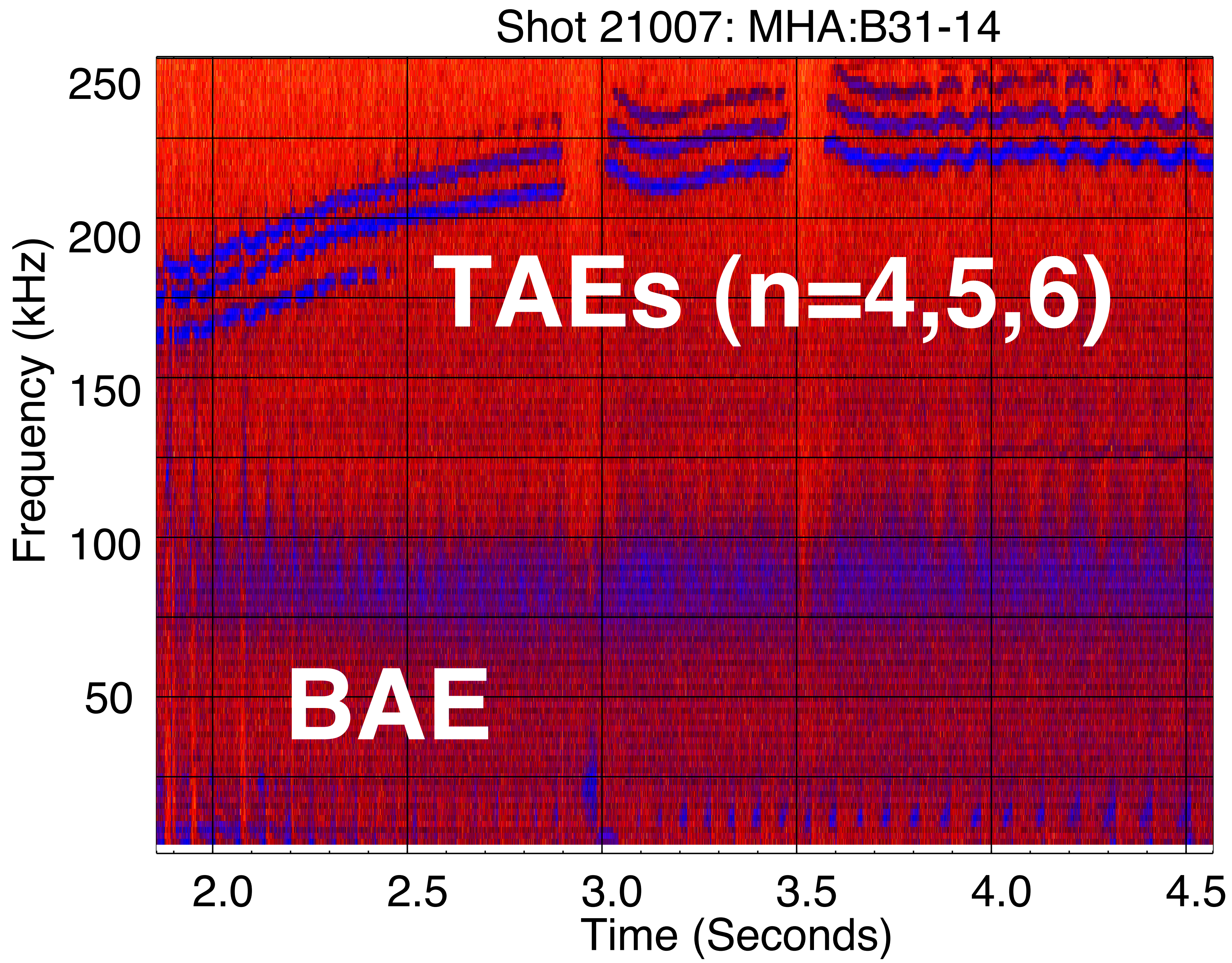

radiative damping: cross-scale coupling of global shear Alfvén waves and KAWs

radiative damping: kinetic Alfven waves 'tunnels' into TAE

[Mett, Mahajan, 1992
Berk 1993, Candy & Rosenbluth 1994, Breizman& Sharapov 1995,…]

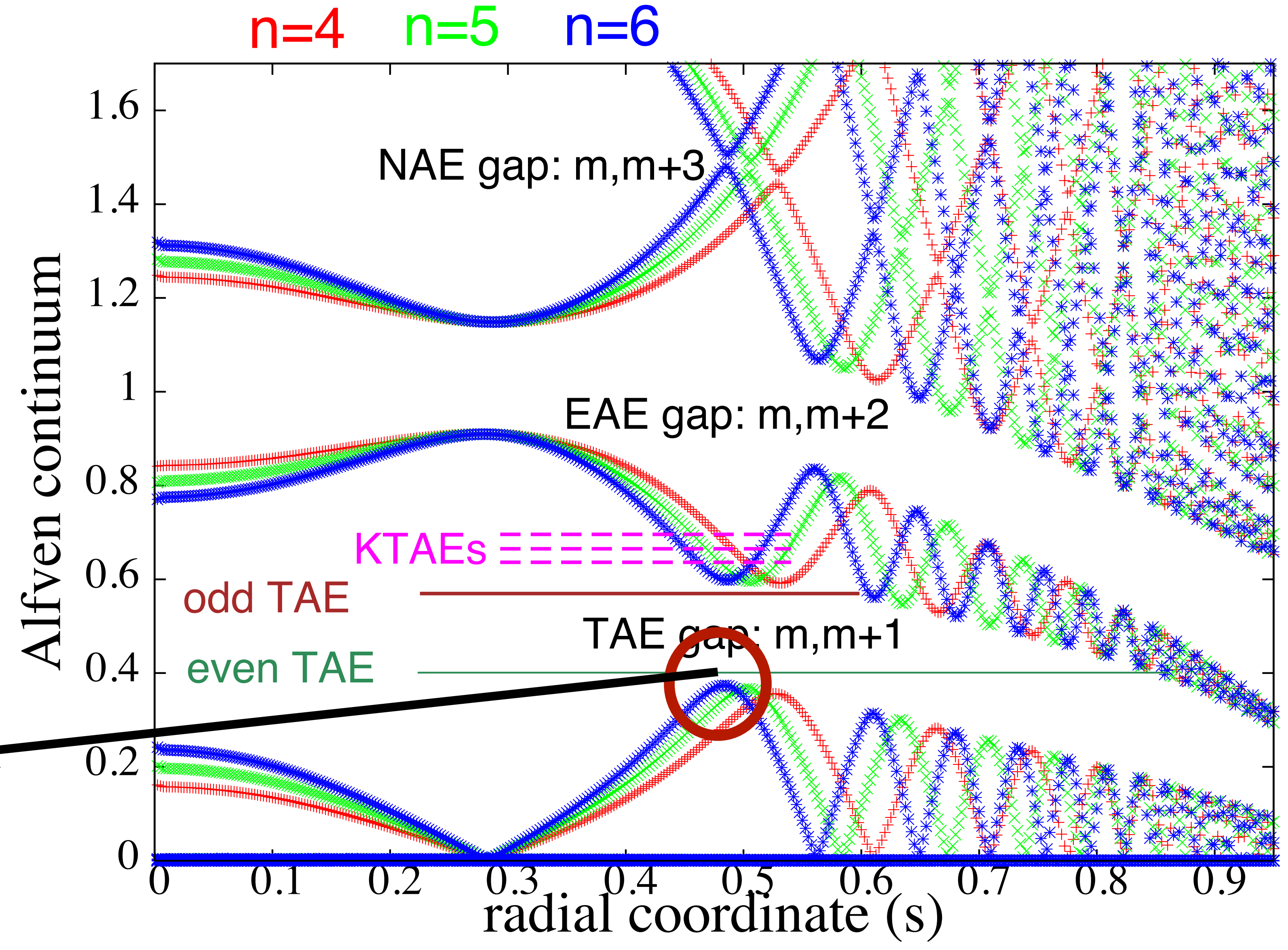

ASDEX Upgrade Alfvén continuum

coupling strength determined by non-ideal parameter:

$$\lambda \equiv 4 \frac{\rho_i}{r_m} \frac{mS}{\varepsilon^{3/2}} \left(\frac{3}{4} + \frac{T_e}{T_i} \right)^{1/2}$$

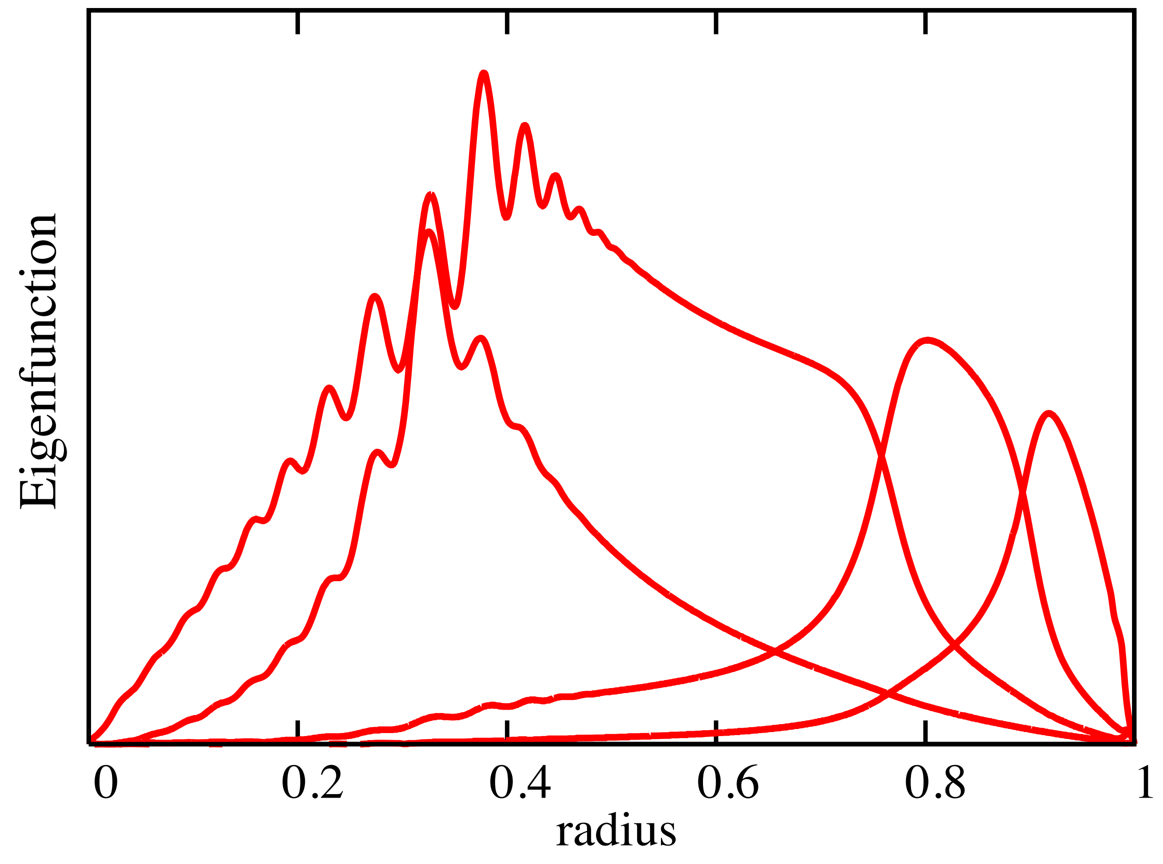

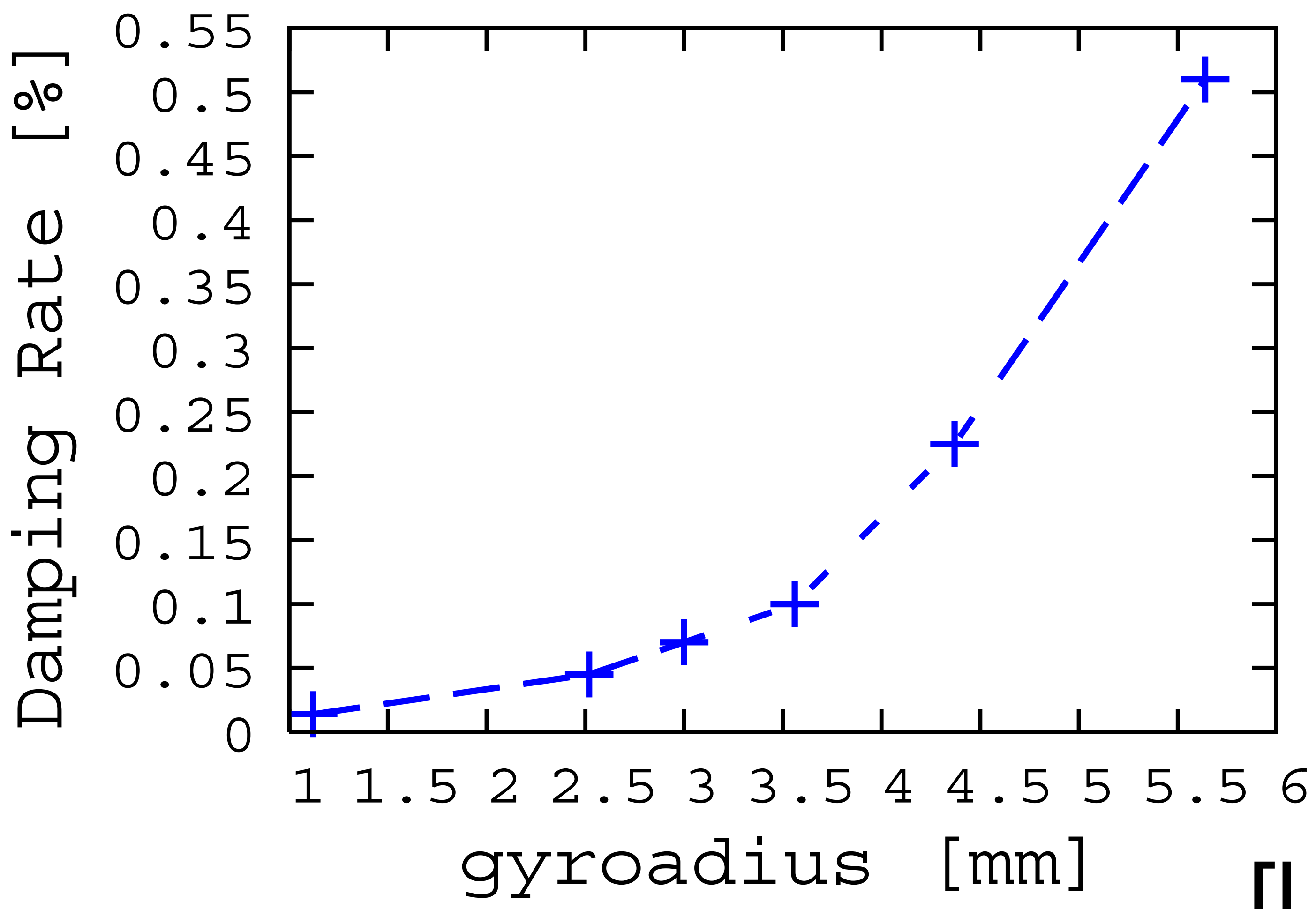

[Lauber, PoP 2005]

non-local continuum damping

[F. Zonca et al PRL 1992, Rosenbluth et al 1992, Berk et al 1992]

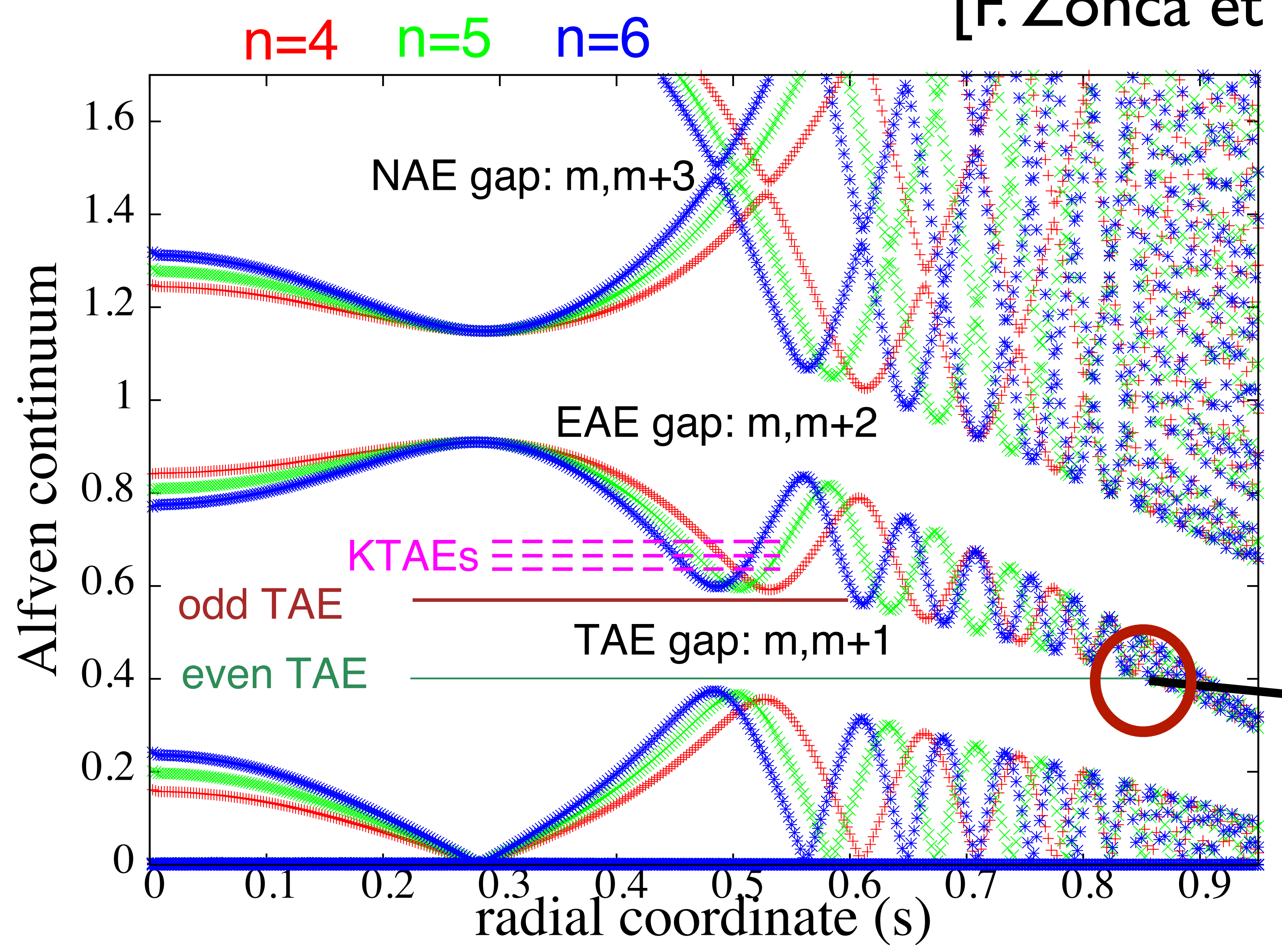

ASDEX Upgrade Alfvén continuum

continuum damping: mode conversion to kinetic Alfven wave

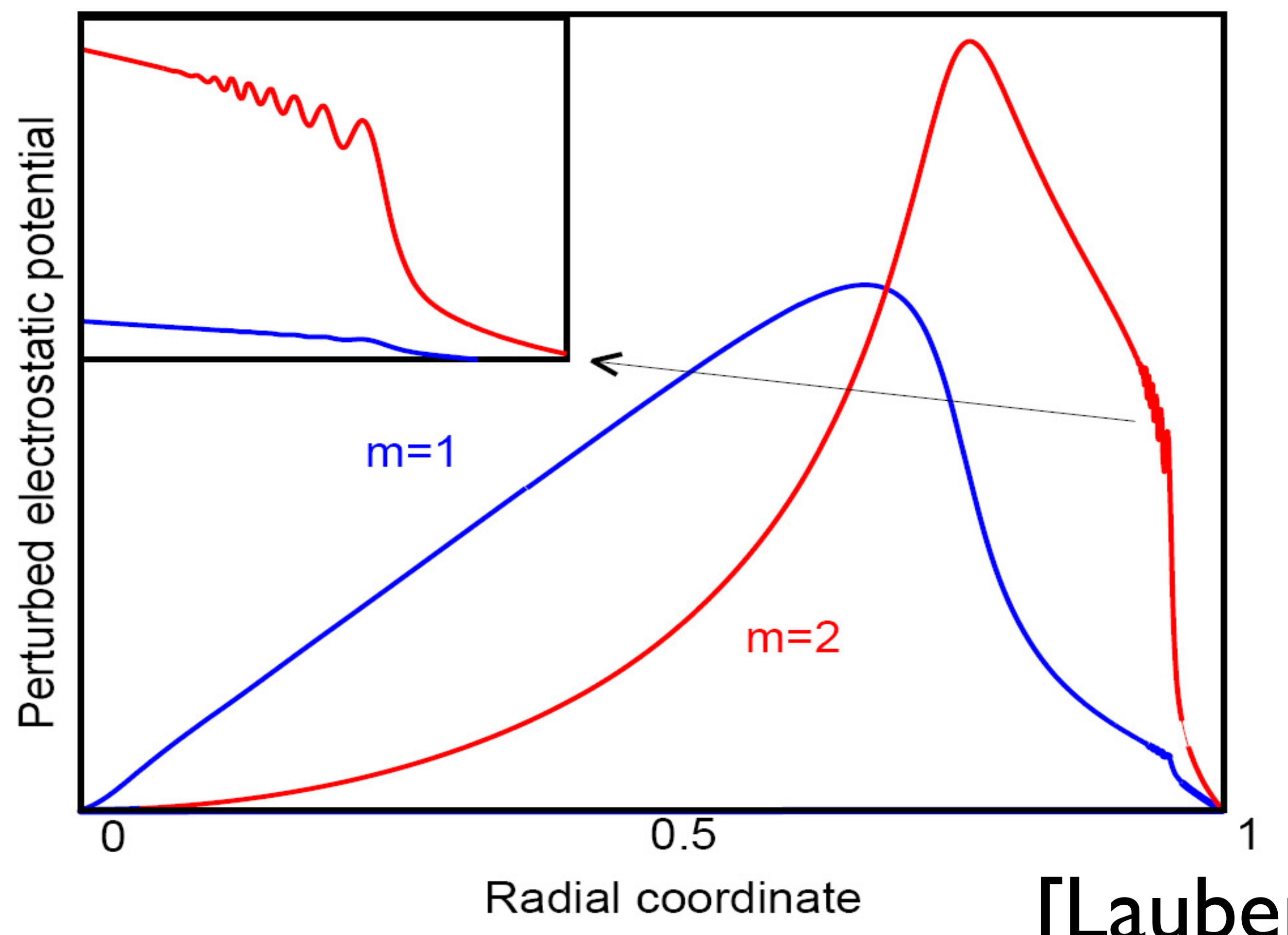

[Lauber,2005]

TFTR: [Wong, Phys. Lett A, 1996]

global mode driven by EPs - short wave-length structure detected at intersection points with continuum

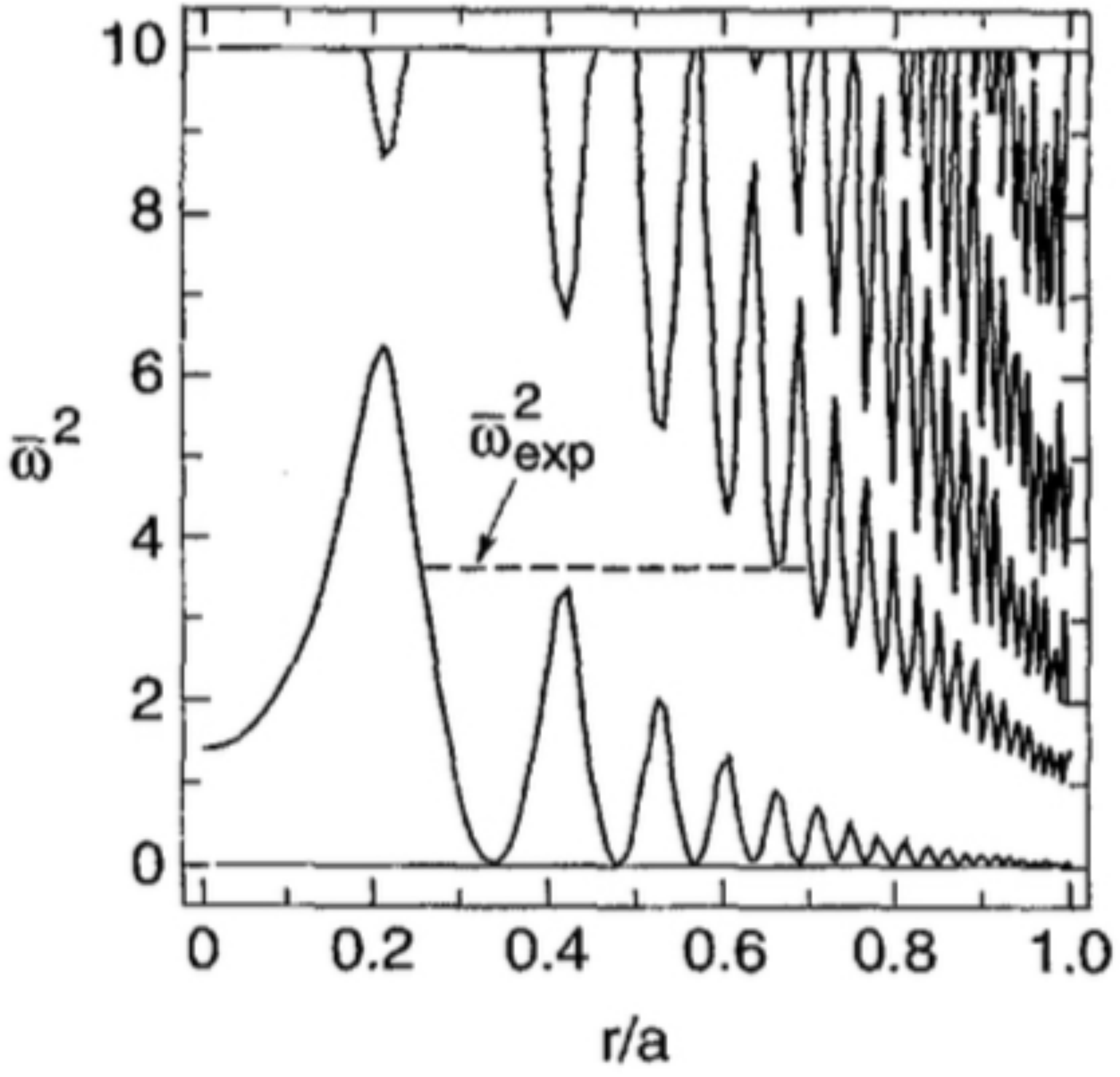

microwave scattering

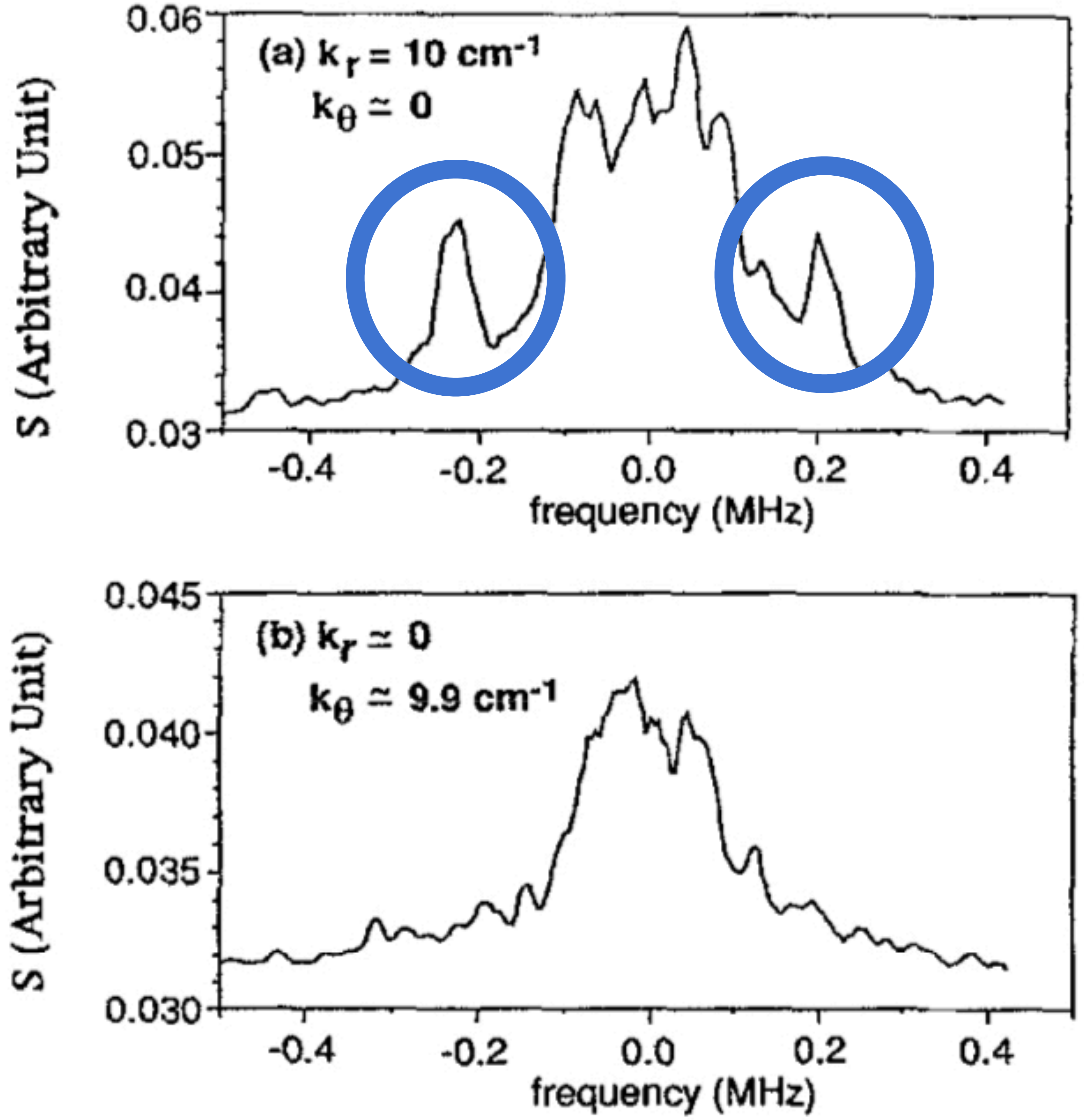

great confirmation of theory - demonstrating non-local nature of KAW physics

global, linear GK model, multi-species, general 2D geometry

LIGKA [Qin 1998, Lauber 2003, JPC 2007, Lauber PLREP 2013, Bierwage&Lauber 2017, Lauber JPCS 2018]

https://git.iter.org/projects/STAB/repos/ligka/

- gyrokinetic moment equation (GKM):

shear Alfvén law

$$-\frac{\partial}{\partial t}\left[\nabla\cdot\frac{1}{v_A^2}\nabla_\perp\phi\right]+\boldsymbol{B}\cdot\nabla\frac{\nabla\times(\nabla\times(\frac{\nabla\psi}{i\omega})_\parallel\boldsymbol{b})}{B}+(\boldsymbol{b}\times\nabla(\frac{\nabla\psi}{i\omega})_\parallel\boldsymbol{b})\cdot\nabla\frac{\mu_0 j_\parallel}{B}$$

$$=-\sum_a\mu_0\int \mathrm{d}^2v\, e_a\left\{\boldsymbol{v}_\mathrm{d}\cdot\nabla J_0 f\right\}_a+\sum_a\left[\boldsymbol{b}\times\nabla\left(\frac{\beta_{a\perp}}{2\Omega_a}\right)\right]\cdot\nabla\nabla_\perp^2\phi$$

$$+\sum_a\frac{3v_{th,a}^2}{8v_A^2\Omega_a^2}\nabla_\perp^4\frac{\partial\phi}{\partial t}+\boldsymbol{B}\cdot\nabla\frac{1}{B}\sum_a\frac{\beta_a}{4}\nabla_\perp^2(\frac{\nabla\psi}{i\omega})_\parallel\boldsymbol{b}$$

'pressure' tensor - curvature drift coupling

reduced MHD as limit

- quasi neutrality (QN):

$$0=\sum_a e_a\int \mathrm{d}^2v\left\{J_0 f\right\}_a+\nabla_\perp\cdot\frac{m_\mathrm{i}n_\mathrm{i}\nabla_\perp\phi}{B^2}$$

- non-adiabatic response for perturbed distribution function:

propagator → resonance

$$\hat{h}\ =\ ie\sum_m\int_{-\infty}^{t}dt'e^{i\left[n(\varphi'-\varphi)-m(\theta'-\theta)-\omega(t'-t)\right]}e^{-im\theta}$$

$$\frac{\partial F_0}{\partial E}\left[\omega-\hat{\omega}_*\right]J_0^2(k_\perp\varrho_i)\left[\phi_m(r')-(1-\frac{\omega_d(r',\theta')}{\omega})\psi_m(r')\right]$$

free energy

resonances (circ/trapped):

$\omega_{AE}-\omega_{prec}-(nq-m+k)\cdot\omega_t=0$

$\omega_{AE}-\omega_{prec}-k\cdot\omega_b=0$

for all species , including electrons and energetic particles

LIGKA: linear GK model, multi-species, general 2D geometry

equations are solved in different limits and approximations, sharing same infrastructure:

- local, analytical estimates
- local reduced MHD - shear Alfvén spectra
- local kinetic (w/o numerical coefficients, i.e. orbits given by GC code) [Zonca 1996, Lauber 2009]
- local kinetic with FLR/FOW (w/o numerical coefficients) [Zonca 1998,Lauber JPC 2018]

- global reduced MHD - global eigenfunction
- global kinetic (w/o numerical coefficients): 2 solvers
- global kinetic track mode (w/o numerical coefficients)

- typically modes are called in sequence - to large part automated (workflow, IMAS format)

- toolbox ready for the use in various transport models: Eurofusion 'ATEP' Enabling research project [Lauber, Falessi et al 2021]

[V.-A. Popa, master thesis TUM 2020]

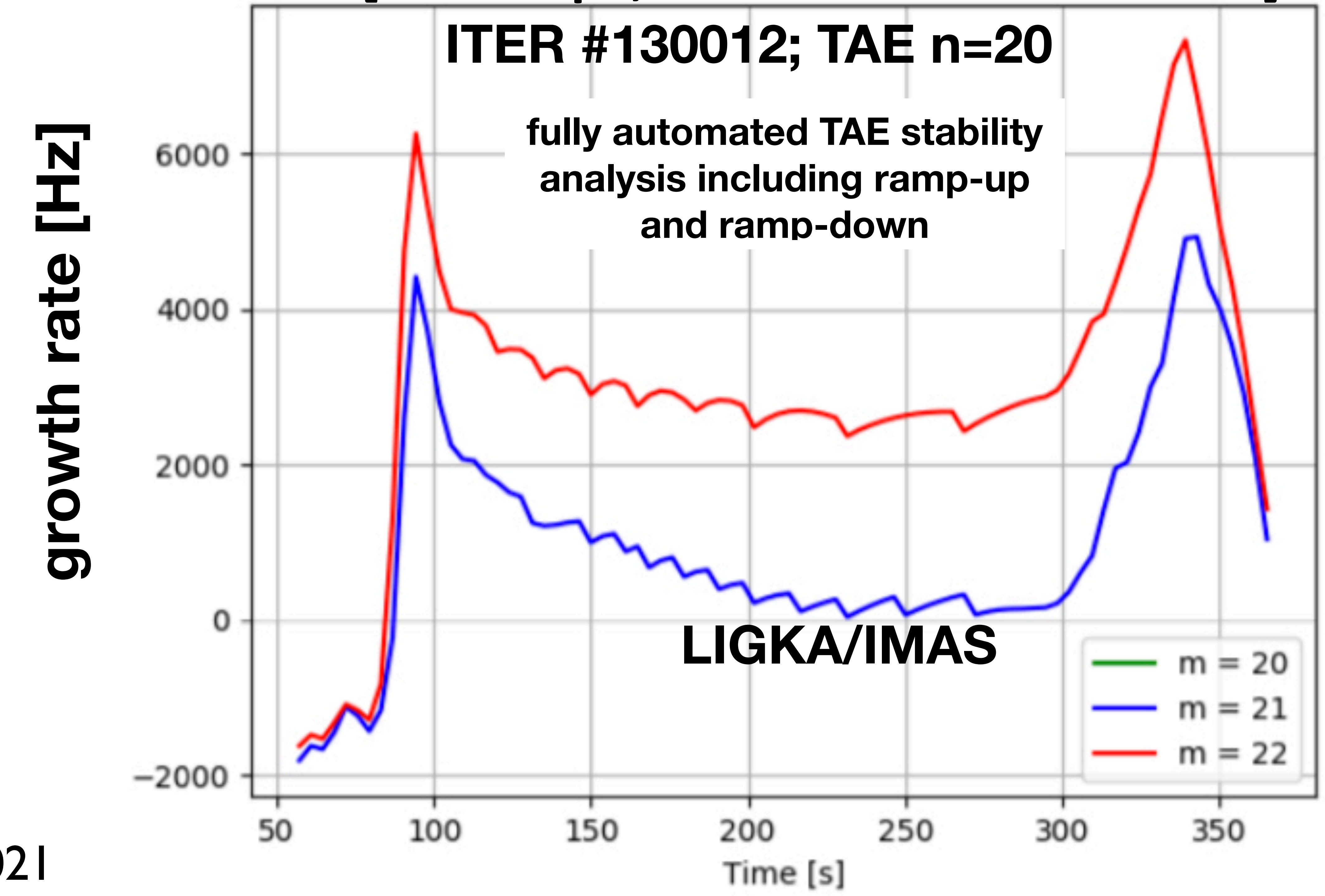

the role of kinetic Alfvén waves (KAWs) in Tokamaks: JET

JET TAE antenna

[Fasoli, Testa, Panis, Puglia, Tinguely,… 1995-2021]

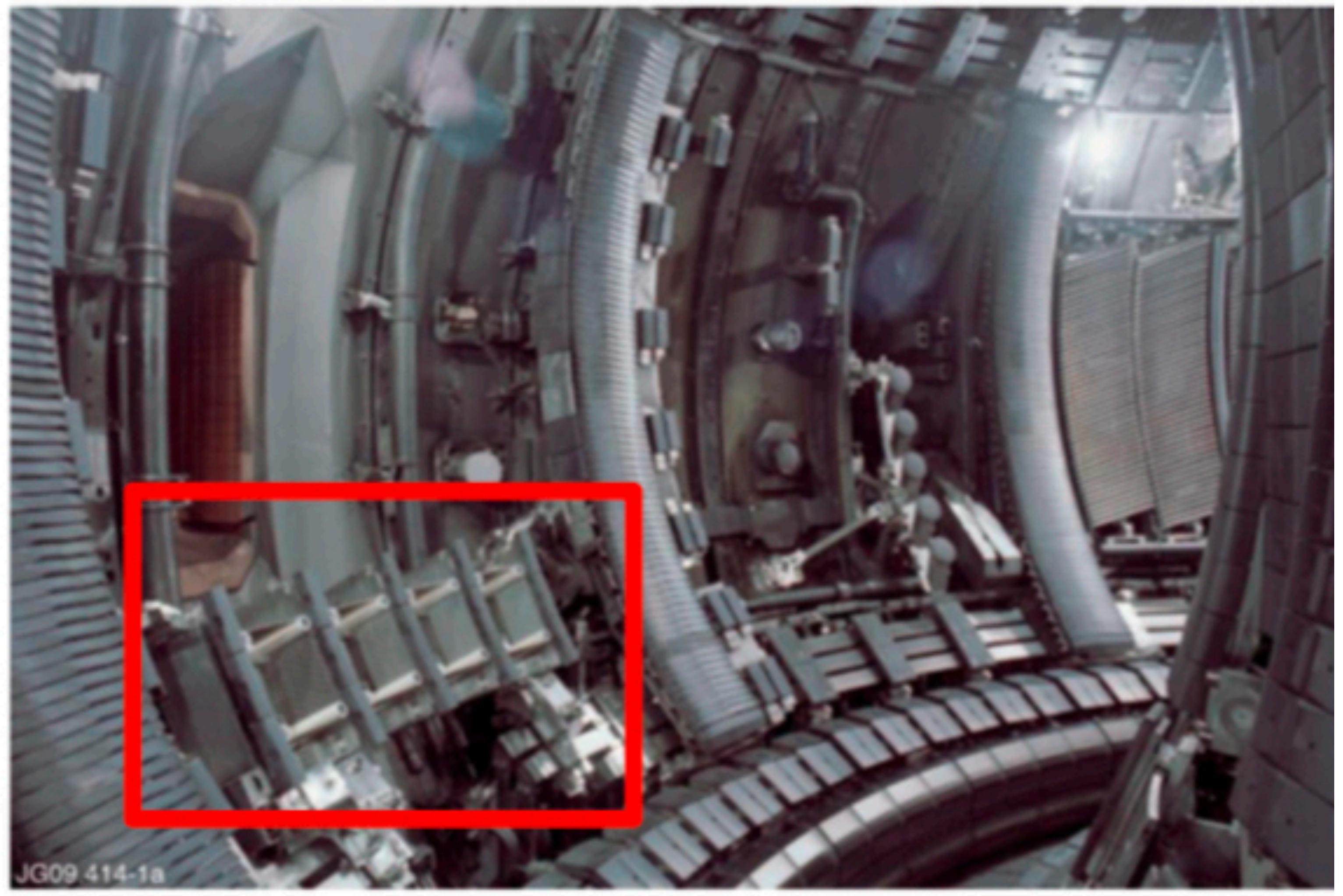

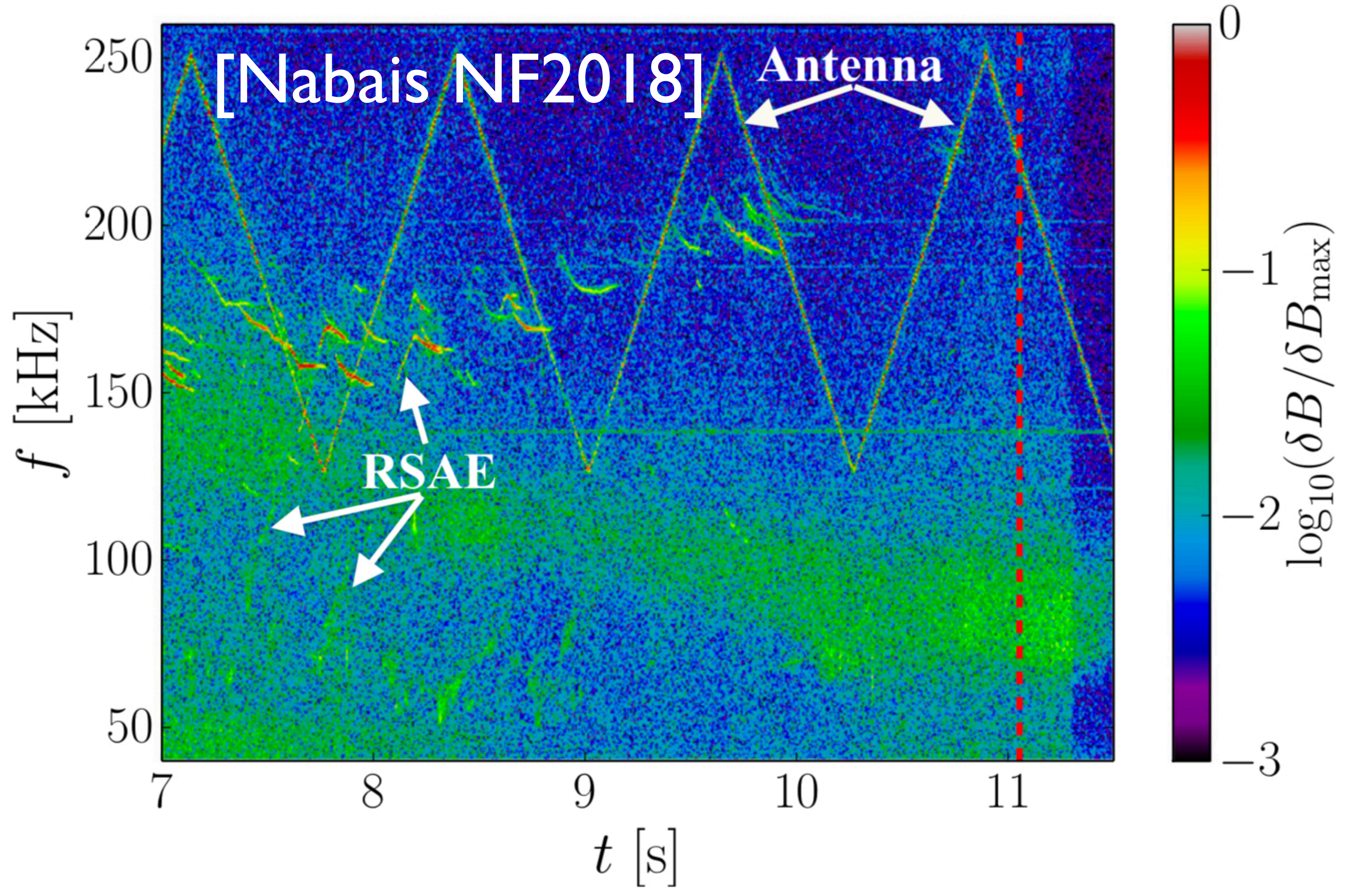

Tinguely IAEA FEC 2021

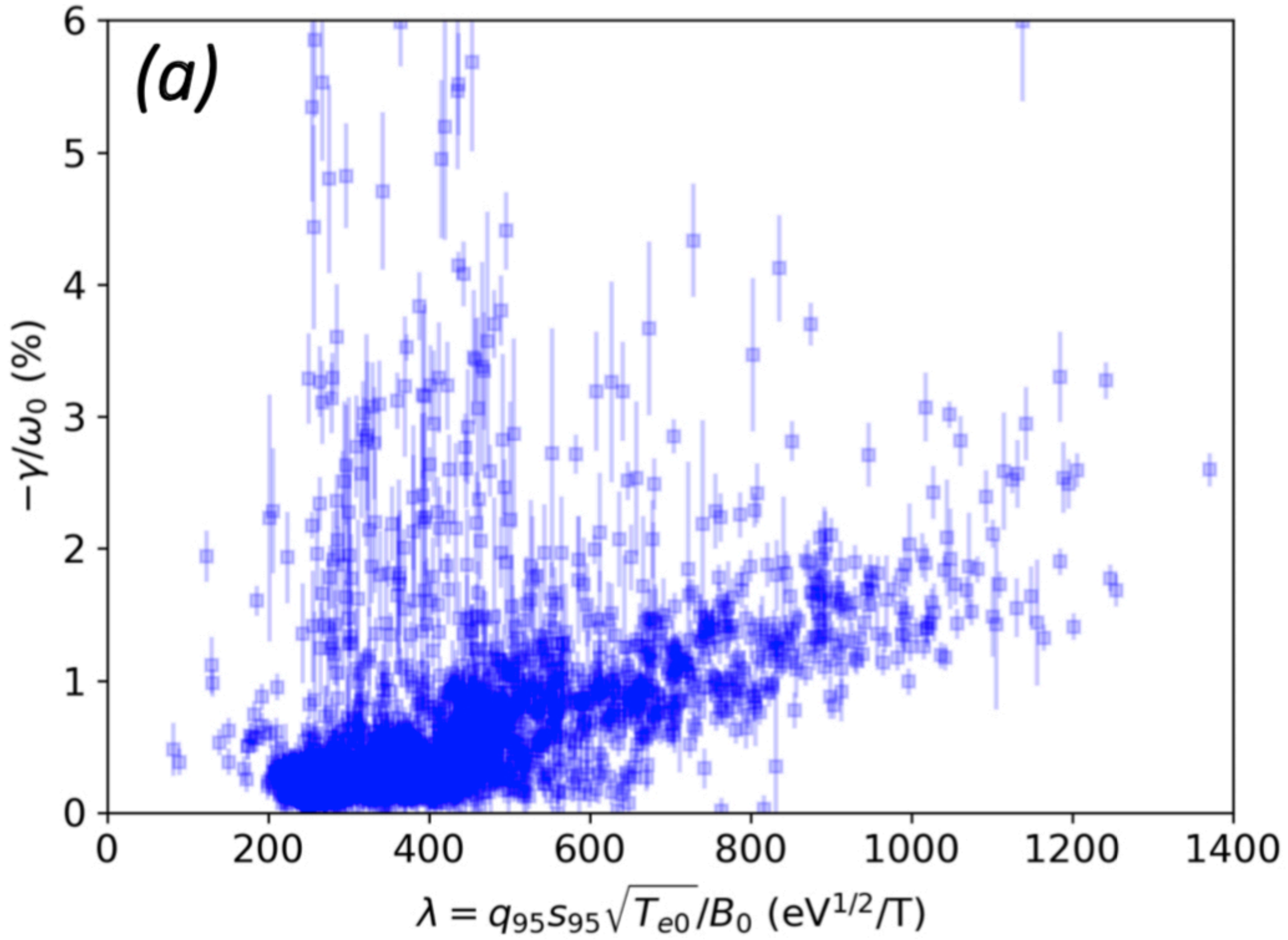

- probe plasma at typical AE frequencies and measure plasma response - determination of damping rate
- if gap is open, clear correlation with non-ideal parameter is found
- indication that KAW physics is very prominent in JET AE physics, as confirmed by ITPA EP effort [Lauber et al 2010] in 2010, and resistive MHD model [Nabais, NF 2018]

JET TAE damping

[ITPA group, Lauber et al IAEA FEC 2010]

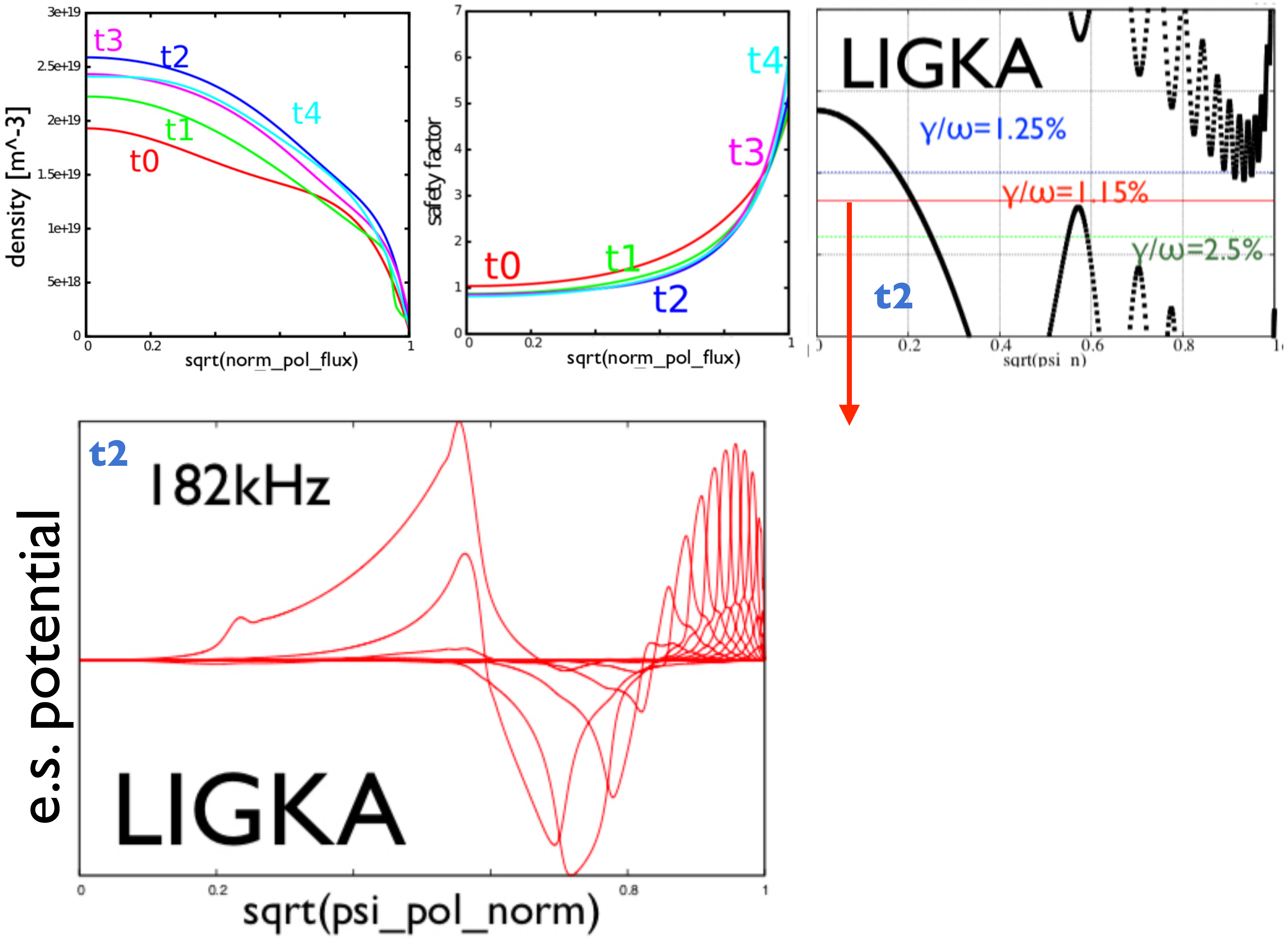

- 'far'continumm intersection, small ion LD
- radiative damping dominates - core and edge contribution global nature of TAE
- experiment: 1.5%

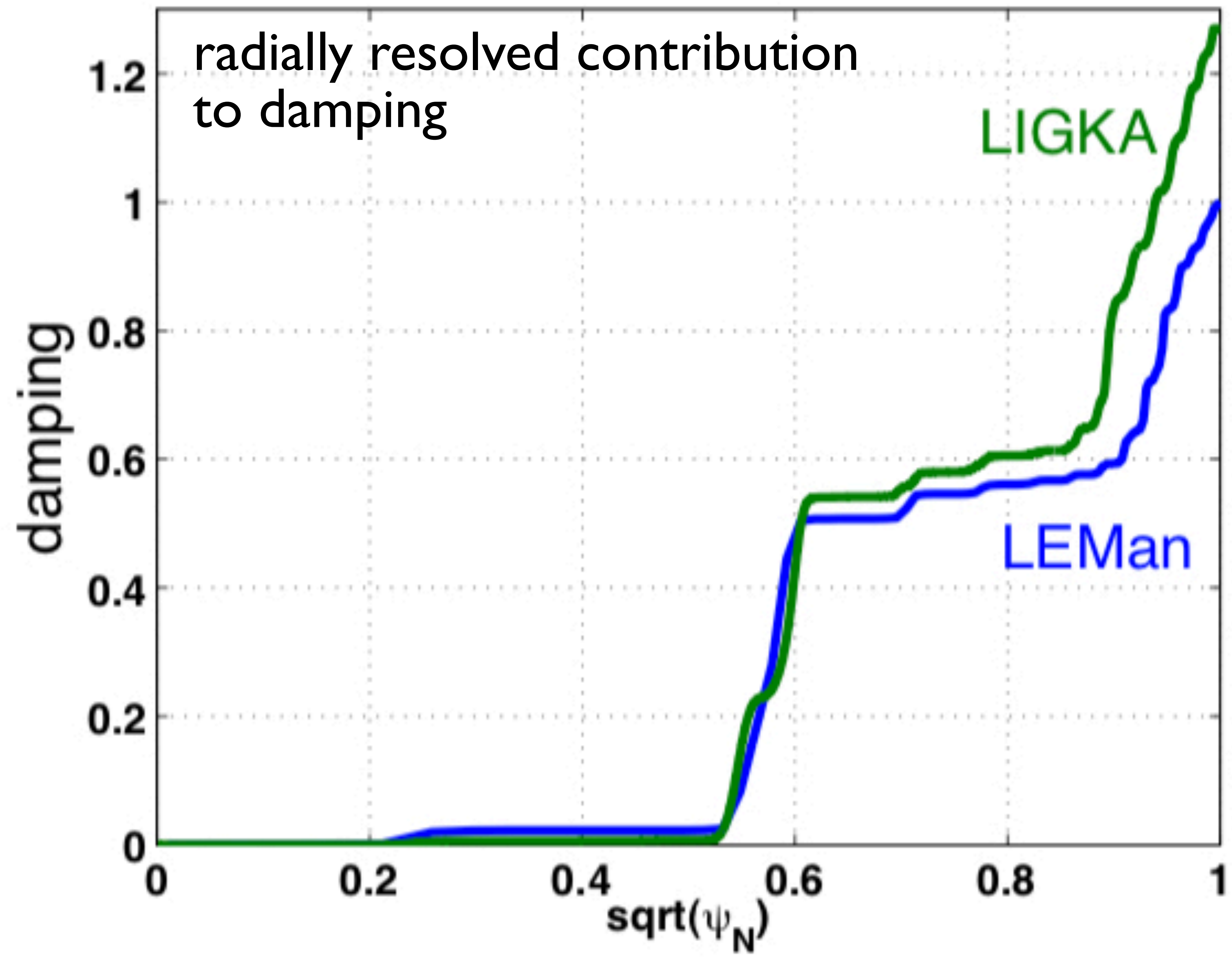

vicinity to continuum (s≈0.5,s>0.9) correlates with locations of damping: concept of 'tunneling' [Mett, Mahajan]

successful code validation -capture trend of elongation scan

JET-like case: elevated q case as candidate for DT scenario

similar to [M Fitzgerald et al in prep 2021]

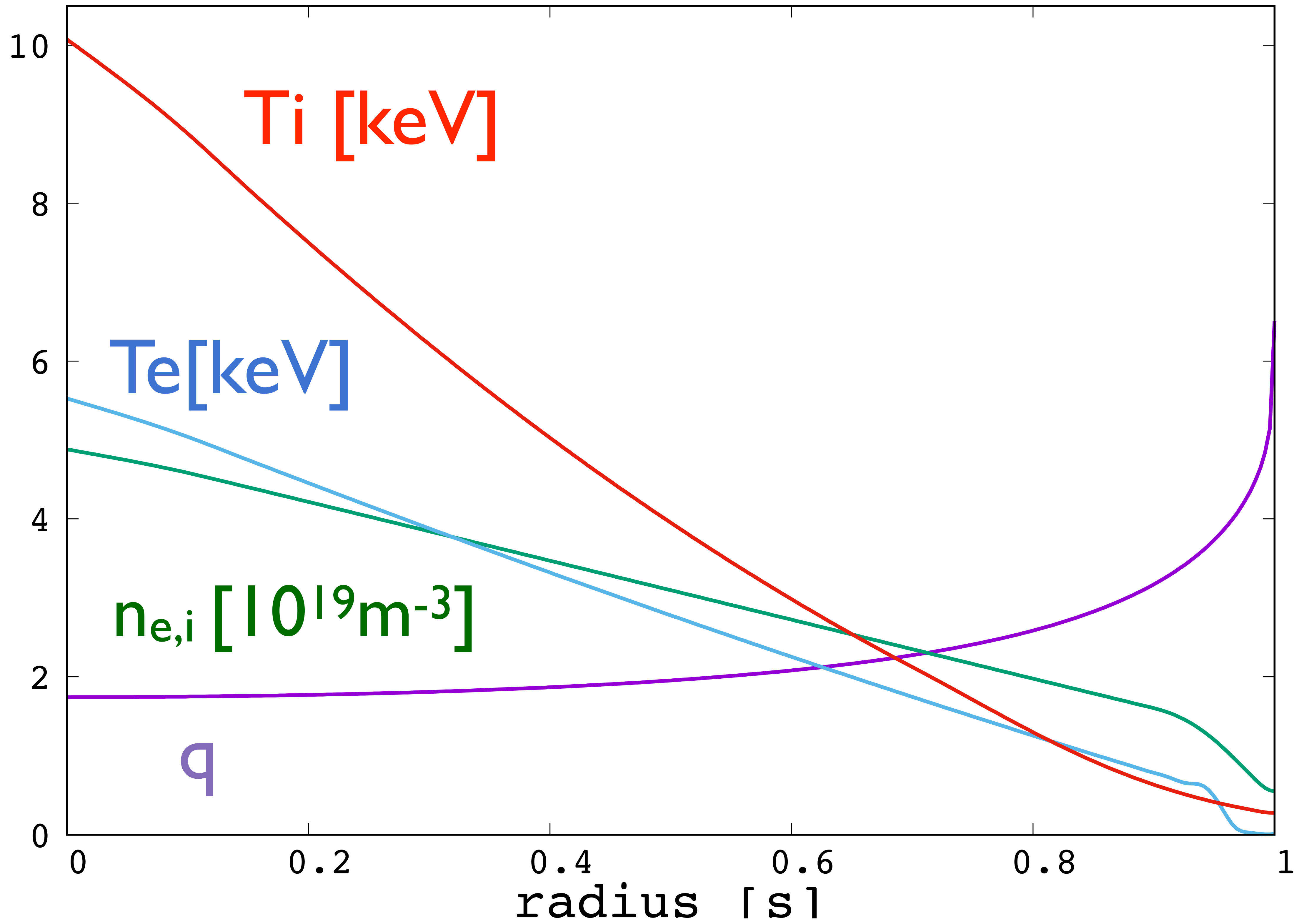

B0=3.4, R0=2.97m

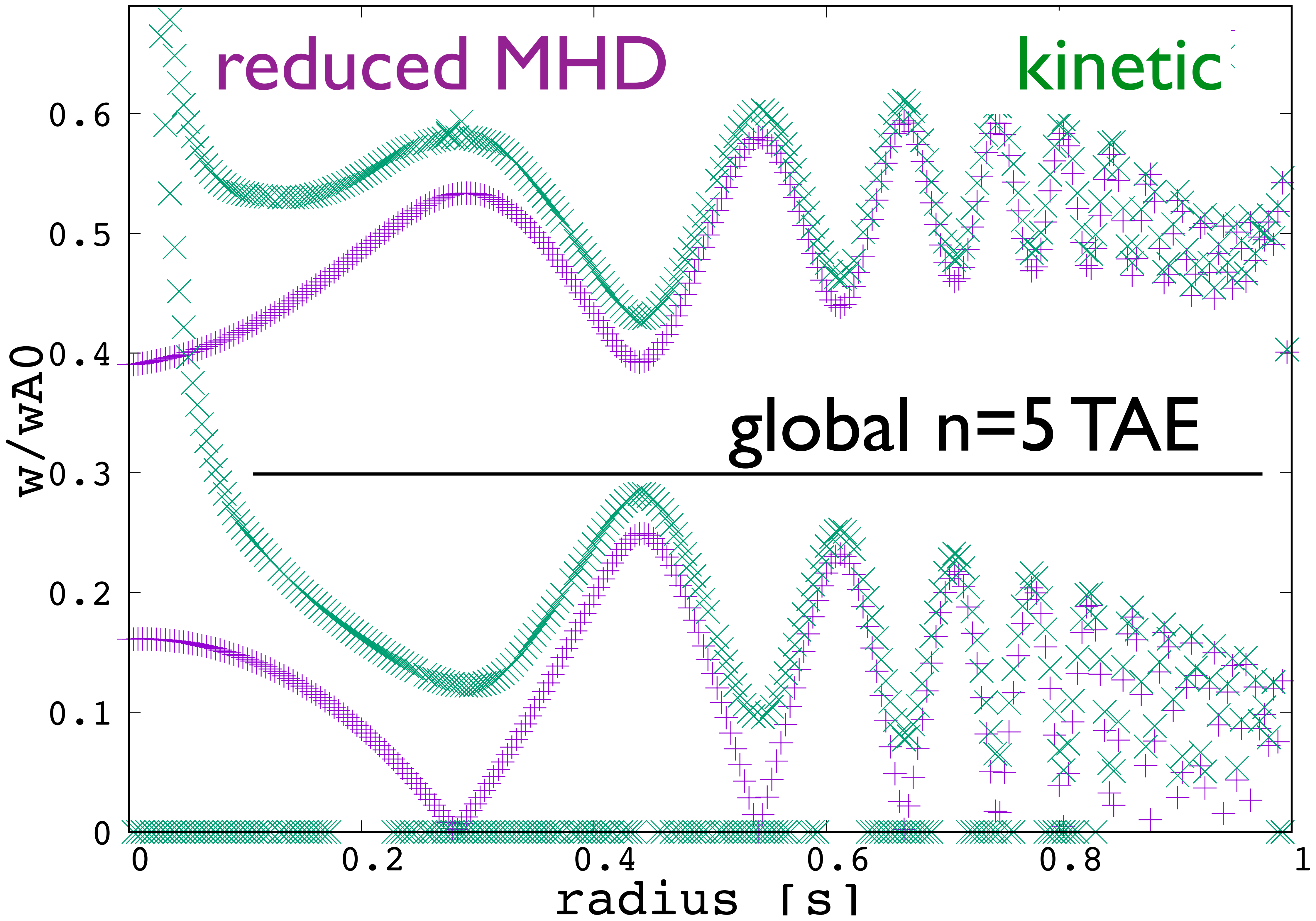

What is the role of KAWs for the damping of low-n TAEs?

analyse ion and electron contributions, structure of mode structures and $E_{//}$:

JET-like case: ion resonances

analyse damping:

- plot: use n=5,m=9 harmonic for evaluating resonance condition at TAE position in velocity space
- only higher order resonances e.g. k=4 reach Ti range (10keV)
- deuterium ions are too slow to efficiently interact with TAE
- consequence: **low thermal ion LD**
- neutral beam ions with energies between 30-80keV usually contribute to damping
- use afterglow phase without neutral beam ions to analyse α-driven modes

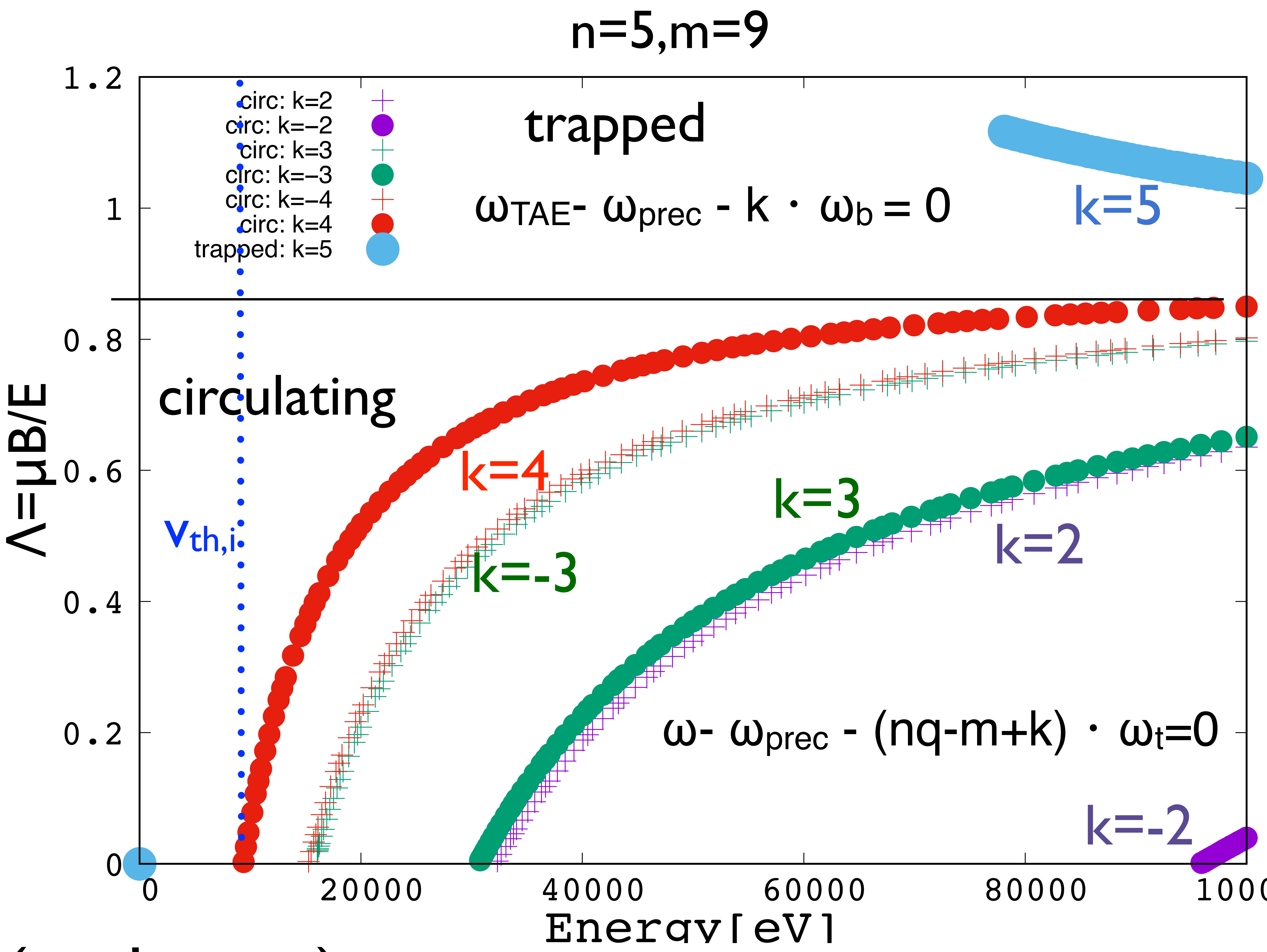

thermal ion LD damping: γ/ω = -0.16% (no electrons)

JET-like case: analysis of damping

adding step by step electron resonances:

no electron LD damping:

γ/ω = -0.16% (ion LD)

adding circulating k=0 resonance:

γ/ω = -0.67% (ion LD+circ el)

adding circulating k=±1 sidebands:

γ/ω = -0.77% (ion LD+circ el+sb)

adding trapped electrons:

γ/ω = -0.87% (ion LD+all el)

electron resonances for main TAE harmonic (n=5,m=9)

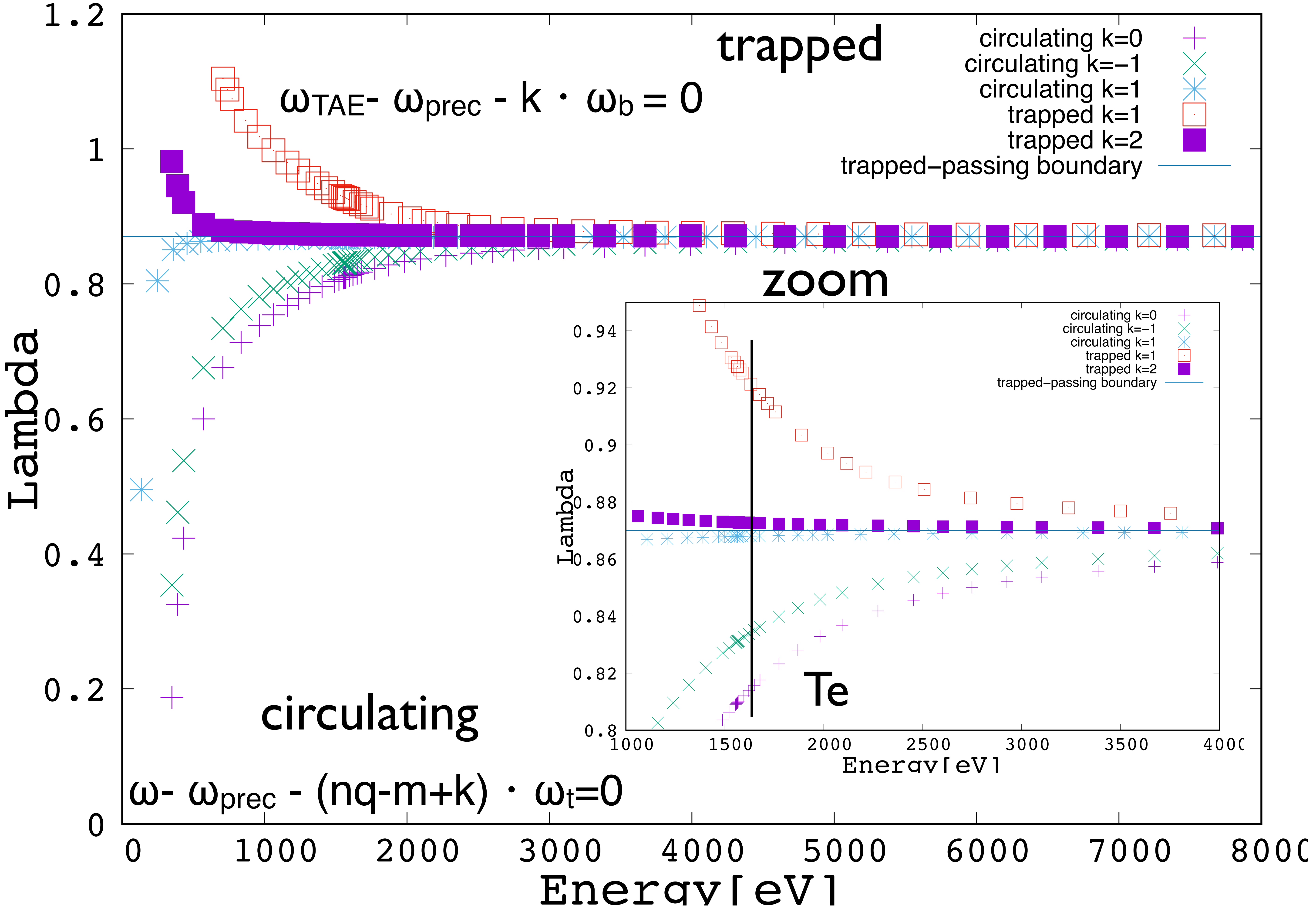

ratio el:ion: ~4:1 - non-perturbative, non strictly additive

JET-like case: analysis of mode structures

adding step by step electron resonances:
no electron LD damping:

γ/ω = -0.16% (ion LD)

adding circulating k=0 resonance:

γ/ω = -0.67% (ion LD+circ el)

adding circulating k=±1 sidebands:

γ/ω = -0.77% (ion LD+circ el+sb)

adding trapped electrons:

γ/ω = -0.87% (ion LD+all el)

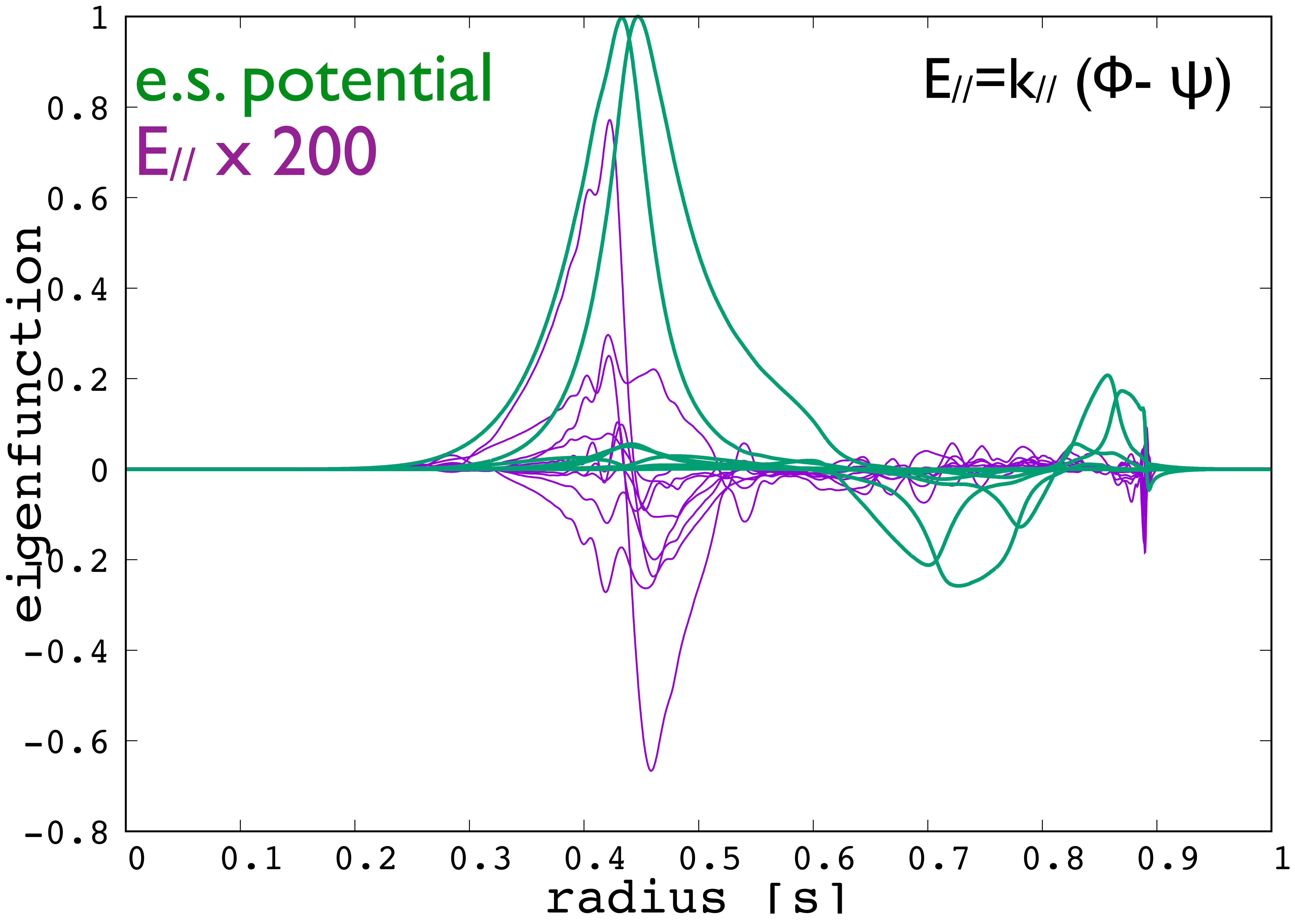

smooth structure - KAW coupling visible in E//
mode structure differs from MHD result - **non-perturbative**

JET-like case: analysis of mode structures

adding step by step electron resonances:
no electron LD damping:

γ/ω = -0.16% (ion LD)

adding circulating k=0 resonance:

γ/ω = -0.67% (ion LD+circ el)

adding circulating k=±1 sidebands:

γ/ω = -0.77% (ion LD+circ el+sb)

adding trapped electrons:

γ/ω = -0.87% (ion LD+all el)

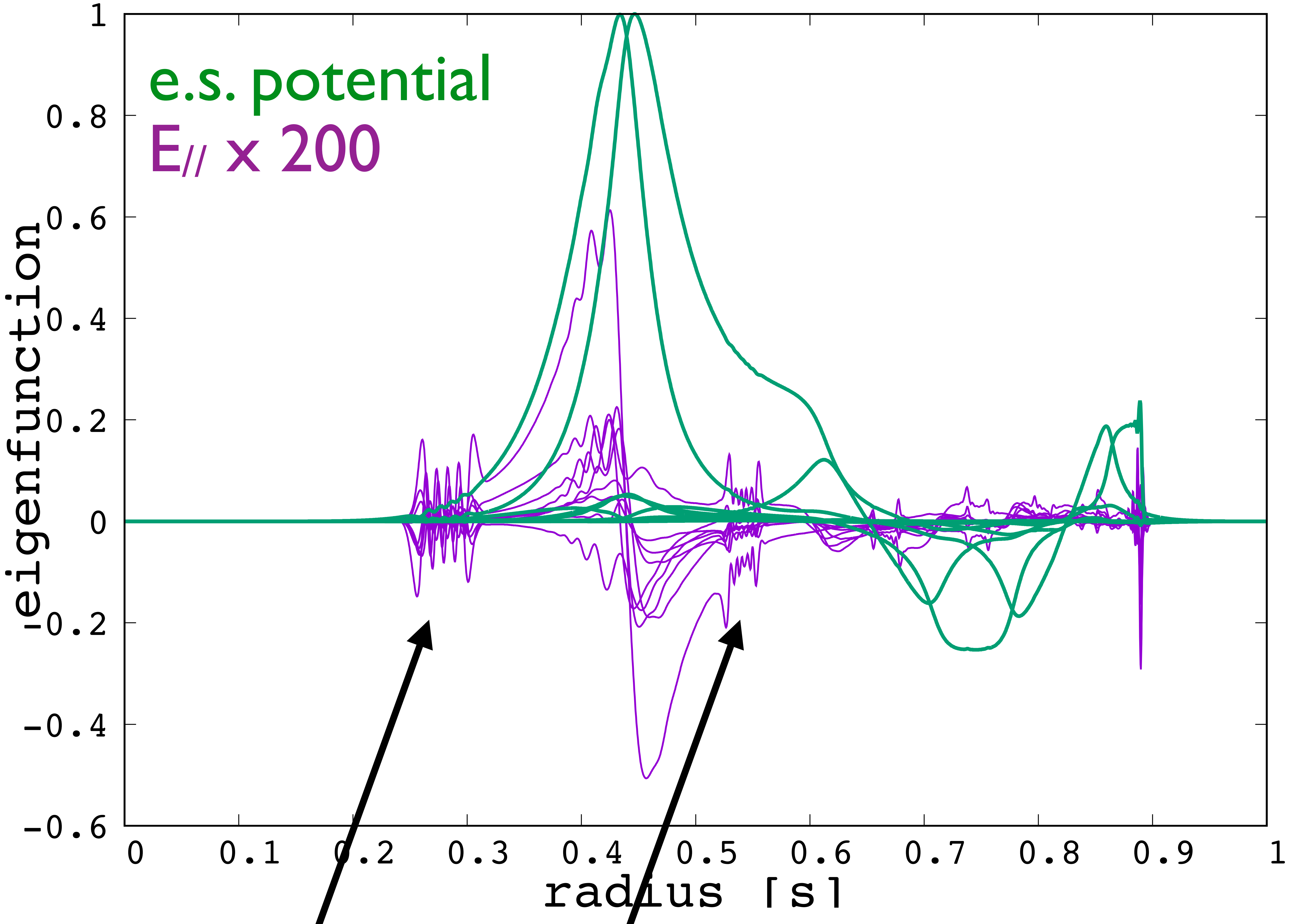

missing trapped electrons lead to weakly damped region close to k//=0

adding step by step electron resonances:
no electron LD damping:

γ/ω = -0.16% (ion LD)

adding circulating k=0 resonance:

γ/ω = -0.67% (ion LD+circ el)

adding circulating k=±1 sidebands:

γ/ω = -0.77% (ion LD+circ el+sb)

adding trapped electrons:

γ/ω = -0.87% (ion LD+all el)

Im[circ. el response coefficient]
Im[trapped el response coefficient]

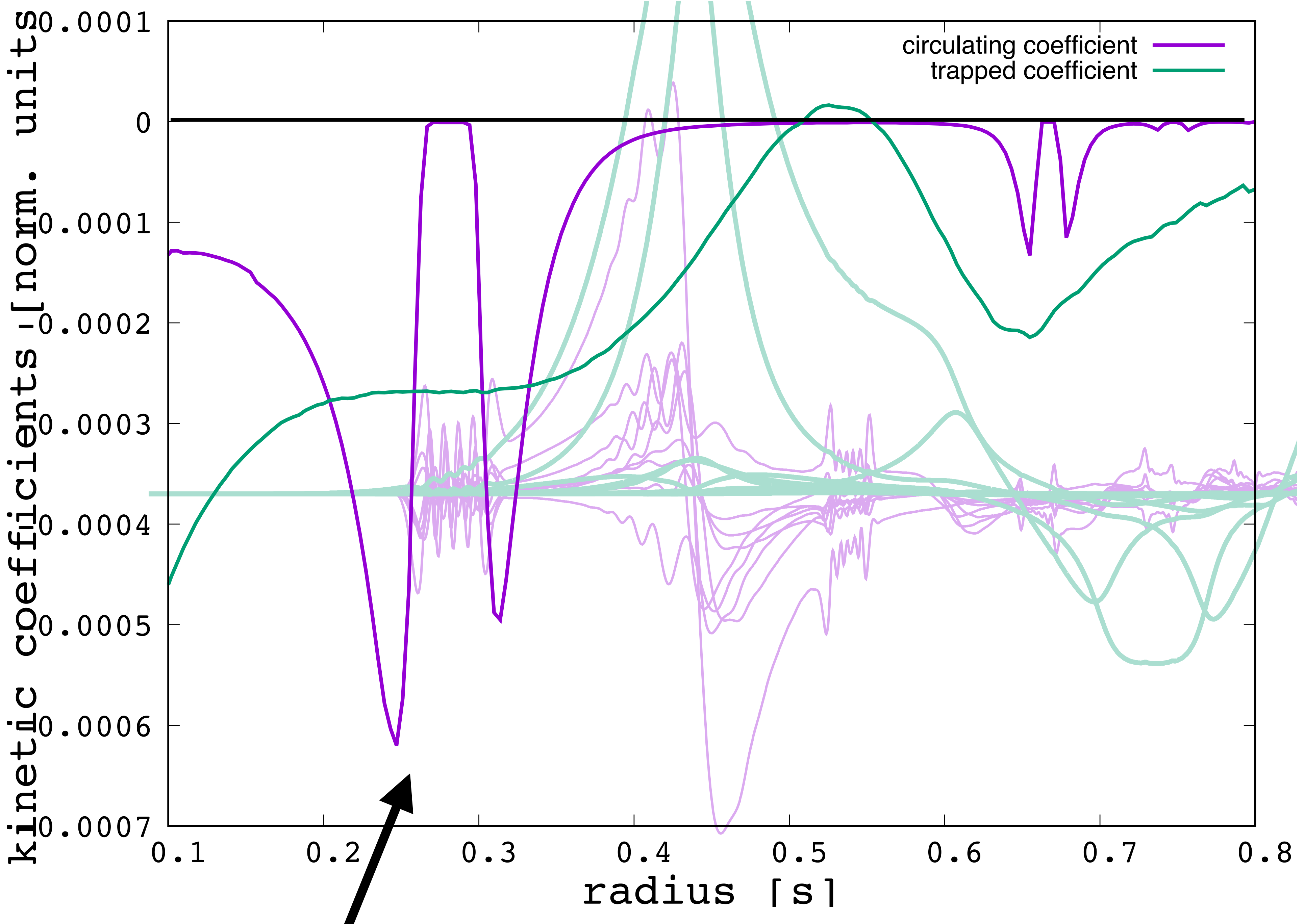

missing trapped electrons lead to weakly damped region close to k//=0 - non-local, non-perturbative effects are crucial

JET-like case: analysis of mode structures

adding step by step electron resonances:
no electron LD damping:

γ/ω = -0.16% (ion LD)

adding circulating k=0 resonance:

γ/ω = -0.67% (ion LD+circ el)

adding circulating k=±1 sidebands:

γ/ω = -0.77% (ion LD+circ el+sb)

adding trapped electrons:

γ/ω = -0.87% (ion LD+all el)

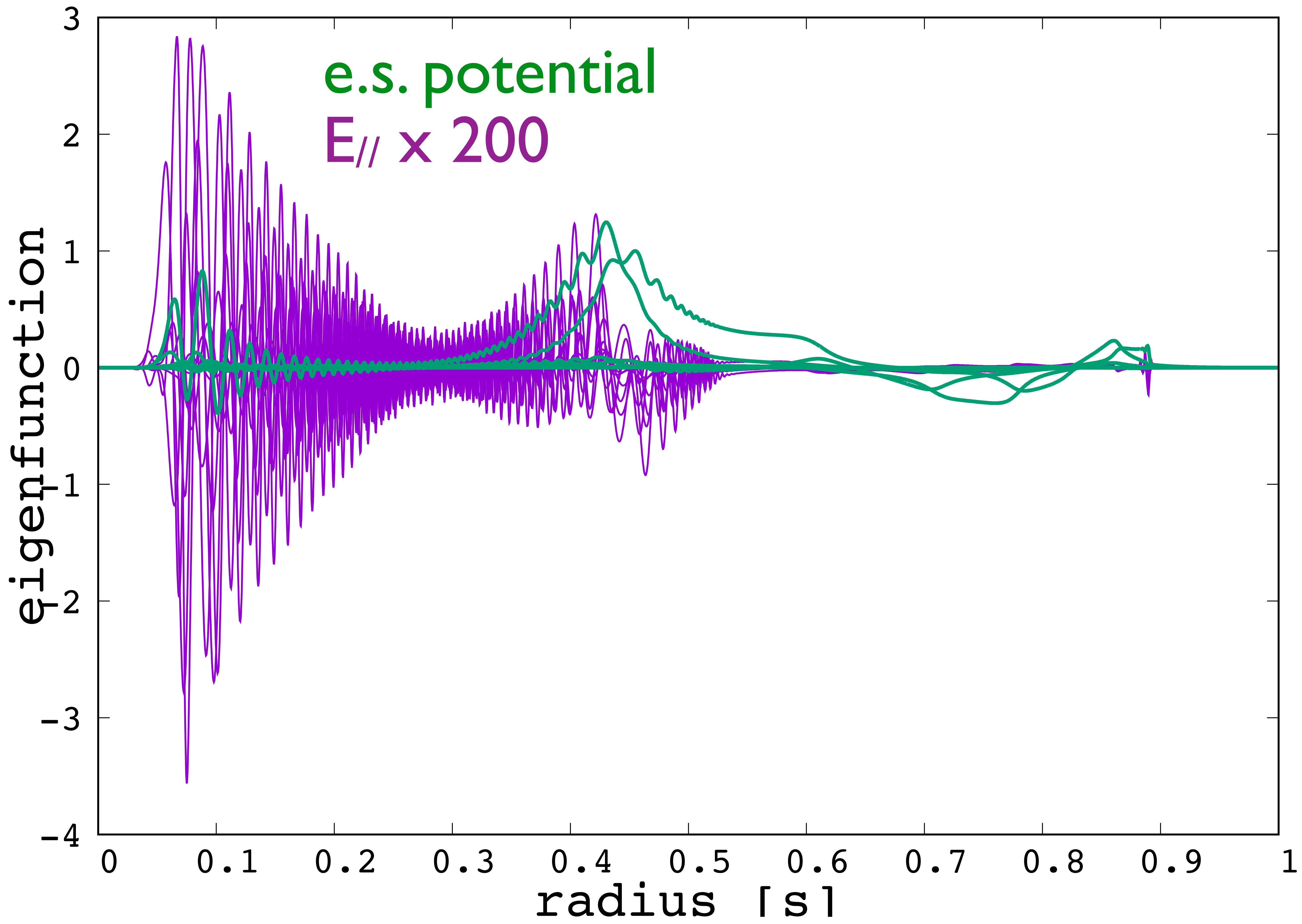

almost undamped KAW - in agreement with theory

JET-like case: electron mass ratio scan - cheaper non-linear simulations

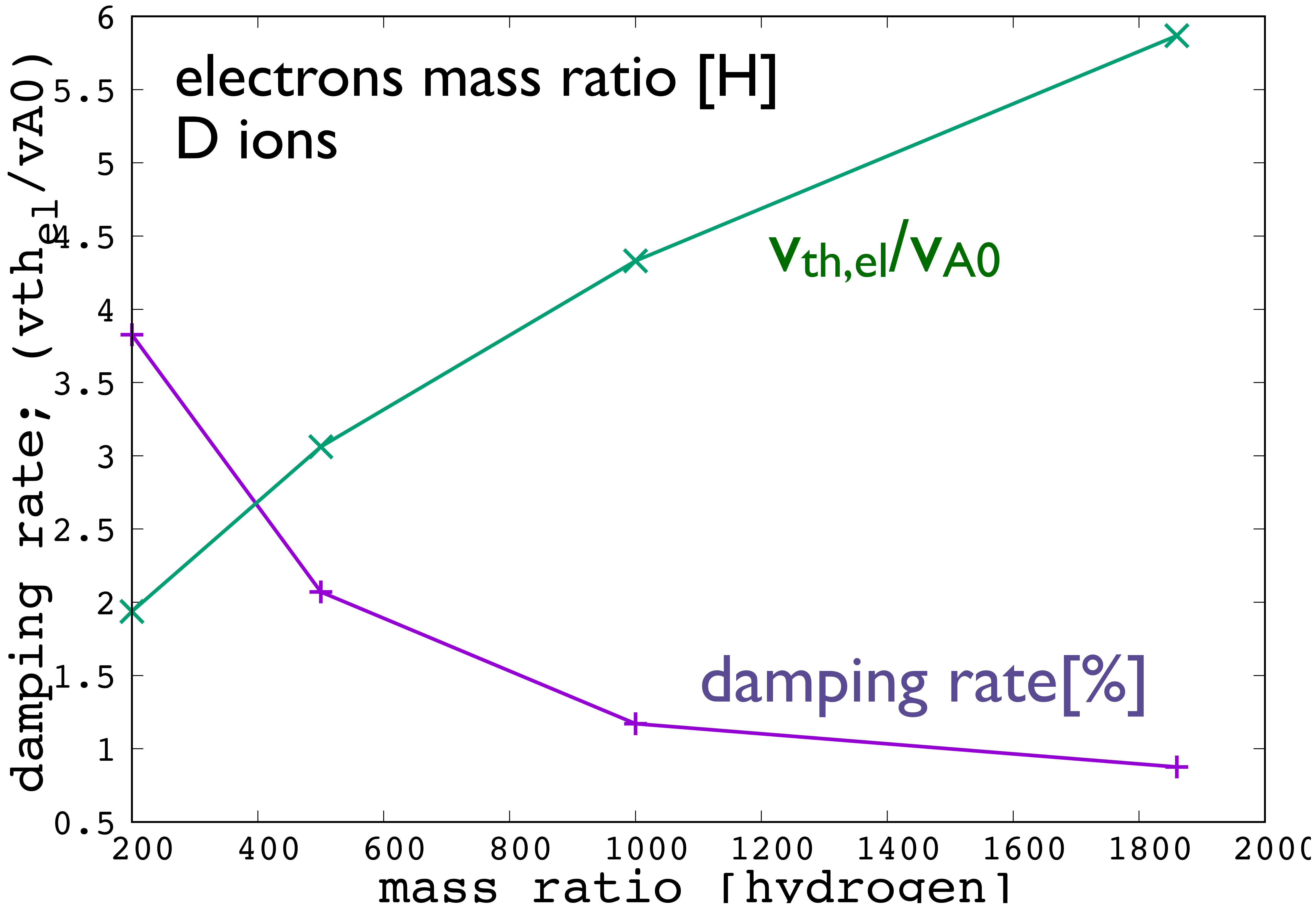

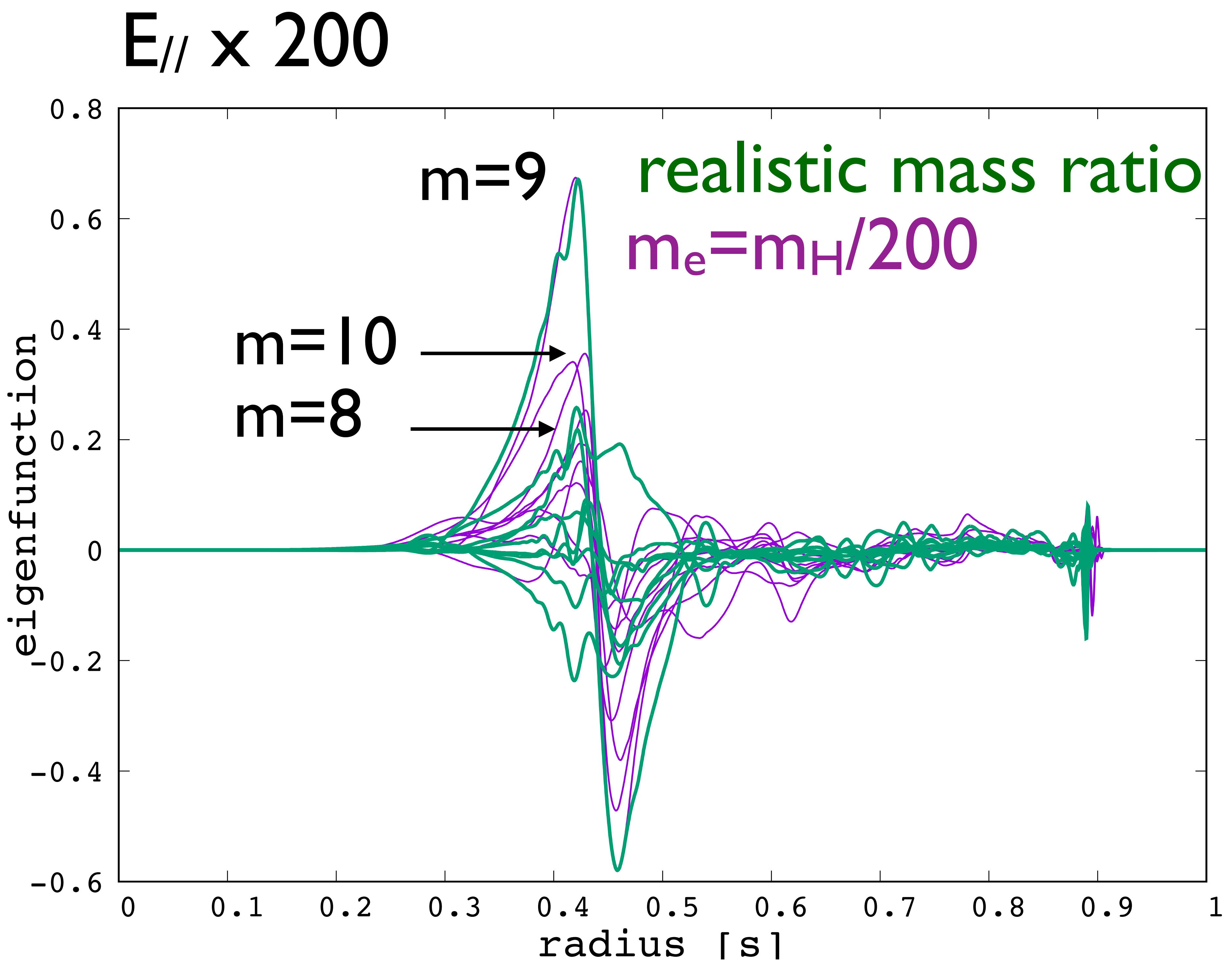

modifications of E// sidebands
influence on non-linear generation of ZS/ZF?

[Chen&Zonca 2012, RMP 2016]

damping rate increases when thermal 'electron' velocity reaches $v_{Alfvén}$

Kinetic Alfven Waves (KAWs) in multi-scale problems: ITER

ITER 15 MA DT [ITER database, very similar to #131018,13]

[A. R. POLEVOI ET AL. J. Plasma Fusion Res., 5 (2002)]

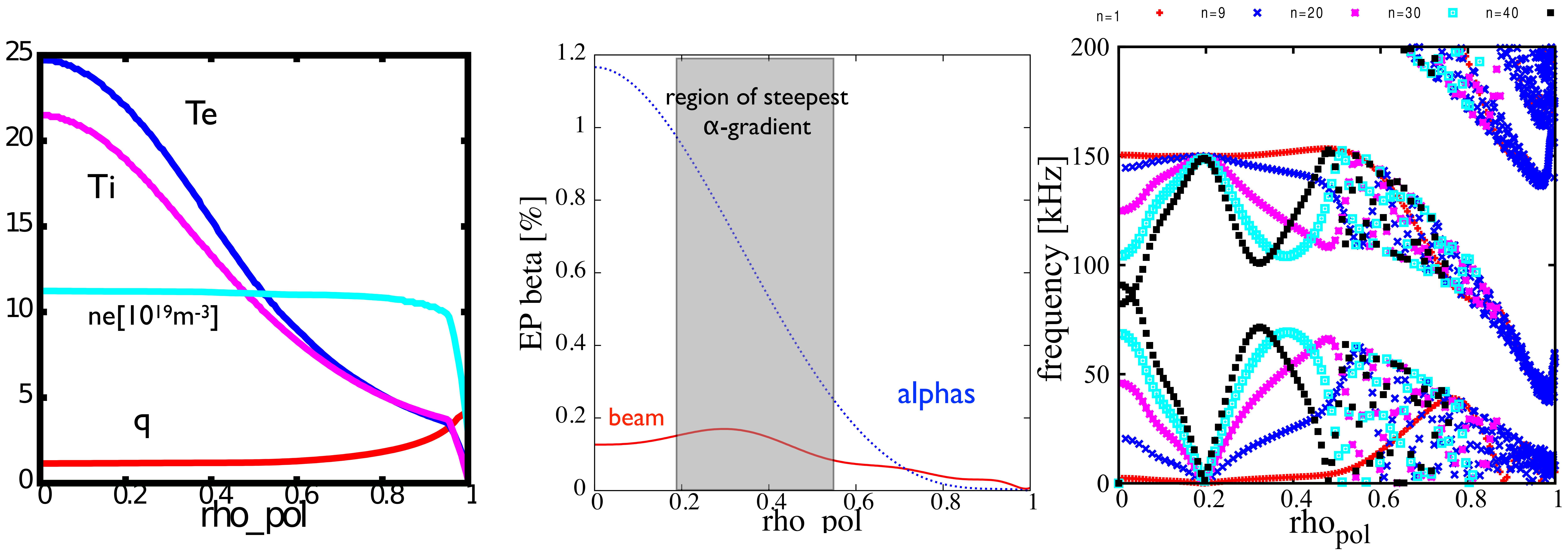

B0=5.3T, R0=6.2m, D,T,He-ash, Be,α,NNBI-D

[S.D. Pinches et al PoP , 2015
Ph. Lauber PPCF 2015]

dense TAE cluster for $\rho_{pol} > 0.4$

damping > ~1%
various TAE branches with same n due to alignment of SAW gaps

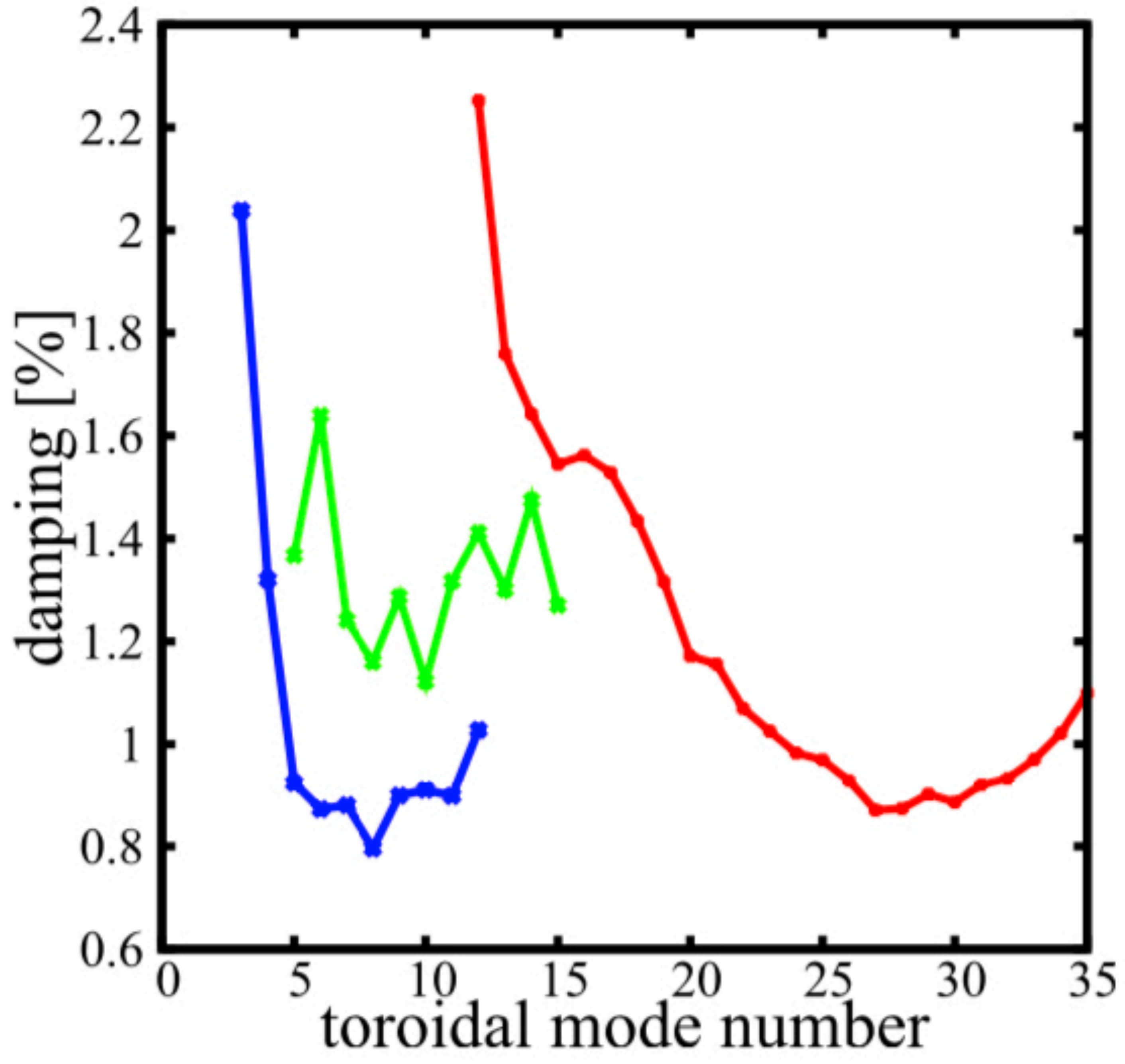

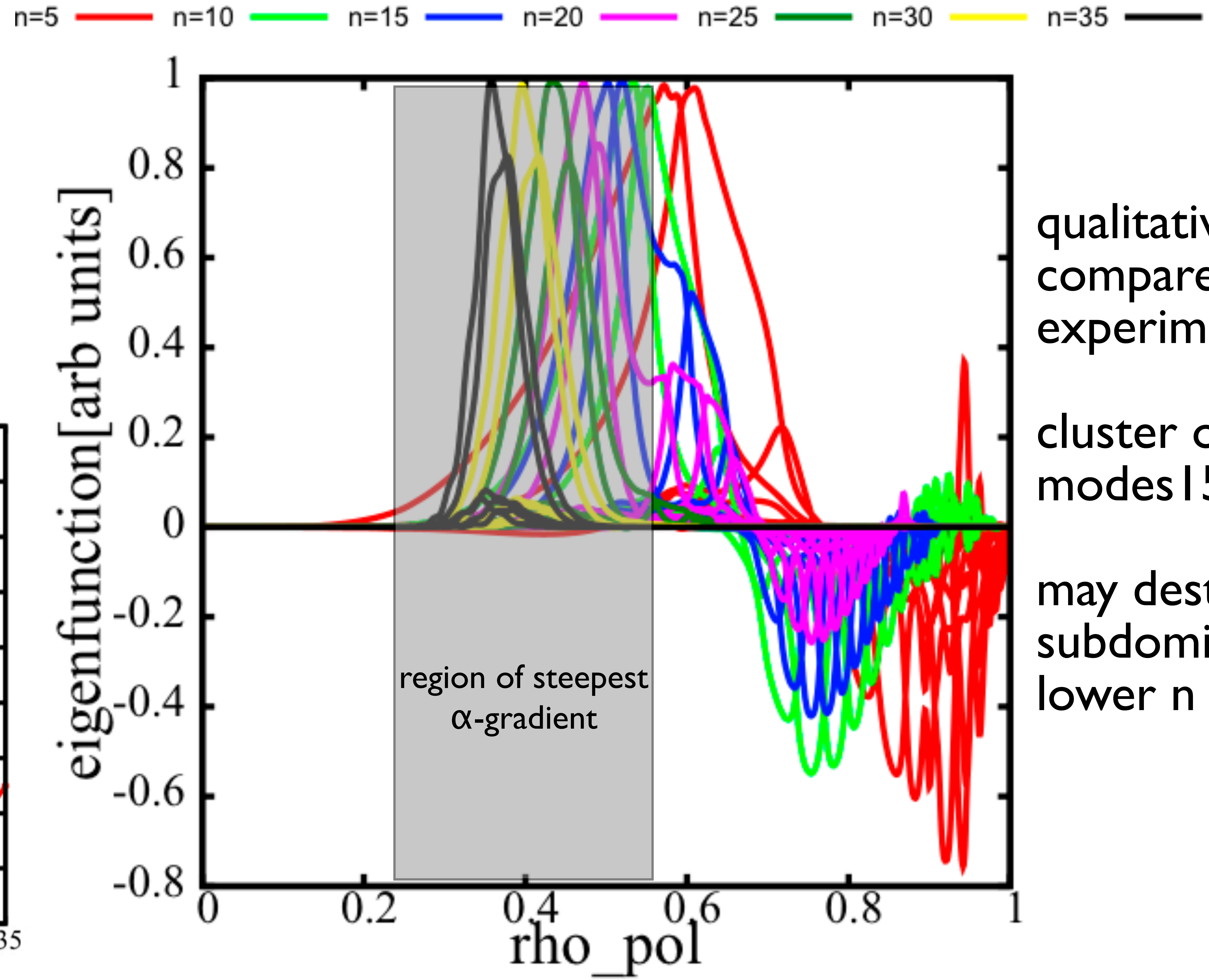

qualitatively new situation compared to present-day experiments:

cluster of most unstable modes 15<n<25

may destabilise subdominant modes with lower n in outer core

ITER case: ion and electron LD for n=26 TAE

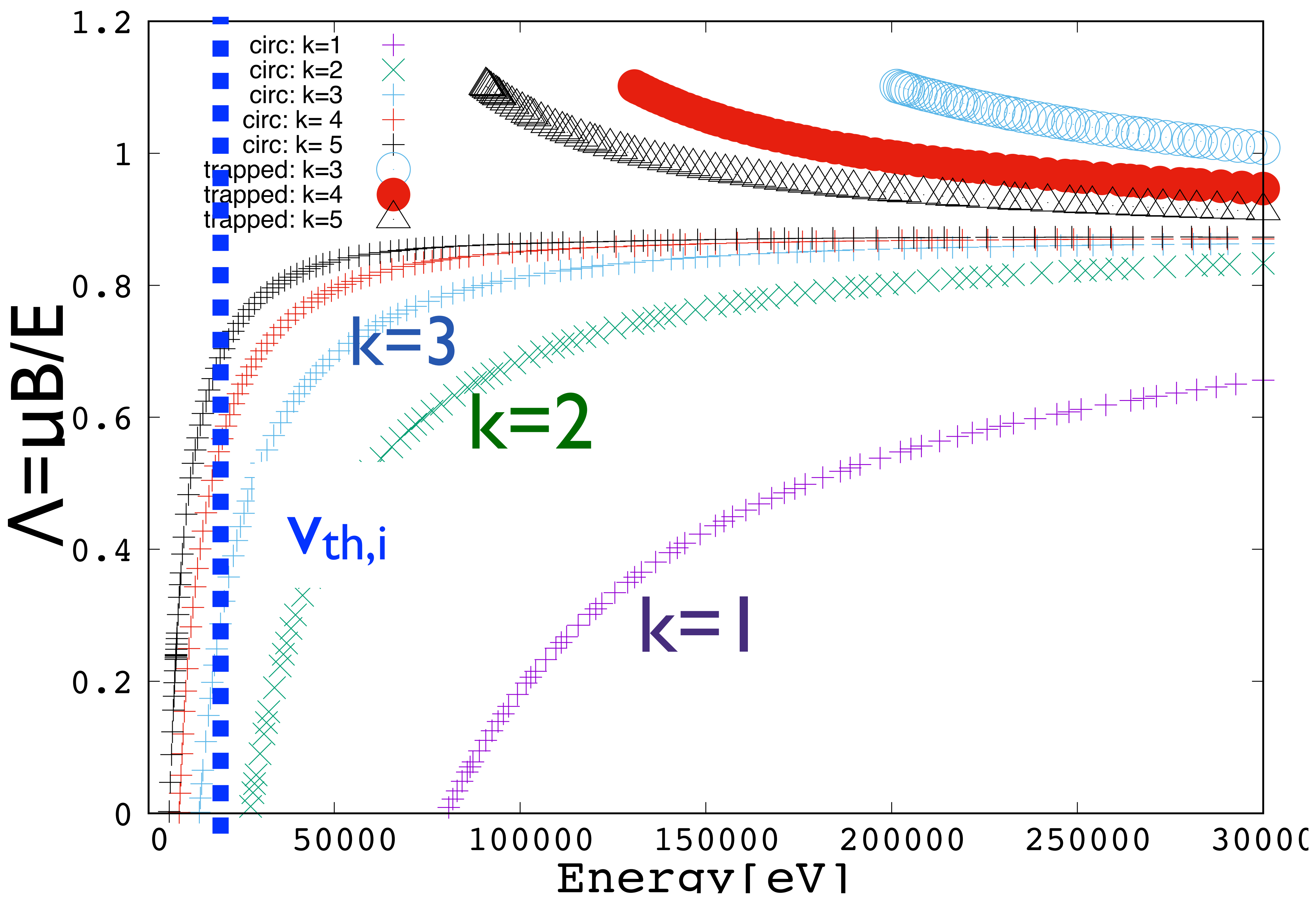

el, DT-hybrid: all species (k=-5…+5): ω/ω_{A0}: 0.487; -1.296 [%]
el, DT-hybrid: no trapped electrons: ω/ω_{A0}: 0.485; -1.106 [%]
el, DT-hybrid: adiabatic electrons: ω/ω_{A0}: 0.483; -0.305 [%]

contribution to damping: electrons: ~1%, ions 0.3% - larger than in JET due to higher Ti

ITER will have hydrogen and deuterium phases before going to DT 50:50 mix

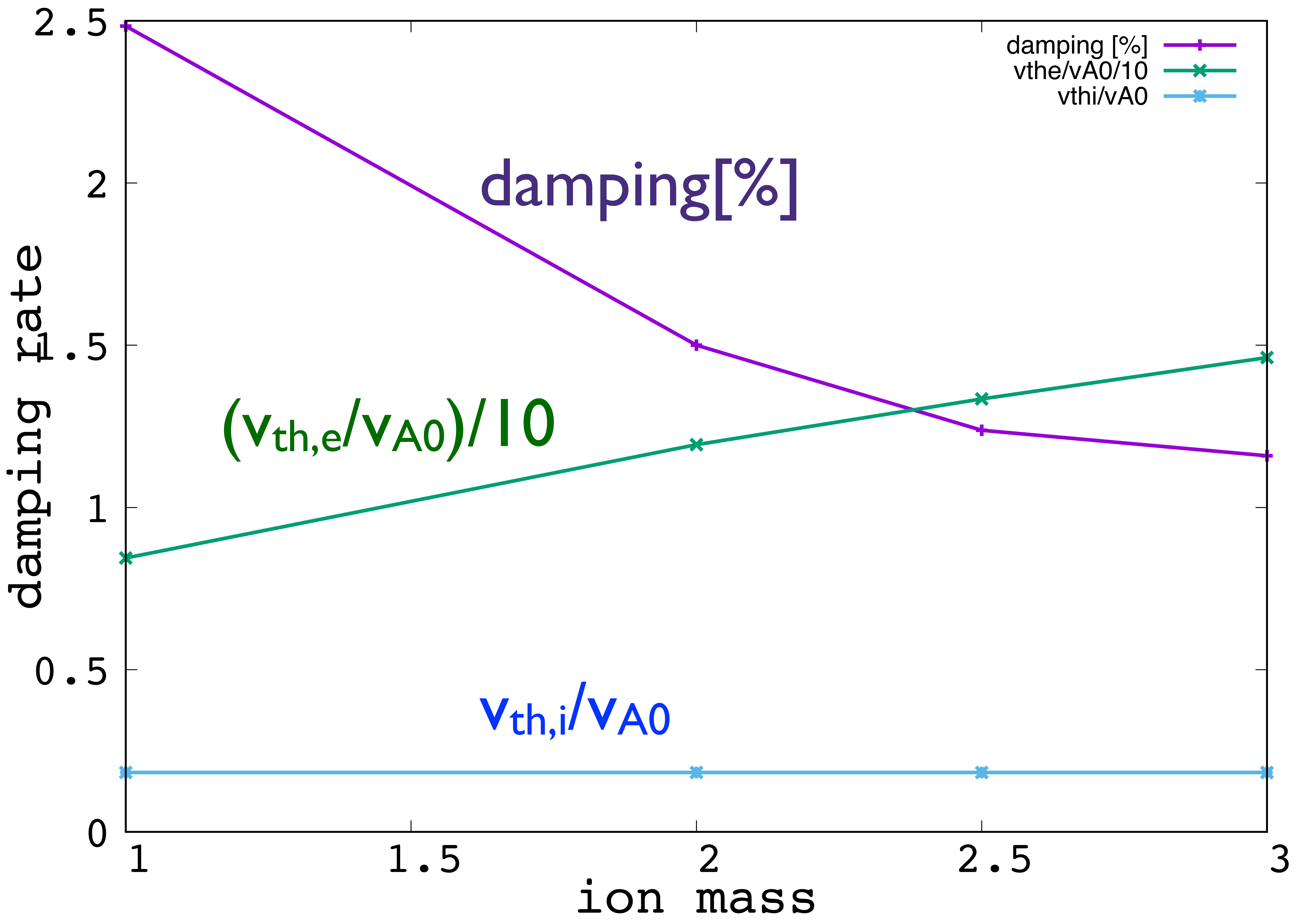

- TAEs will be less damped in burning plasmas compared to early H operation
- since ion LD scales with $\sim(v_{A0}/v_{th,i})^{3/2}\exp-[v_A/(3\ v_{th,i})]^2$, ion mass cancels for ion LD
- but situation is more complex since ITER will have species mix due to He ash, Be, Ne etc..
- increase in damping due to KAWs /electron LD

ITER: isotope scan - non-perturbative mode structures

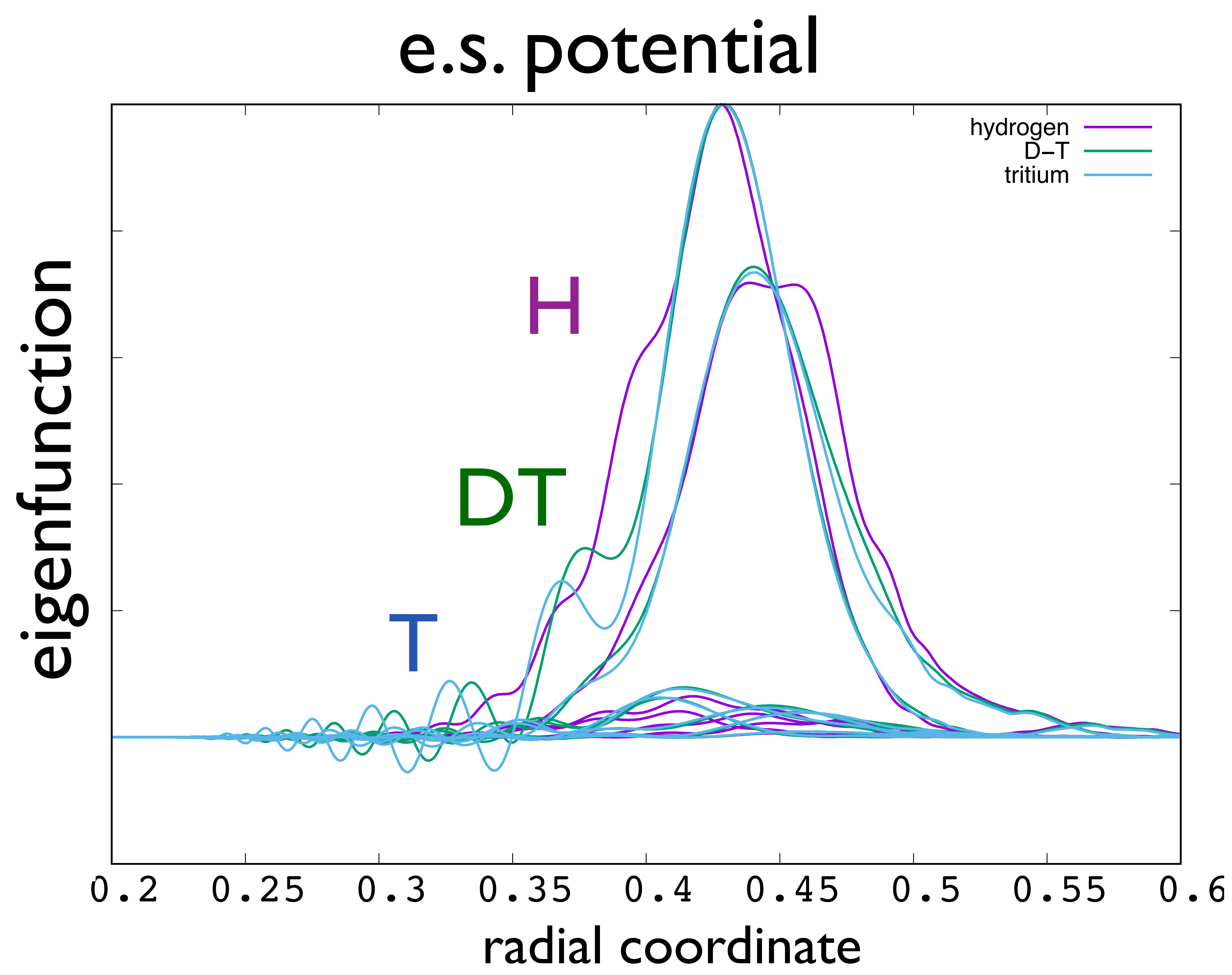

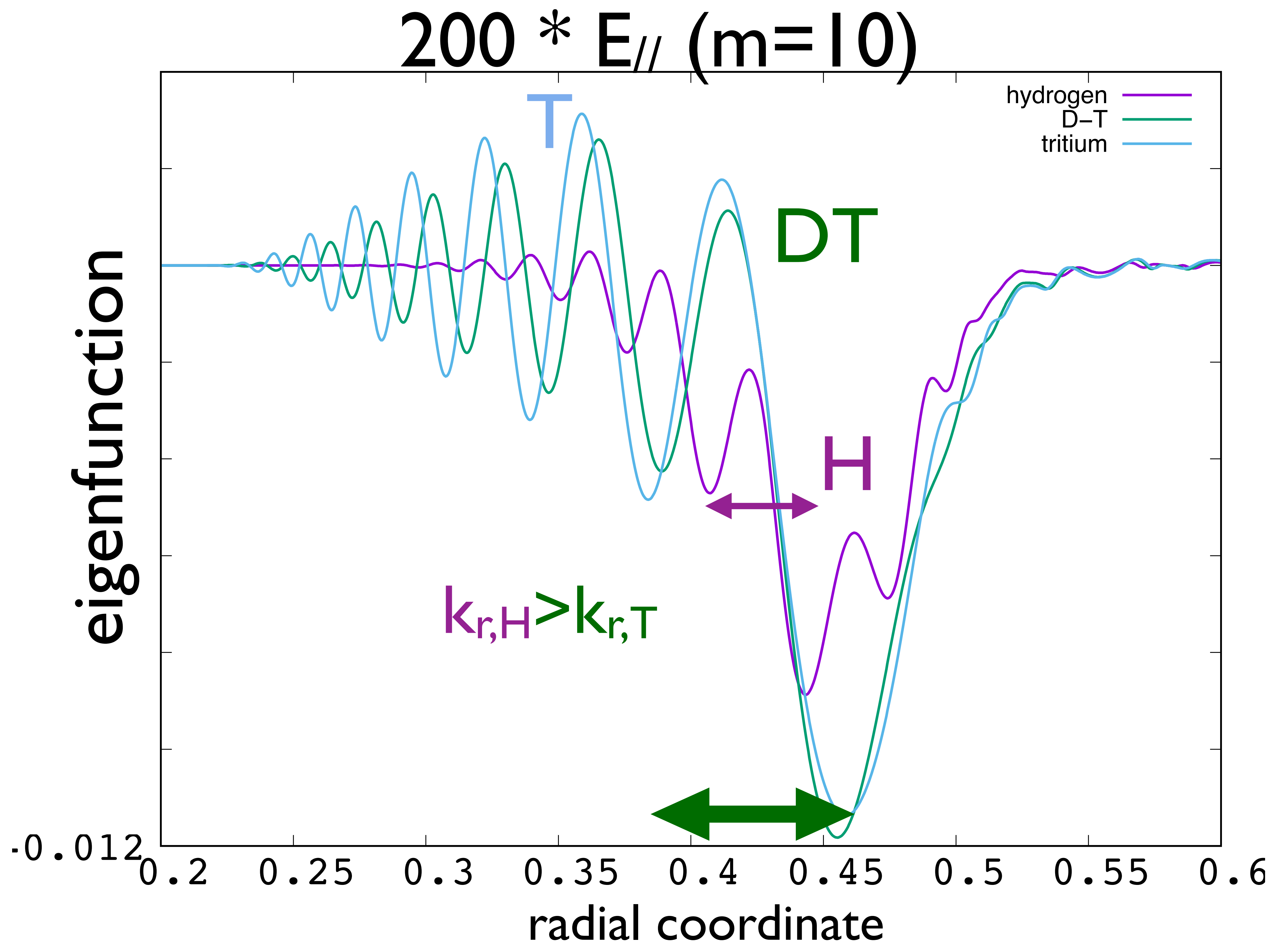

damping ~ $(k_\perp \rho_i)^2$

checking a posteriori: $\rho_i k_\perp = (\sqrt{k_r^2 + k_\theta^2})\ \rho_i \approx 0.13 \ll 1$, long wave-length approximation valid

- global modes (n=8-15) add non-local complexity to problem
- energetic α-particles drive modes unstable, but also affect mode structures (e.g. p_{EP} changes f-distance to continuum - larger coupling parameter)

non-linear consequences

ITER using linear spectrum for non-linear perturbative runs: add energetic ions, calculate wave-particle power transfer until non-linear saturation

HAGIS/LIGKA model, ITER 15 MA TAEs [Schneller, 2015]

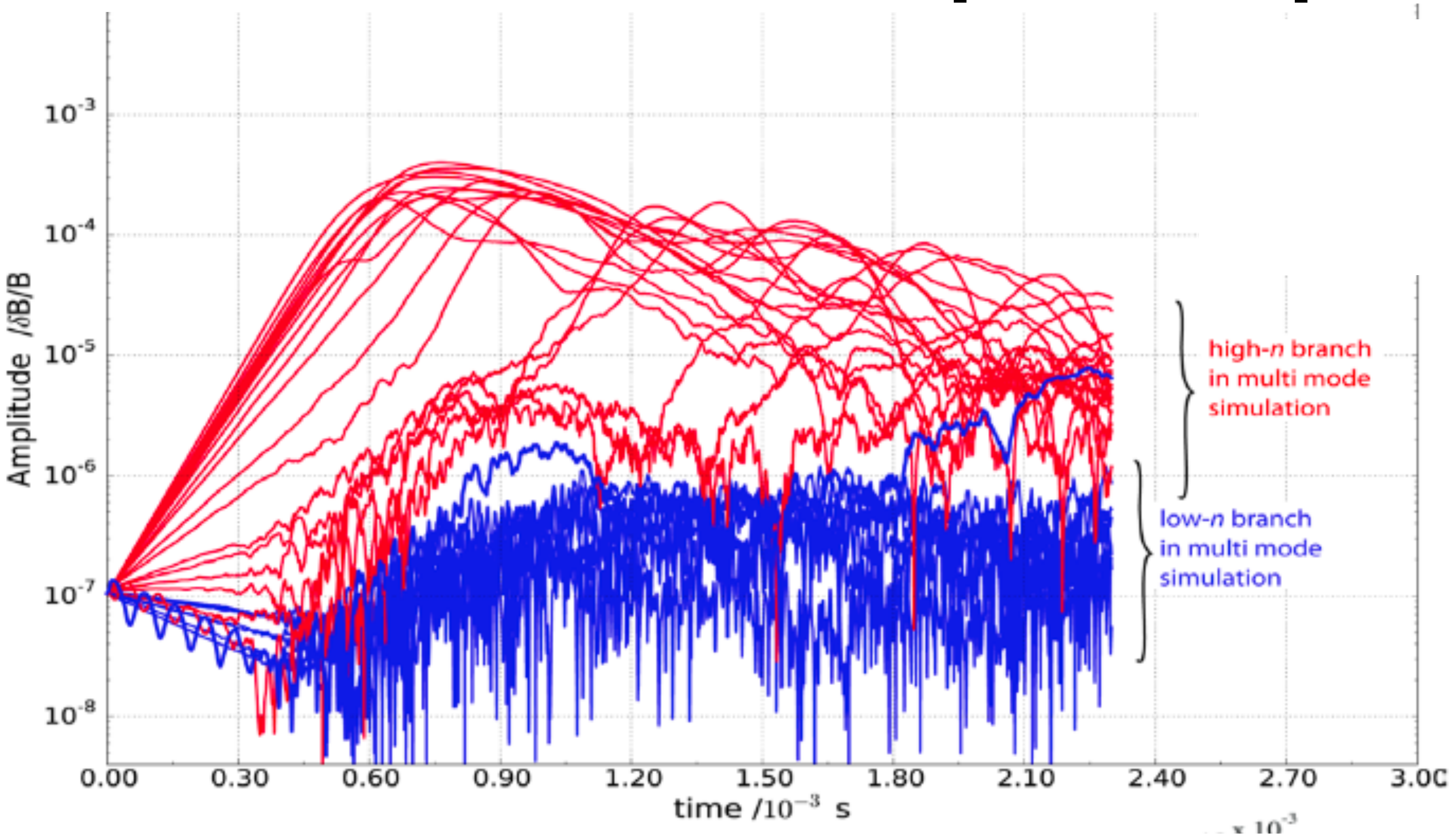

'sea' of weakly unstable TAEs expected with small EP transport;
agreement with QL estimates

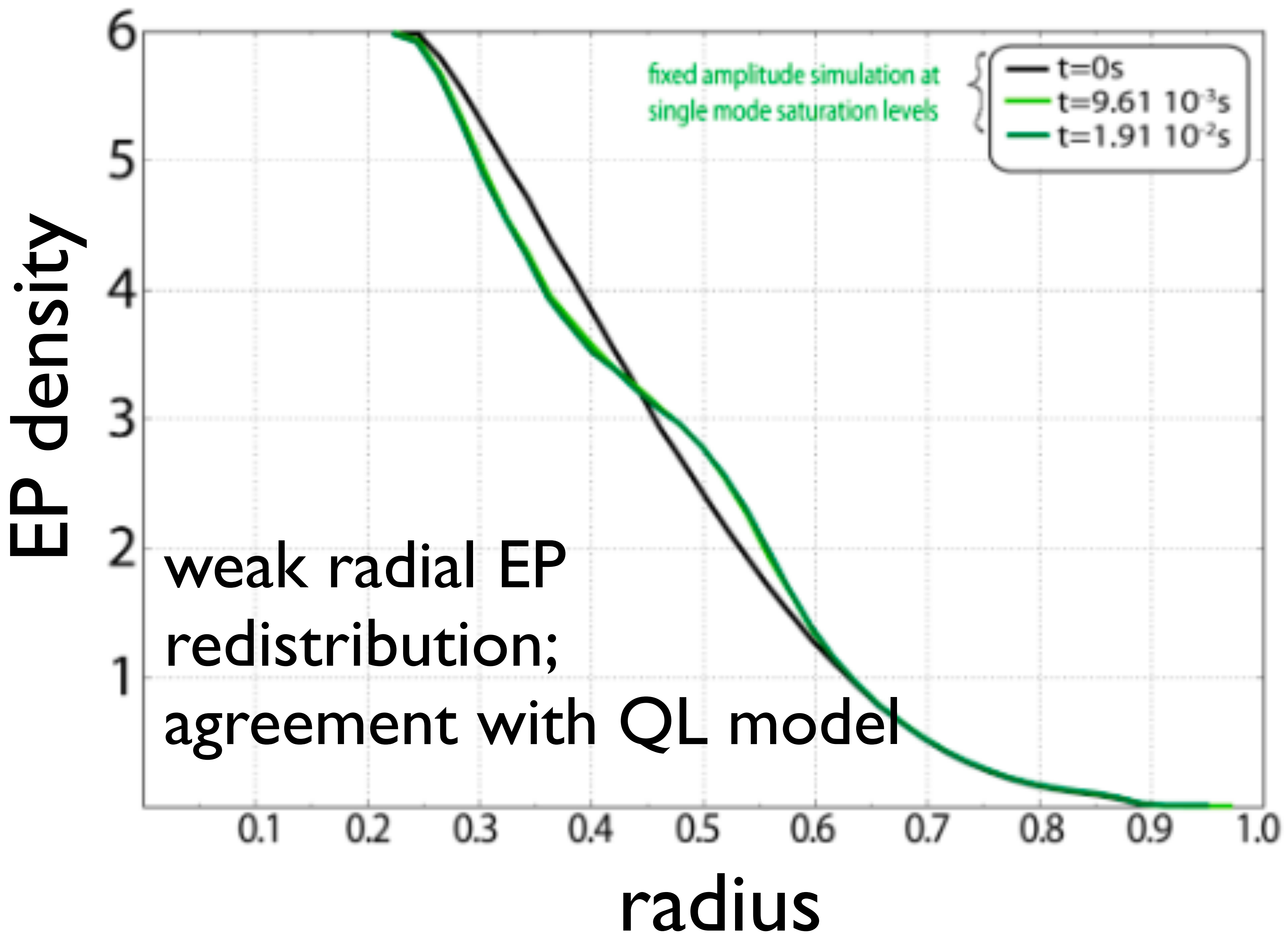

can be used to check QL linear resonance broadening models [Berk, 1995, Gorelenkov 2015…]

QL boundaries? for artificially higher EP pressure (~2 times), energetic particle avalanches are found

HAGIS/LIGKA model, ITER 15 MA TAEs [Schneller, 2015]

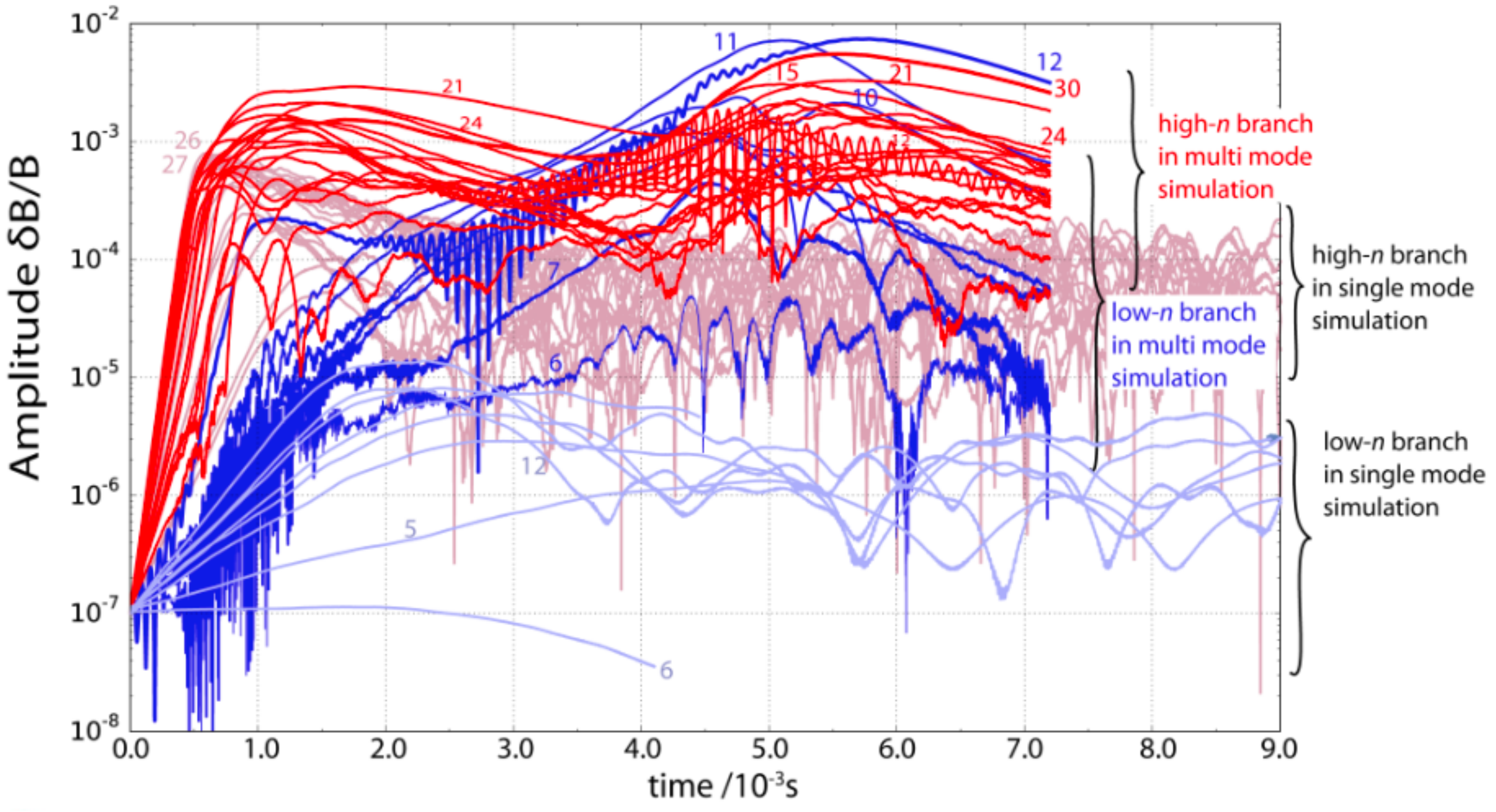

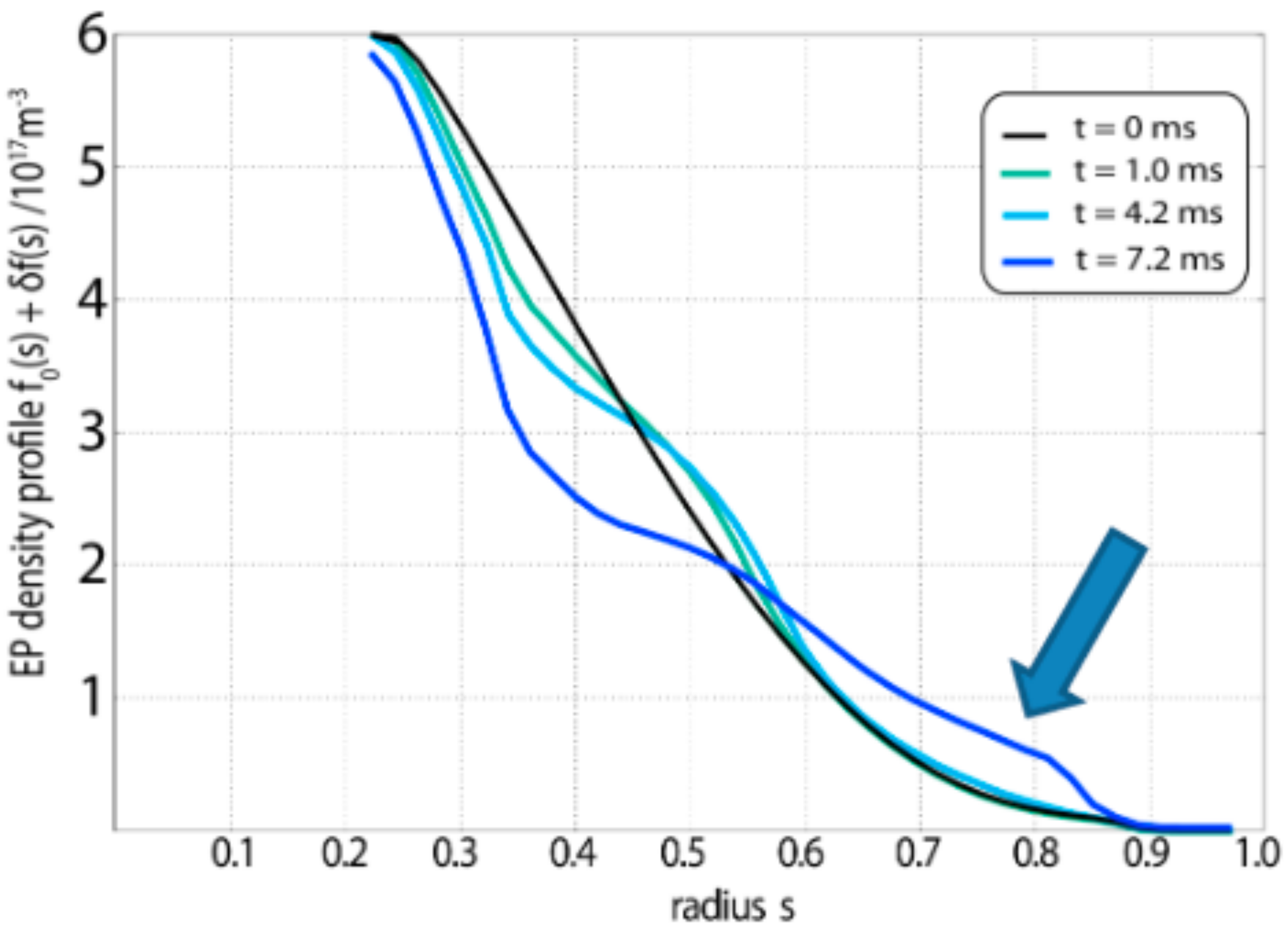

- also found in reduced descriptions: 1d beam plasma model [Carlevaro, 2015-17,2021]
- above simulations do not consider wave-wave non-linearities [Z. Qiu at this session]
- collisions influence saturation level [see talk by C Slaby at this conference]
- not found in works with similar non-linear model but different linear mode spectrum [Fitzgerald NF 2016]

successful comparison with global non-linear GK code ORB5

HAGIS/LIGKA model, ITER 15 MA TAEs [Schneller, 2015]

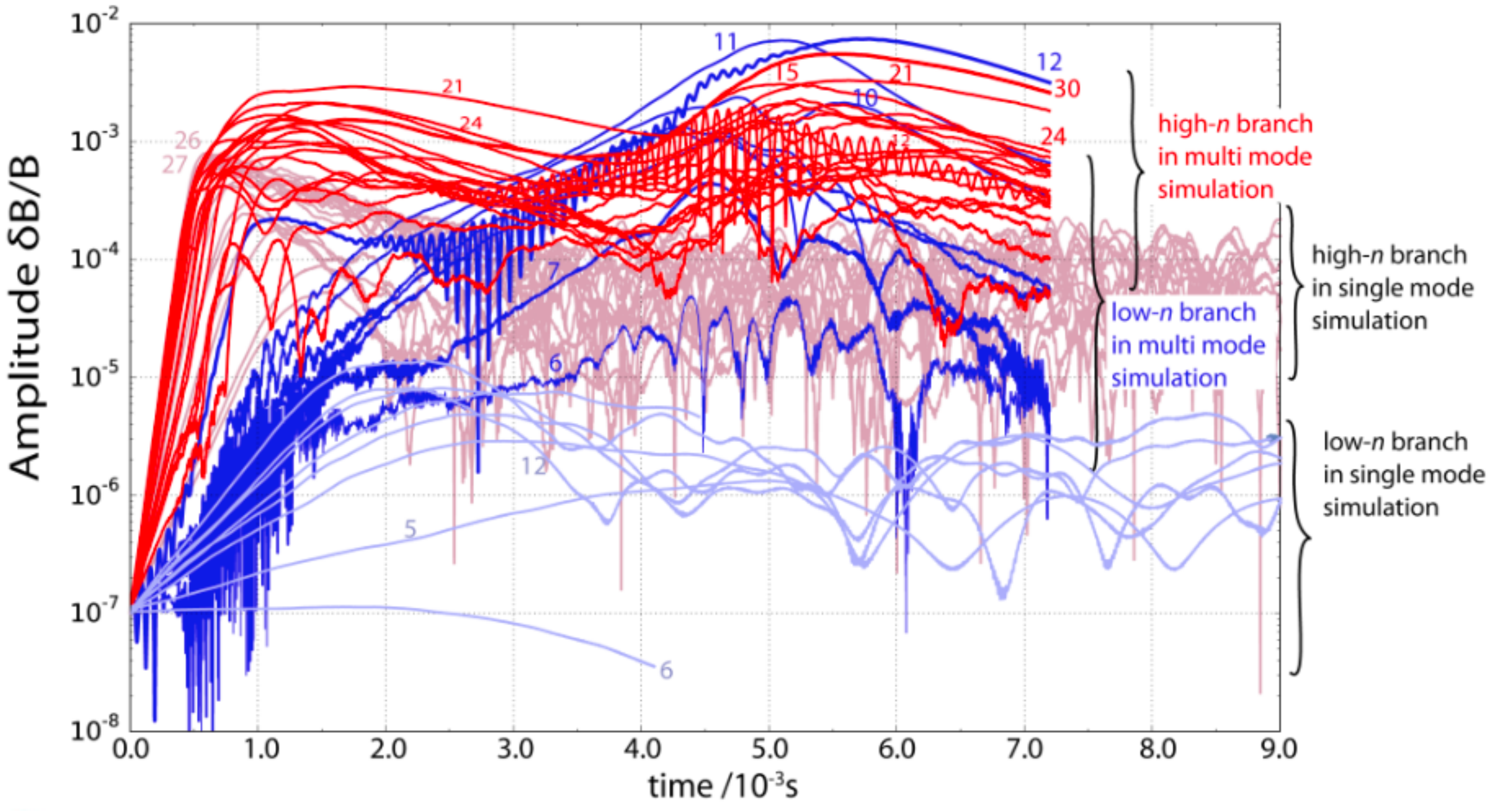

ITER 15 MA case - ORB5 [T Hayward-Schneider NF 2021]

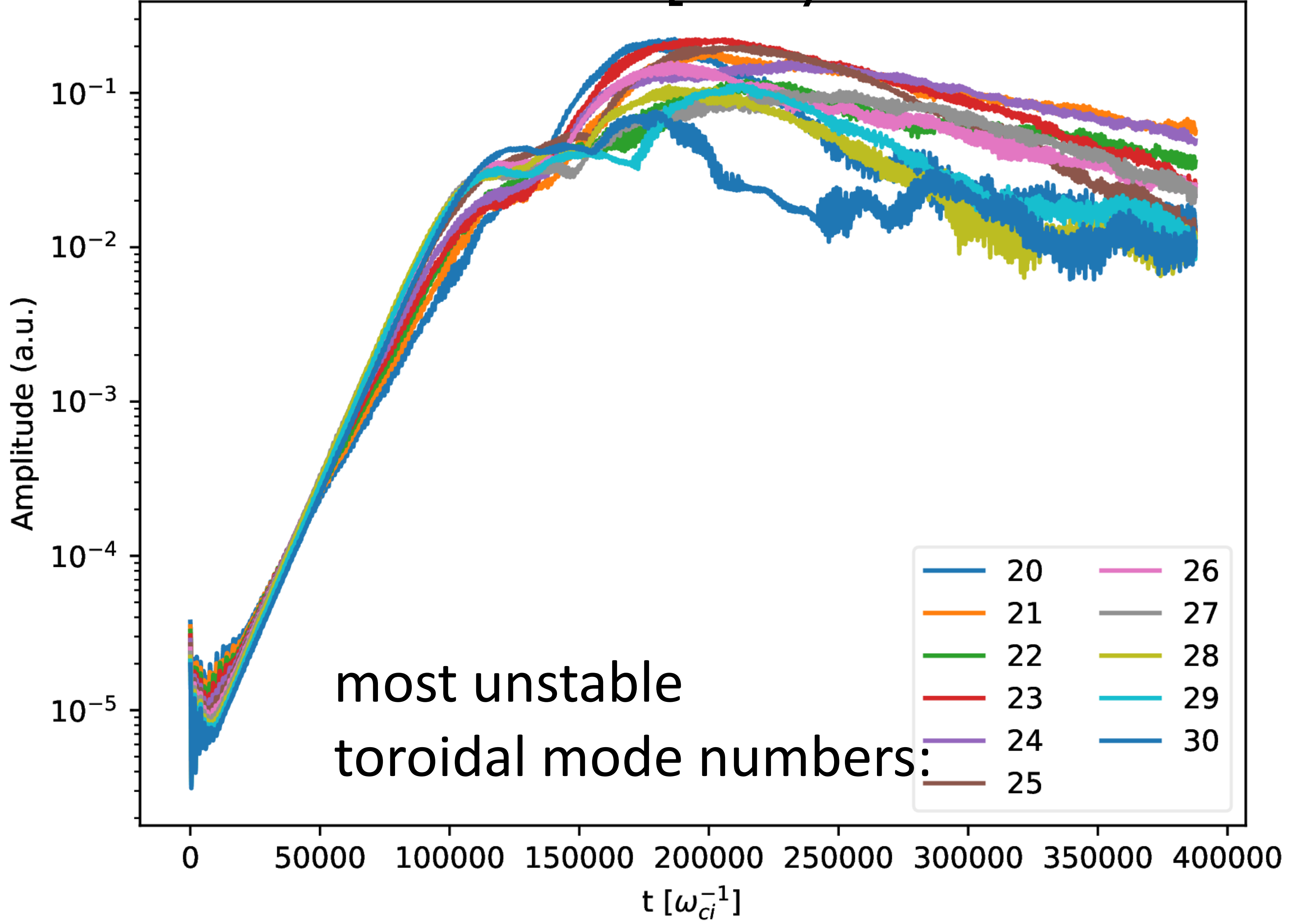

- compare LIGKA/HAGIS model to ORB5: global electromagnetic gyrokinetic code using the PIC approach in toroidal geometry [Lanti CPC 2020, for EP physics: Biancalani, Bottino, Hayward-Schneider, Vannini,… 2012-21]
- Effectively mitigates with the so-called cancellation problem using the pullback scheme (leads to an order of magn. increase of time step) [Mishchenko CPC 2019]
- very similar linear and non-linear properties of ITER 15 MA case were found [T Hayward-Schneider 2021, AAPPS-DPP 2020]

KAW physics with ORB5

[T Hayward-Schneider, EPPI 2019]

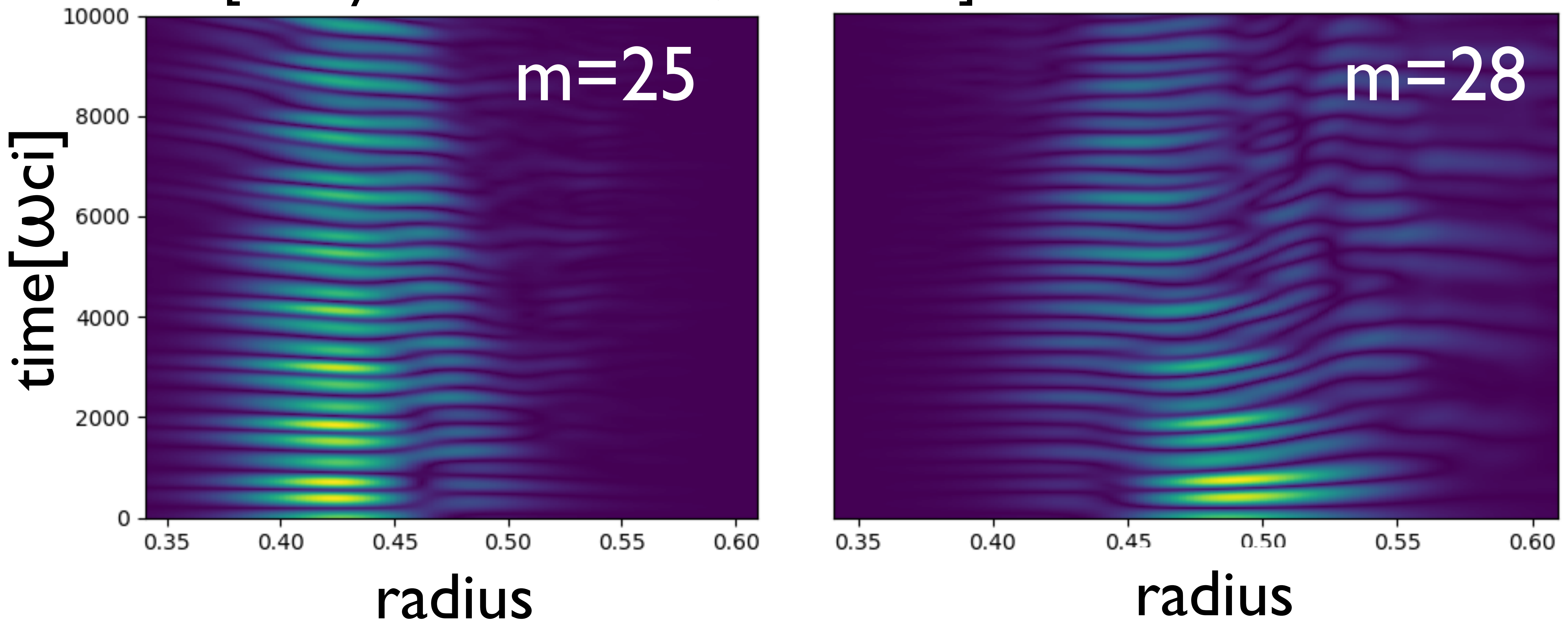

ITER n=26:
radially inwards and outwards propagating wavefronts can be clearly seen - finite k_r

- short -wavelength features can be directly seen [ITPA TAE case, A. Konies NF 2018]
- electron and ion damping have been investigated in detail with ORB5- consistent with LIGKA results [F.Vannini, PoP 2020]
- also other symmetry breaking processes leading to radial propagation under investigation (EP profile non-uniformity) [G. Meng, et al. NF, 2020(056017)subm. PST 2021, F. Zonca, NF 2005, L. Chen RMP 2016, Z. Lu, et al., NF 2018]

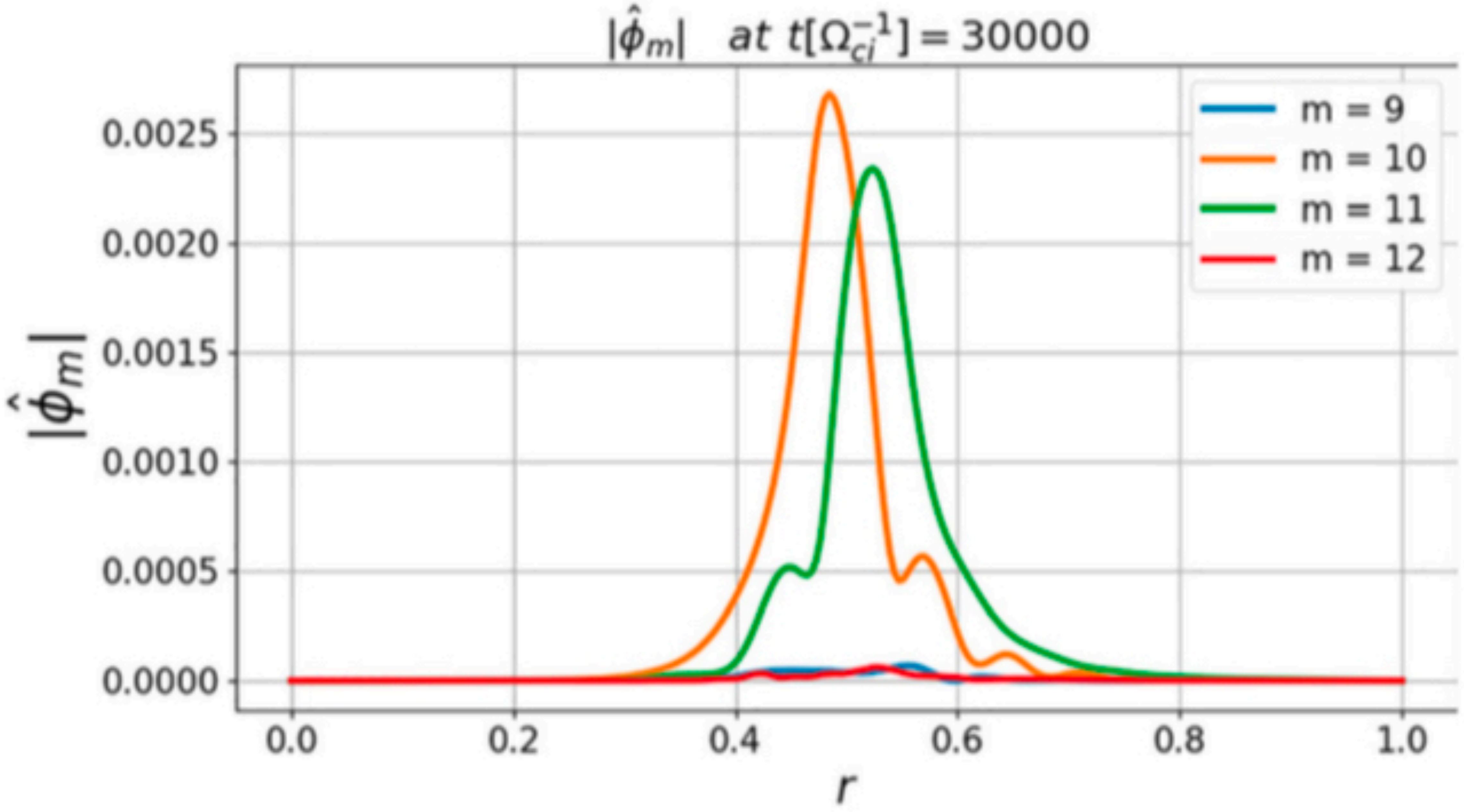

Kinetic Alfven Waves (KAWs) in multi-scale problems: ASDEX Upgrade (AUG)

AUG EP-'supershot' scenarios

[Lauber FEC 2018,2021; Horvath NF 56 2016]

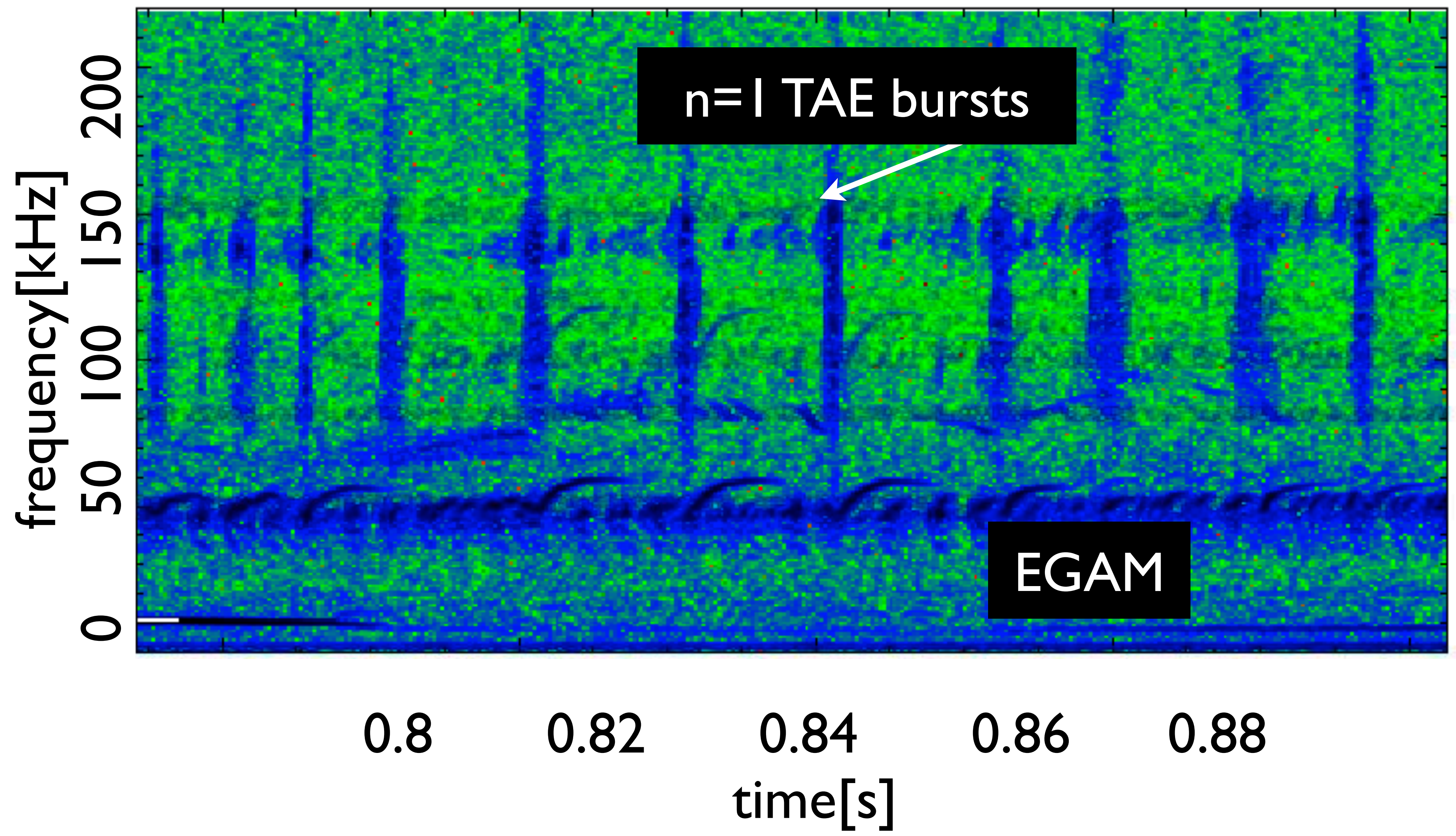

- minimize ion and electron LD by:
- cold core plasma despite strong EP drive (NBI)
- let impurities accumulate in core, heat only off-axis
- EP pressure dominated plasma - very useful for validation [benchmark paper Vlad et al NF 2021] of non-linear physics
- reaches for EP physics relevant parameters: $\beta_{EP}/\beta_{thermal} \sim 1$, $E_{NBI}/T_{i,e} \approx 100$

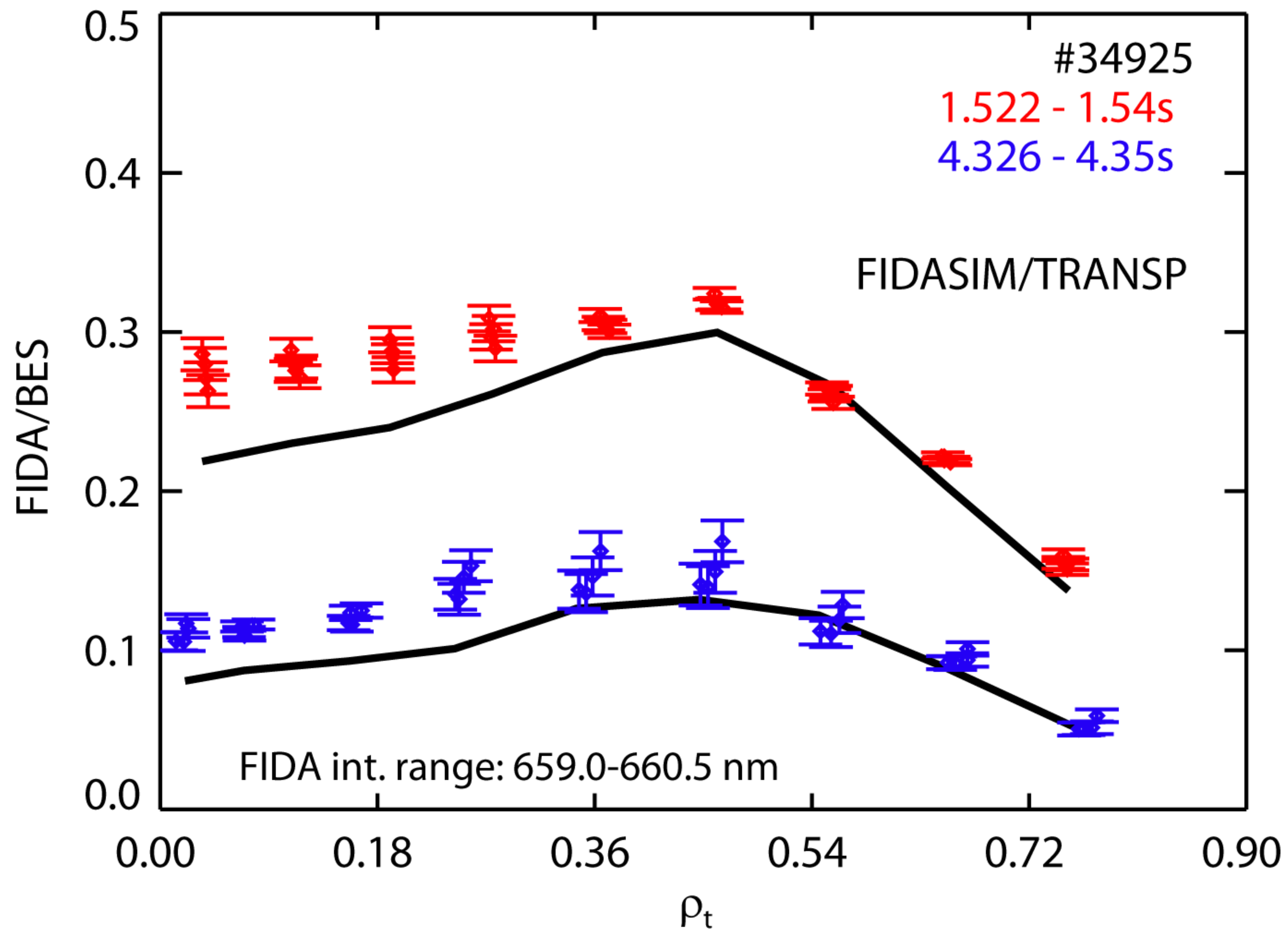

- off-axis peaked EP profile
- modes are driven by negative and positive EP gradients
- measurable inwards EP transport with change-exchange measurements

AUG EP-'supershot' scenarios

[Lauber FEC 2018,2021; Horvath NF 56 2016]

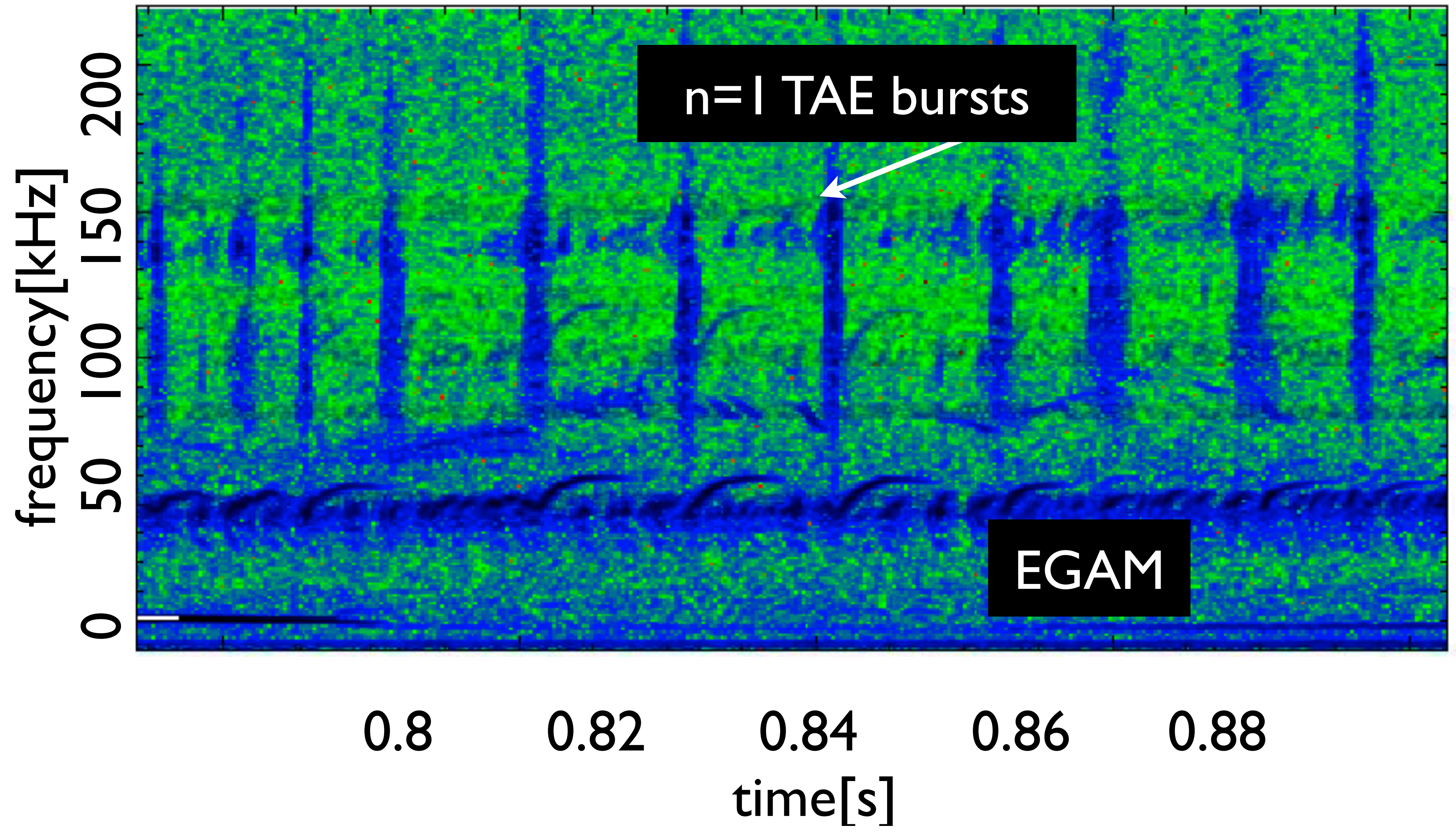

- minimize ion and electron LD by:
- cold core plasma despite strong EP drive (NBI)
- let impurities accumulate in core, heat only off-axis
- EP pressure dominated plasma - very useful for validation [benchmark paper Vlad et al NF 2021] of non-linear physics
- reaches for EP physics relevant parameters: $\beta_{EP}/\beta_{thermal} \sim 1$, $E_{NBI}/T_{i,e} \approx 100$

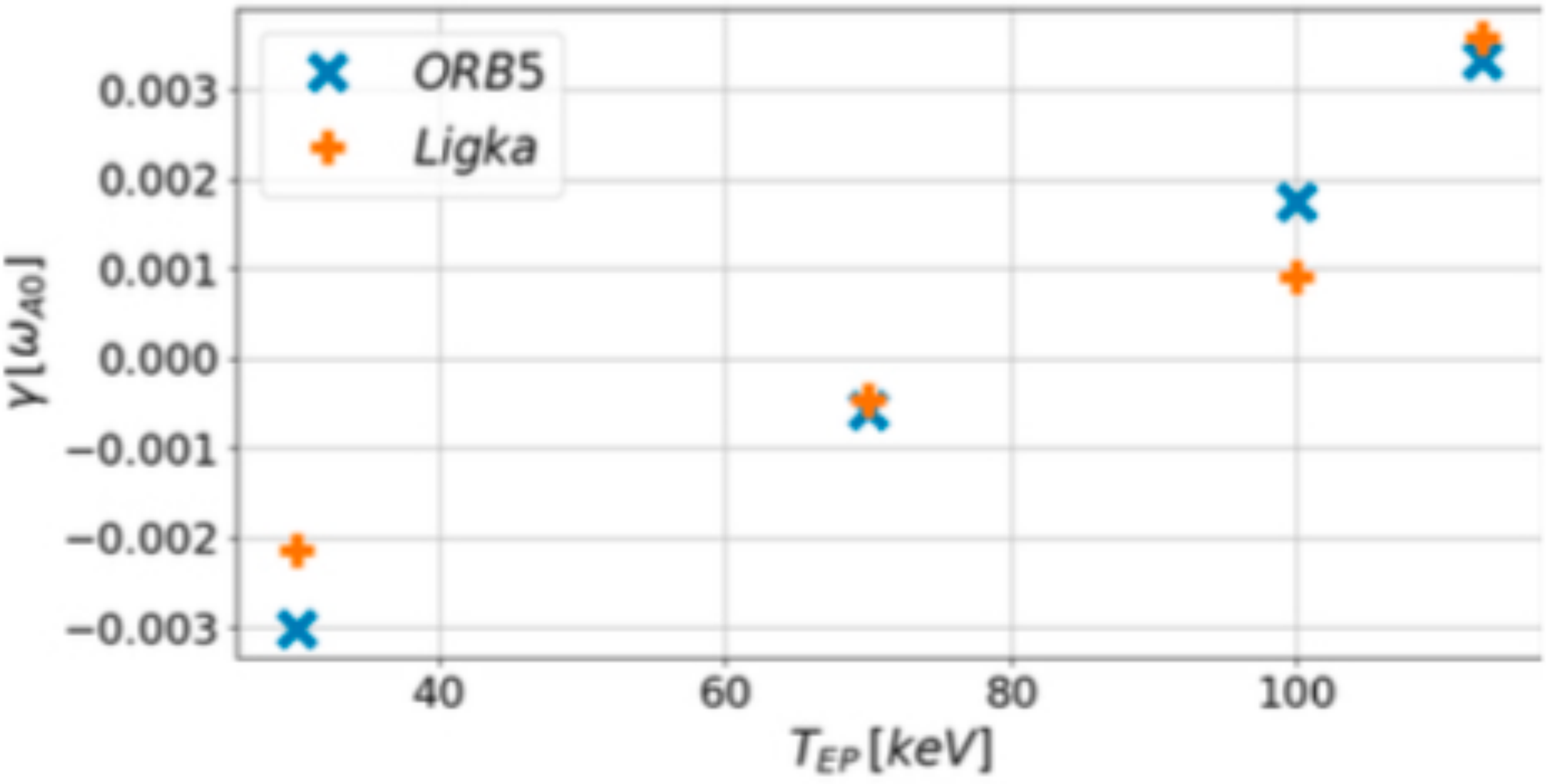

reasonable agreement for damping and linear growth rates [Vannini PoP 2020, Vlad NF 2021]

AUG EP-supershot scenarios

[Lauber FEC 2018,2021; Horvath NF 56 2016]

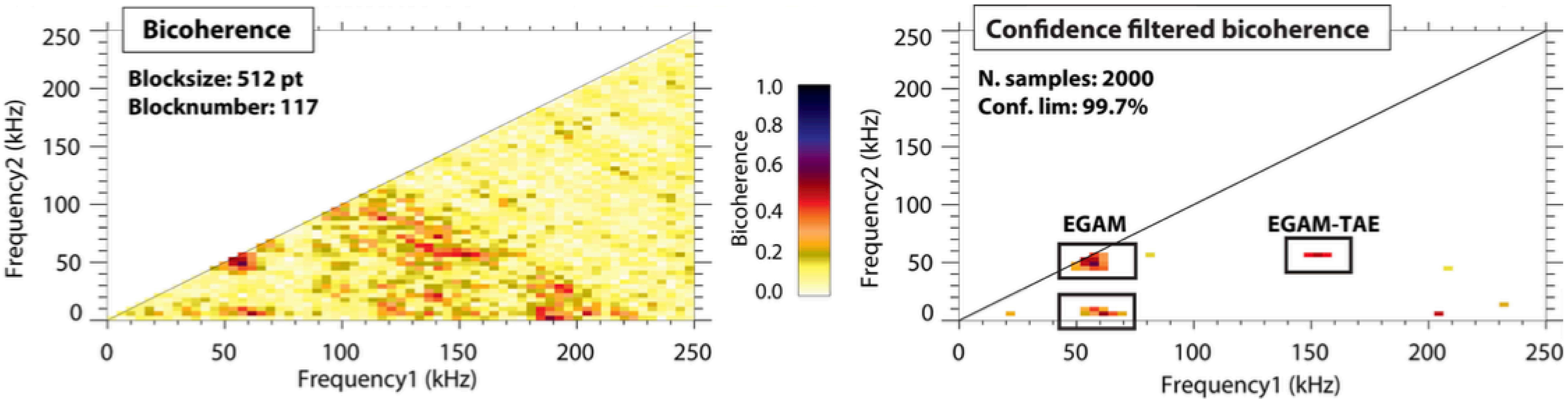

[P Poloskei et al IAEA TCM 2017, Lauber FEC 2018]

bicoherence analysis shows non-linear interaction between TAE and n=0 (EGAM) frequency band - which non-linearity?

aspects of non-linear saturation of EP-driven modes and related transport

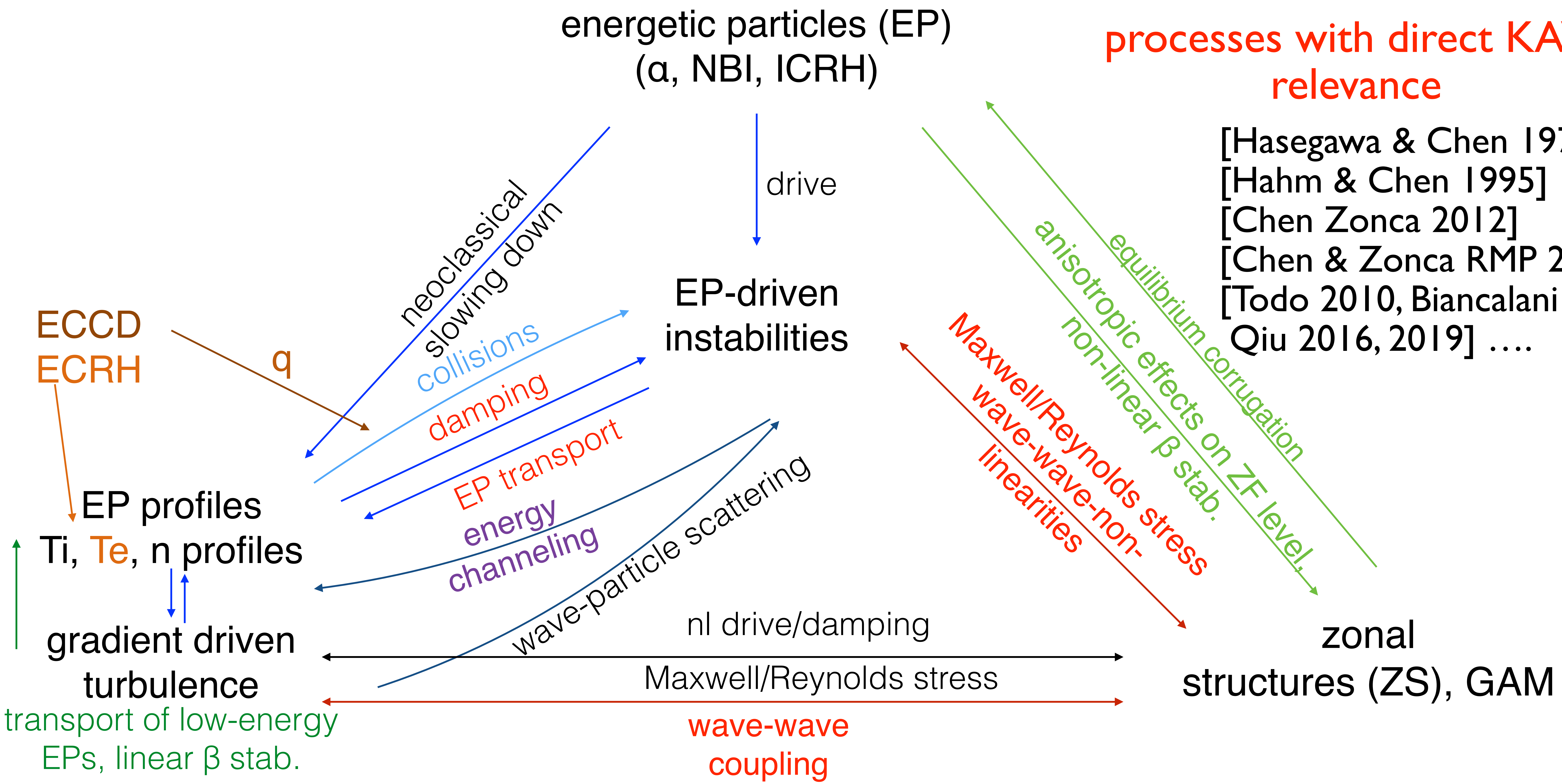

processes with direct KAW relevance

[Hasegawa & Chen 1976]
[Hahm & Chen 1995]
[Chen Zonca 2012]
[Chen & Zonca RMP 2016]
[Todo 2010, Biancalani 2020, Qiu 2016, 2019] ….

AUG: non-linear interaction of TAEs and ZS

[Vannini, PoP 2021, Qiu, NF 2019]

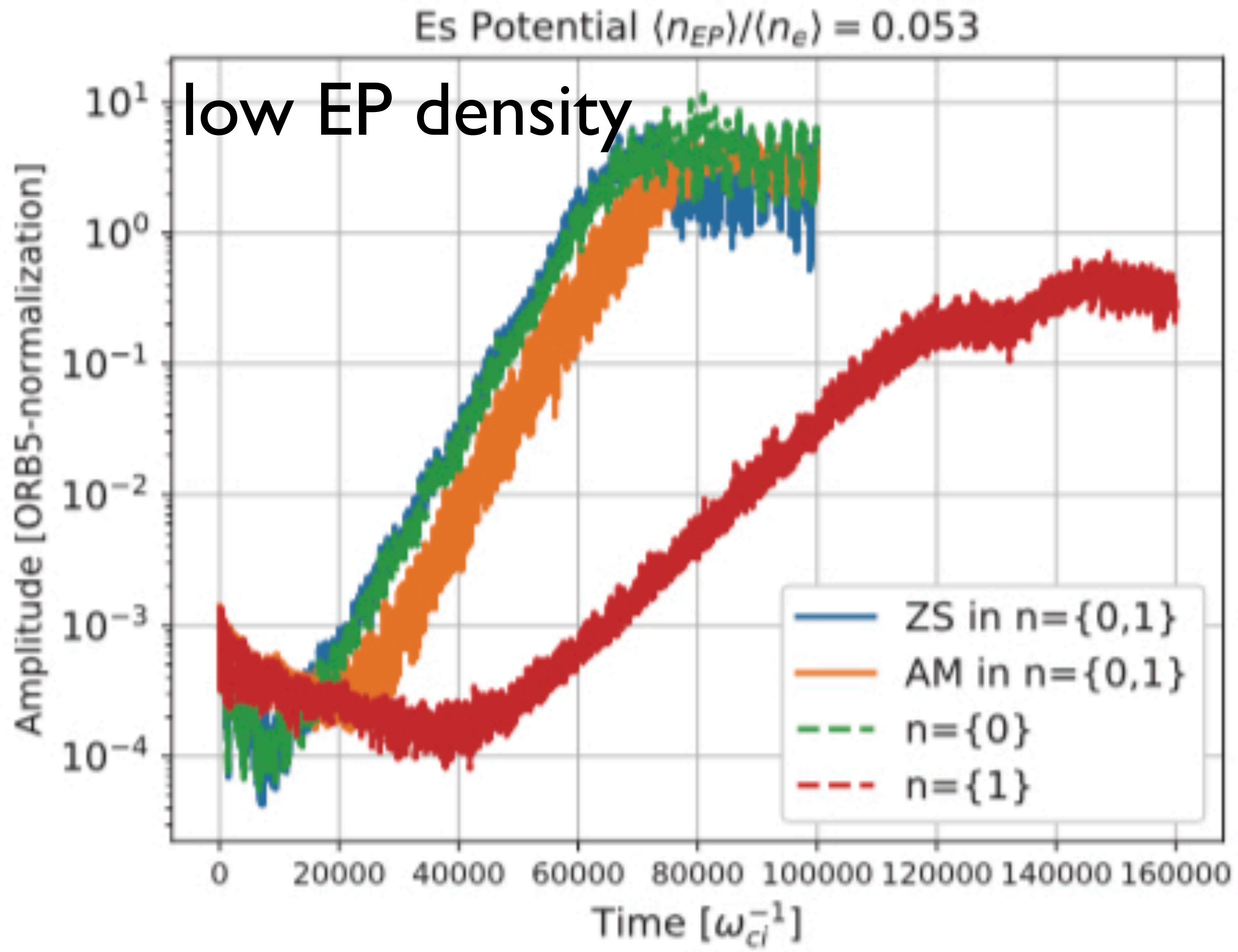

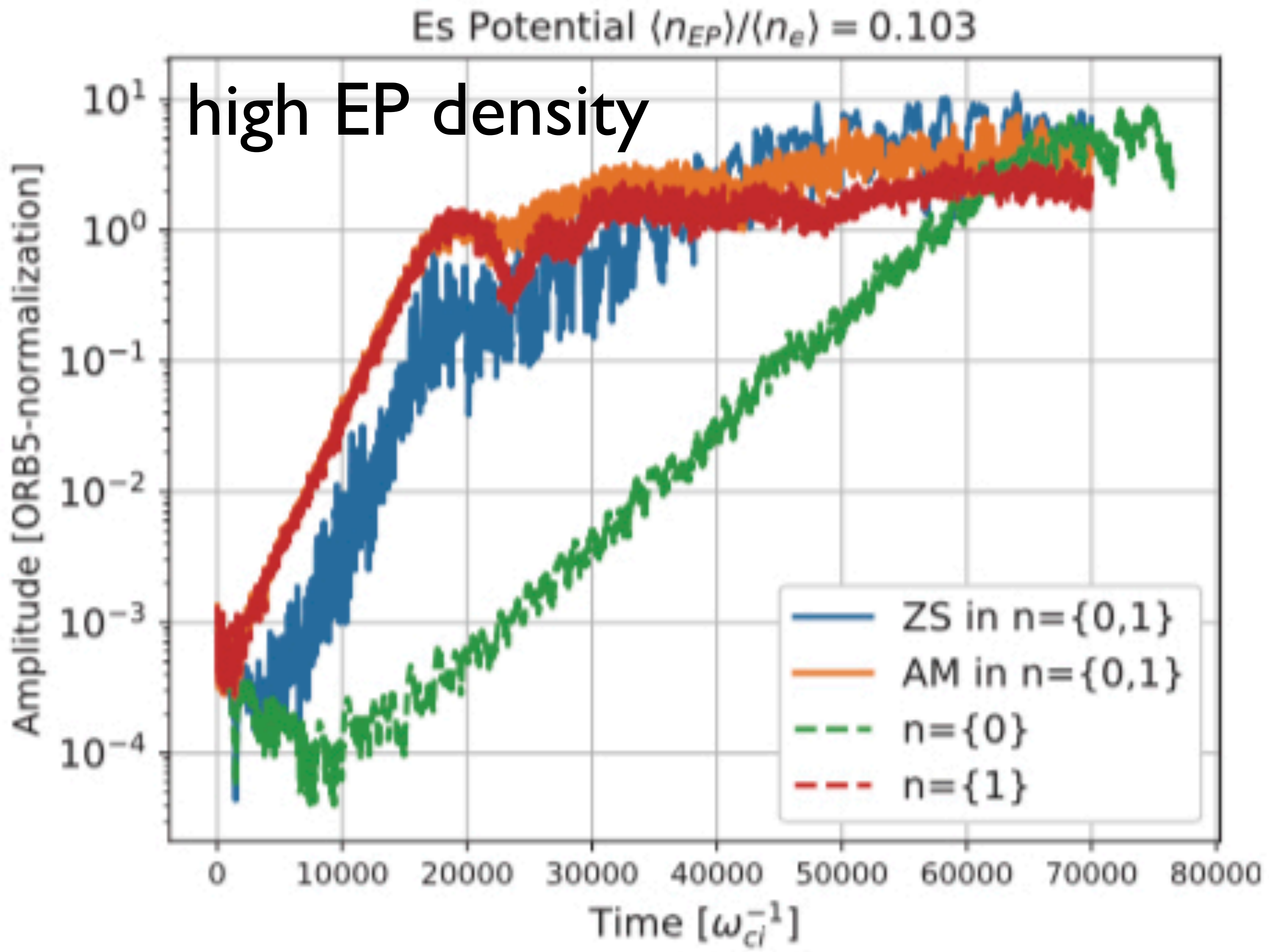

- non-linear ORB5 run, only EP non-linearities are kept
- AUG NLED EQ; bump-on tail EP distribution, radial gradient as in experiment, realistic electron-ion mass ratio
- single mode runs (keeping only n=0 or n=1 TAE) are compared with runs with n=0,1 both present
- considerable modifications of saturation levels found - nl forced-driven excitation [Todo 2010, Biancalani 2020, Qiu 2016]
- for further quantitative comparison, realistic F_{EP} has been implemented [T Hayward-Schneider, B. Rettino prep. 2021]

conclusions & outlook

- KAW physics is crucial for determining the self-organisation processes in a burning plasma
- both linear and non-linear processes depend on the details of cross-scale couplings of shear Alfven waves and KAWs: E//, parametric decay and zonal structures
- also other processes, like q=1 physics may be in influences by KAWs [M. S. Chu et al 2006]
- not discussed here: compressional Alfvén waves - KAW coupling [Belova, Lestz, 2015…2021]
- numerical tools, both linear and non-linear are evolving to capture relevant, non-perturbative, global physics elements

- dedicated experiments and diagnostics are needed for providing data-base in relevant parameter regimes - extended AUG scenarios to L,H mode, isotope scans

- interaction of EPs, AE, and turbulence [Liu AAPPS-DPP, 2020, Ishizawa FEC 2021, Biancalani PoP 2021, diSiena PRL 2021, Mazzi 2021] presently under investigation

- reduced models needed for analysis on transport time scales - general GK transport theory framework available capturing all elements discussed in the talk [Zonca & ChenNJP 2015, RMP 2016 , Falessi 2019,2021] - presently implemented in various hierarchal levels within Eurofusion Enabling Research Project (ATEP)

additional slides

radial propagation also due to other symmetry breaking meachnisms:

[G. Meng, et al. NF, 2020(056017), inv. talk AAPPS-DPP, 2020, subm. PST 2021]

- radial non-uniformities of background/EP profiles leads to symmetry breaking (S.B.) of Alfvén eigenmode structures - finite kr: asymmetric EP gradient w.r.t. mode rational surface of AE (here RSAE)

F. Zonca, NF 2005, L. Chen RMP 2016, Z. Lu, et al., NF 2018

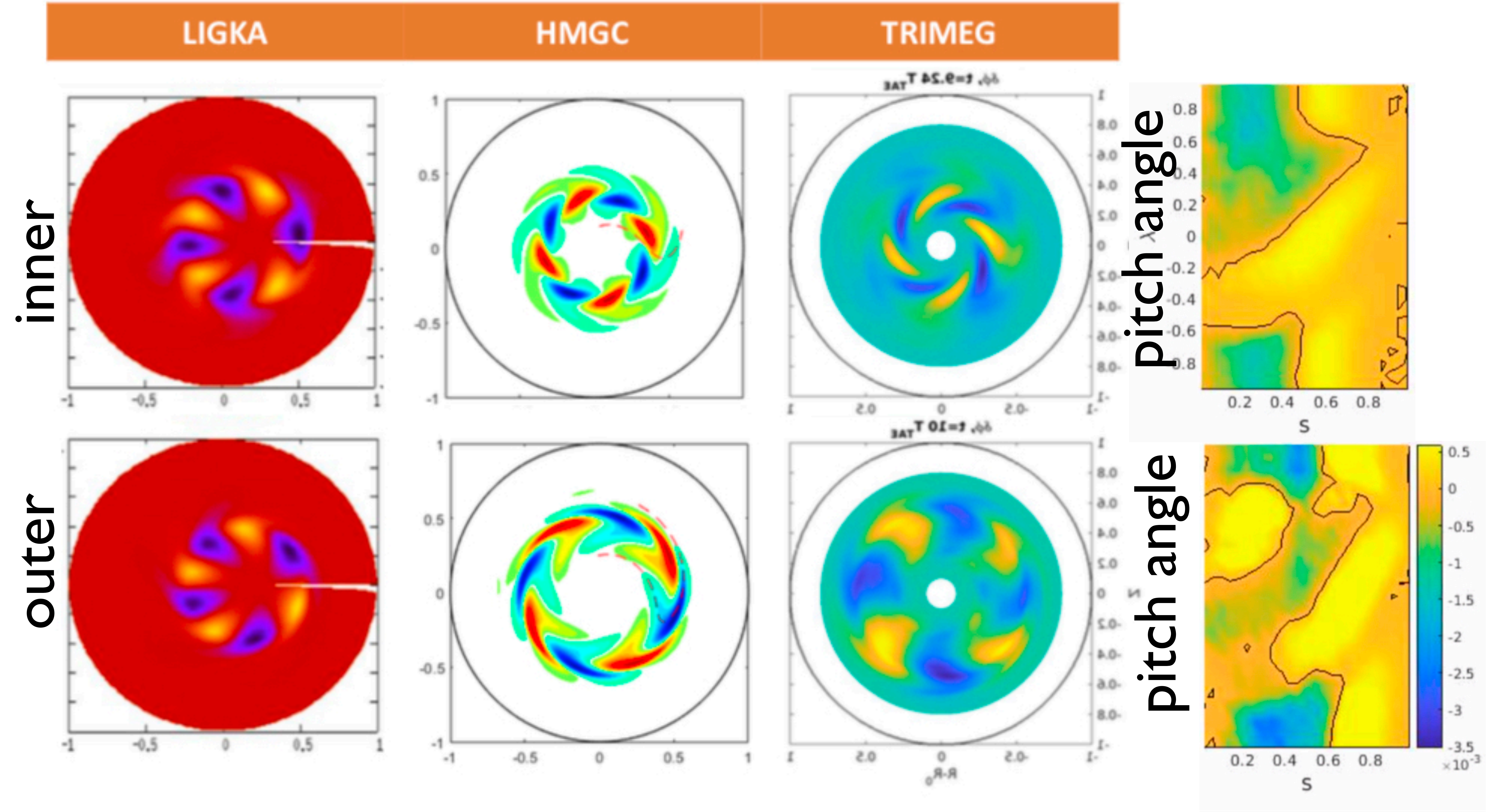

Parallel velocity radial distribution:

$u_{\parallel} = \int \delta f \cdot v_{\parallel}\, dv^3 / \int f\, dv^3$

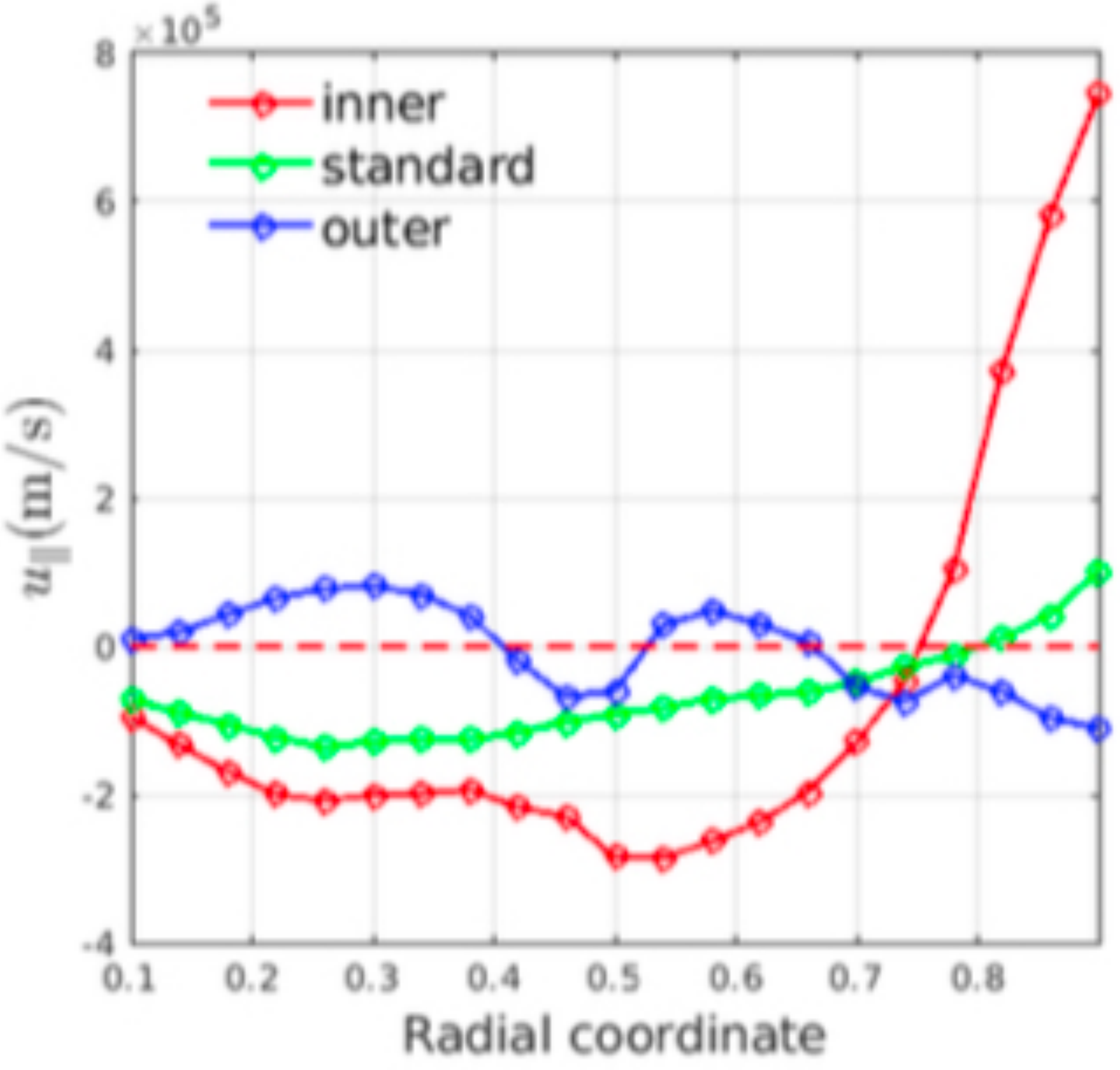

Result: mode symmetry breaking leads to anisotropies in phase space, even distribution, while growth rates and saturation amplitude remain very similar.

important role of sub-dominant modes

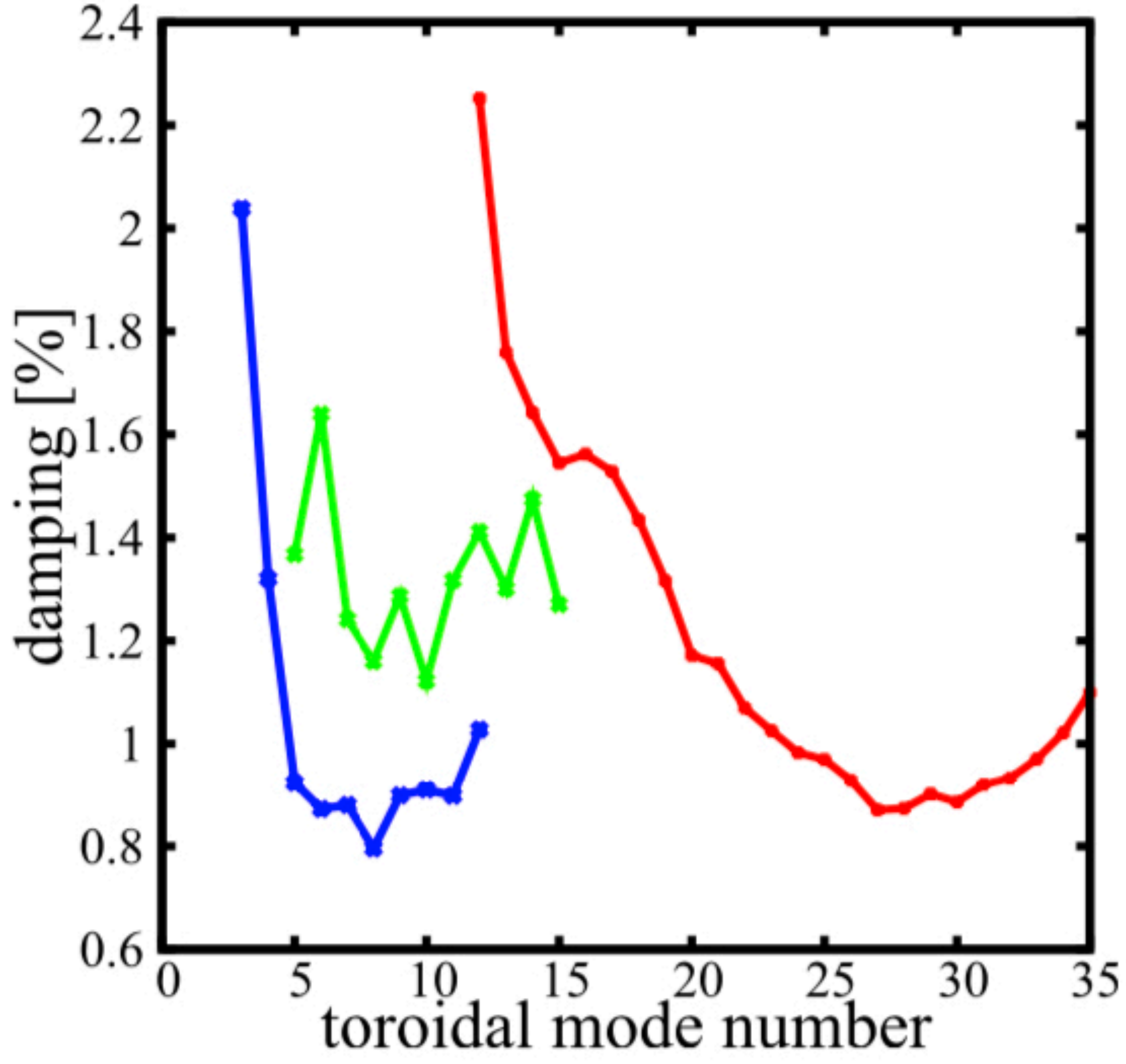

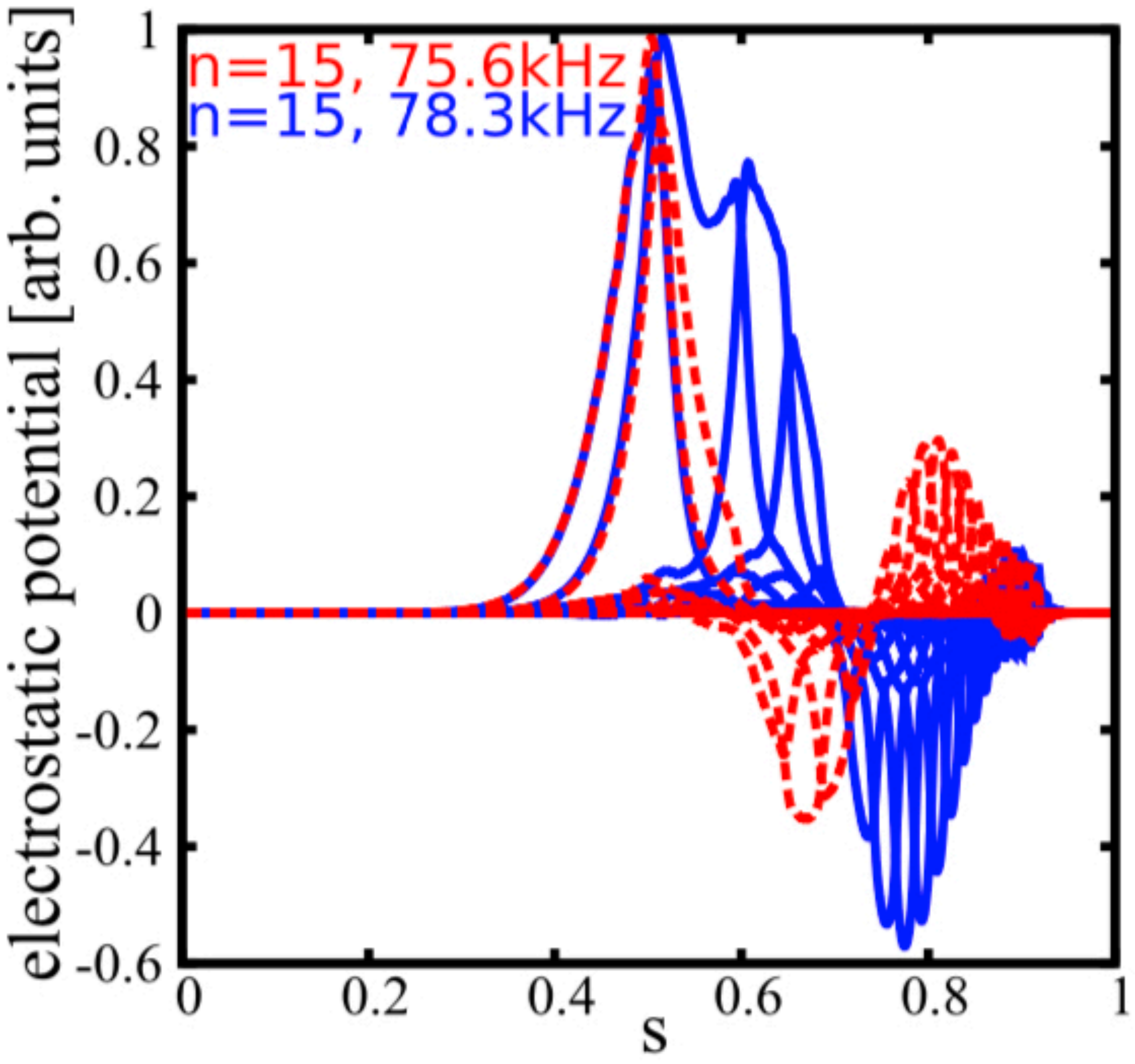

damping > ~1%

for n<15 more than one TAE branch is found to be weakly damped

different alignment of TAE gaps from core-edge

may destabilise subdominant modes with lower n in outer core

ITER case: electron mass ratio scan

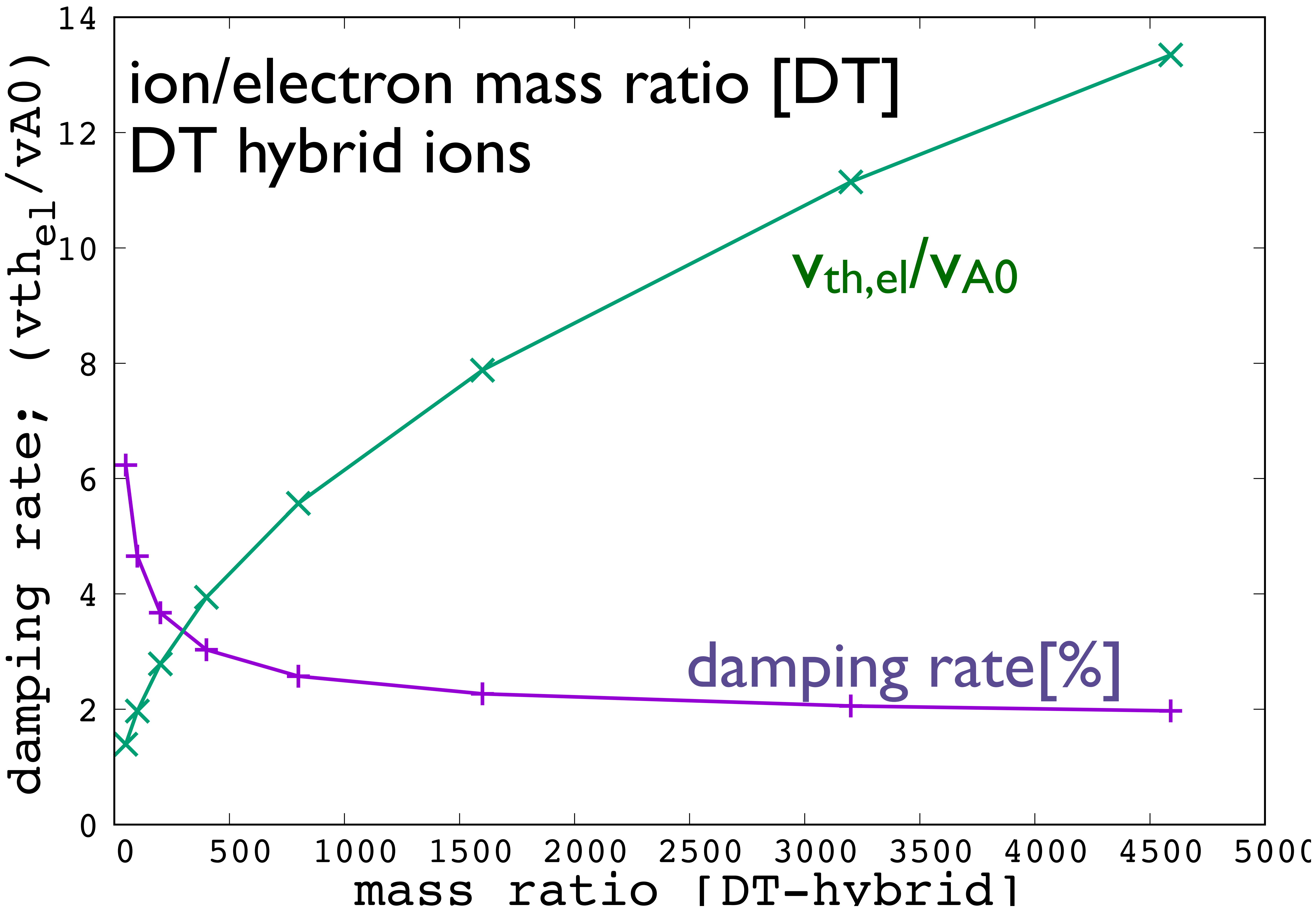

[T Hayward-Schneider NF 2021]

damping is almost independent of electron mass ratio over large range